Streptococcus mitis bacteriocins drive contact-dependent lysis of *S. pneumoniae* facilitating transformation in multispecies environments

João Borralho[1], João Lança,[1], Joana Bryton[1], Wilson Antunes[2], Raquel Sá-Leão[1]*

[1] Laboratory of Molecular Microbiology of Human Pathogens, Instituto de Tecnologia Química e Biológica António Xavier, Universidade Nova de Lisboa, Oeiras, Portugal

[2] Centro de Investigação da Academia Militar (CINAMIL), Unidade Militar Laboratorial de Defesa Biológica e Química (UMLDBQ), Av. Dr. Alfredo Bensaúde, 1849-012, Lisboa, Portugal.

* Corresponding author: rsaleao@itqb.unl.pt

Author Contributions: R. Sá-Leão and J. Borralho contributed to the concept and design of the study. R. Sá-Leão contributed with reagents and materials. Data acquisition was performed by J. Borralho, J. Lança, J. Bryton and W. Antunes. Data was interpreted by J. Borralho, J. Lança, J. Bryton, W. Antunes and R. Sá-Leão. The manuscript was drafted by J. Borralho and R. Sá-Leão. All authors critically revised and approved the final version of the manuscript.

Competing Interest Statement: Universidade NOVA de Lisboa has filed a provisional patent application that covers pharmaceutical compositions comprising strain G22 and/or bacteriocin molecules, and derivatives thereof, which can inhibit the growth and persistence of the pathogen *S. pneumoniae* (PT119647).

Keywords: Horizontal gene transfer, competence, interspecies interactions, predation, biofilms

Abstract

Natural competence allows bacterial species like *Streptococcus pneumoniae* and *S. mitis* to acquire environmental DNA, driving horizontal gene transfer (HGT) and adaptation. In *S. pneumoniae*, a human pathogen, competence-induced predation is well characterized and involves the release of bacteriocins and a murein hydrolase to lyse noncompetent siblings and liberate DNA. In contrast, in the human commensal *S. mitis*, mechanisms mediating DNA acquisition remain poorly understood. Here, we identify a diverse set of competence-associated bacteriocins (*cab*) that are produced by *S. mitis* during the late phase of competence. We focus on one bacteriocin pair, CabAB, that triggers contact-dependent growth inhibition and lysis of *S. pneumoniae* through activation of the major pneumococcal autolysin LytA. We demonstrate that CabAB compromises *S. pneumoniae* membrane integrity, leading to formation of intracellular membrane aggregates and the release of cytoplasmatic content, thereby increasing available DNA, which enhances HGT from *S. pneumoniae* to *S. mitis* in biofilms. These findings uncover a mechanism of interspecies predation and gene acquisition, revealing a critical role for competence-associated bacteriocins in shaping evolutionary dynamics of streptococci.

Significance Statement

Many streptococci are naturally competent, acquiring environmental DNA through transformation. This includes pathogens like *S. pneumoniae* and commensals like *S. mitis,* which can exchange genetic material through horizontal gene transfer (HGT). For example, *S. mitis* can acquire pneumococcal capsules, leading to its misidentification in polymicrobial samples such as those obtained from the upper respiratory tract. Understanding the drivers of HGT between these species is therefore critical. Here, we characterize a competence-induced bacteriocin cluster in *S. mitis*. These bacteriocins lyse pneumococci, promoting DNA release and enhancing gene transfer in dual-species biofilms. Our findings uncover a mechanism by which competence-associated predation promotes interspecies HGT, shaping the evolution and epidemiology of streptococcal populations.

Main Text

Introduction

Natural competence for genetic transformation is a developmental program found in certain bacterial species that enables the uptake of naked DNA from the environment. Once internalized, this DNA can be incorporated into the genome through homologous recombination, making natural transformation one of the main modes of horizontal gene transfer (HGT). This phenomenon was first described in *Streptococcus pneumoniae* (or pneumococcus), a species capable of exchanging pathogenic traits such as the capsule by taking up DNA from other pneumococci (1).

In *S. pneumoniae*, competence is a tightly regulated transient physiological state which is governed by a cell-cell signaling system. The competence-stimulating peptide (CSP), encoded by *comC*, is processed and exported via the ATP-binding cassette transporter ComAB. Extracellular CSP is sensed by the membrane-bound histidine kinase ComD (2-4), which undergoes autophosphorylation triggering subsequent phosphorylation of the response regulator ComE (5). Phosphorylated ComE increases expression of the early competence cascade including *comAB* and *comCDE*, creating a positive feedback loop. It also induces expression of the two copies of the alternative sigma factor (*sigX1* and *sigX2*), marking the onset of the late phase of competence (6).

In the late phase of competence, expression of all genes required for DNA uptake, processing and recombination – the transformasome – is induced (7). Here, pneumococci produce the competence-induced bacteriocins A and B (CibAB), along with the immunity protein CibC, which provides self-immunity to CibAB (8). Because competence is a bistable process, where only a subset of the population becomes competent at any given time, CibAB release on solid media leads to lysis of genetically identical (kin) noncompetent cells that have not yet expressed *cibC*. Additionally, expression of the murein hydrolase CbpD, against which competent cells are protected via ComM expression, is essential for kin predation in liquid cultures. Notably, CbpD has also been implicated in lysis of non-kin, closely related streptococci, thereby expanding the gene pool from which *S. pneumoniae* may acquire DNA (9). CibAB and CbpD have also been associated to competitive

81 interactions *in vivo*, where their expression by colonizing pneumococci provides a competitive
82 advantage over other *S. pneumoniae* invaders (10).

83 A close relative of the pneumococcus, *S. mitis*, is also naturally transformable. *S. mitis* is a
84 common commensal of the human nasopharynx and oral cavity, where it typically establishes long-
85 term colonization without causing disease (11). Despite close phylogenetic relationship with *S.*
86 *pneumoniae*, and a strikingly similar competence regulatory network, *S. mitis* exhibits key differences
87 in terms of bacteriocin content. While *cibAB* is highly conserved in *S. pneumoniae*, most *S. mitis* lack
88 *cibAB*, suggesting that *S. mitis* may rely on an alternative mechanism for predation during
89 competence (12, 13).

90 Although the frequency at which *S. mitis* acquires DNA from *S. pneumoniae* is not well
91 established, such events have been documented. These includes the acquisition of pneumococcal
92 *pbp* mosaic blocks (14, 15), as well as the expression of pneumococcal or pneumococcal-like
93 capsules by certain *S. mitis* strains (16-20).

94 A competence-associated bacteriocin (*cab*) cluster, which is absent in *S. pneumoniae*, has
95 been identified in *S. mitis*. This cluster is located upstream of the competence transporter *comAB* and
96 can encode multiple *cab* bacteriocins distinct from CibAB (12, 13, 21-23). However, the role of *cab* in
97 *S. mitis* predation of kin and non-kin, and its contribution to DNA acquisition, remains unexplored.

98 Here, we characterize the arsenal of *cab* bacteriocins carried by *S. mitis* and provide evidence
99 that some specifically mediate lysis of *S. pneumoniae*. We also show that pneumococcal DNA can
100 be efficiently taken up and recombined by *S. mitis* and that Cab-mediated lysis accelerates gene
101 transfer from *S. pneumoniae* to *S. mitis*. Together, these findings shed light on previous observations
102 of pneumococcal DNA integration in *S. mitis* genomes.

103

104 ## Results

105 ### *S. mitis* encodes a diverse arsenal of competence-associated bacteriocins (*cab*)

106 We previously identified and characterized a limited number of *S. mitis* strains encoding multiple
107 competence-associated bacteriocins (*cab*), most of which lacked the pneumococcal bacteriocins

108 *cibAB* and associated immunity protein *cibC* (23). To investigate the broader distribution of *cab* and
109 *cibAB* in *S. mitis*, we surveyed publicly available genomes, leveraging the conserved genomic context
110 of *cab* clusters – located upstream of *comAB* and downstream of *plsX-acpP*. This region was identified
111 and extracted from 253 of 332 *S. mitis* genomes (Fig. 1A and *SI Appendix*, Table S1). The remaining
112 genomes had contig breaks and were excluded from further analysis.

113 Among the 253 genomes analyzed, 26.9% harbored *cibABC*, a striking contrast with *S.*
114 *pneumoniae*, where these genes are universally present. An additional 13.0% of strains carried *cibC*
115 but not *cibAB* – often referred to as "cheater" phenotype (24), in which strains are immune to CibAB-
116 mediated killing but do not produce the bacteriocins themselves. In contrast, 47.4% of *S. mitis*
117 encoded between one to eleven unique *cab* genes. In total, 95 distinct Cab variants were found, which
118 grouped into 28 clusters based on sequence similarity (Fig. 1B and *SI Appendix*, Fig. S1). Overall,
119 61.3% of *S. mitis* genomes carried at least one *cab* gene or the *cibABC* operon (*SI Appendix*, Table
120 S1).

121 Cab variants were present at low frequencies (<10%) in the *S. mitis* population, with 32 of 95
122 bacteriocin variants only being found in a single strain (Fig. 1B). Despite this extensive diversity,
123 rarefaction analysis suggested that Cab diversity is not yet saturated (Fig. 1C); sequencing more *S.*
124 *mitis* will likely reveal new Cab sequences.

125 These findings highlight *S. mitis* as a reservoir of highly diverse and largely unexplored
126 competence-associated bacteriocins.

127

128 **Cab bacteriocins are expressed in the late phase of competence**

129 *S. mitis* G22, previously described by us, encodes a *cab* operon consisting of two putative bacteriocins
130 and an associated immunity protein (hereafter referred as *cabAB* and *cabC*, respectively) (Fig. 2A)
131 (23). This strain was selected to study *cab* regulation in *S. mitis* and its role in competitive behaviors.
132 Both bacteriocins and the immunity protein it encodes are rare (25) and thus unlikely to encounter
133 pre-existing immunity in other strains. Notably, its *cab* promoter contains five putative binding sites
134 for the alternative sigma factors (SigX boxes) (23), suggesting that *cabABC* may be expressed during
135 the late phase of competence.

136 To investigate the dynamics of *cab* expression, the native *cabABC* promoter was ectopically
137 inserted into the *S. mitis* G22 genome, upstream of a firefly luciferase reporter (*luc*). Expression of
138 *cabABC* was then inferred by expression of *luc* and compared to known early (*comCDE*) and late
139 (*sigX1* and *sigX2*) competence regulators. As expected, we observed that competence was not
140 induced under acidic pH (*SI Appendix*, Fig. S2), unless exogenous cognate competence-stimulating
141 peptide (CSP_{G22}) was supplied (*SI Appendix*, Fig. S3A). Upon CSP_{G22} treatment, *cabABC* expression
142 followed a similar temporal pattern to *comCDE*, *sigX1* and *sigX2*, peaking at approximately 70 min
143 post-induction (*SI Appendix*, Fig. S3B). This response was specific to CSP, as exogenous addition of
144 cognate bacteriocin-like peptide pheromones ($BlpC_1$ and $BlpC_4$), encoded elsewhere in the *S. mitis*
145 G22 genome (25), failed to induce *cabABC* expression (*SI Appendix*, Fig. S4).
146 Deletion of the early regulator *comE* abolished *cabABC* expression, a result expected for both
147 early- and late-regulated genes (Fig. 2B). Individual deletion of *sigX1* or *sigX2* partially reduced
148 expression of *cabABC*, while deletion of both resulted in complete loss of *cabABC* expression,
149 consistent with *cab* being expressed during the late phase.
150 Although multiple SigX boxes have been observed in *cab* promoters previously (13, 23), their
151 functional relevance has not been tested. To assess this, we compared expression driven by the full-
152 length *cabABC* promoter (containing all five SigX boxes) to a truncated version containing only the
153 most proximal SigX box. Deletion of four out of five SigX boxes reduced *cabABC* expression (Fig.
154 2C), indicating that tandem SigX binding sites enhance *cab* expression. In the *S. mitis* collection, all
155 *cab* loci harbored at least two SigX boxes, with one strain containing up to 38 boxes (Fig. 2D and *SI*
156 *Appendix*, Table S1). Larger *cab* loci were associated with higher number of SigX boxes, suggesting
157 accumulation of boxes throughout these sequences.
158 Together, these results demonstrate that *cab* bacteriocins are specifically expressed during
159 the late phase of competence, and that the presence of multiple SigX binding sites amplifies their
160 expression.
161
162 **Expression of *S. mitis cabABC* is induced by pneumococcal CSP-1**

163 Mitis group streptococci naturally produce and recognize different CSP variants, known as pherotypes
164 (26). To investigate the specificity of *cab* expression, synthetic CSP variants from closely related
165 strains were tested for their ability to activate *cabABC*. CSP variants from three other *S. mitis*, one *S.*
166 *oralis*, and one *S. pneumoniae* strain failed to induce *cab* expression in *S. mitis* G22 (Fig. 3A). By
167 contrast, the most prevalent *S. pneumoniae* pheromone, CSP-1 (27), efficiently induced *cab* to the
168 same levels as native CSP_{G22}.

169 Comparison of the amino acid sequences CSP_{G22} and the other CSP variants revealed a
170 single amino acid residue, Q14 (glutamine), that may explain the differences in induction. While both
171 CSP_{G22} and CSP-1 contain Q14, a polar residue, the non-inducing variants contain either a L14
172 (leucine) or a P14 (proline), both nonpolar. To investigate the importance of Q14 and polarity in
173 competence induction, CSP_{G22} variants with single amino acid substitutions at position 14 were tested.
174 Substituting Q14 with L significantly reduced *cab* expression, whereas replacing it with another polar
175 residue (N, asparagine) restored expression (Fig. 3B). This suggests that polarity of amino acid 14 is
176 important for CSP recognition by *S. mitis* G22. However, introducing Q14 into a non-inducing peptide
177 (CSP-2; L14Q) was not sufficient to convert it into a functional inducer, indicating that additional
178 residues beyond Q14 are required for efficient recognition by the membrane-bound histidine kinase
179 ComD of *S. mitis* G22.

180 To assess whether *S. pneumoniae* can also respond to CSP_{G22}, the *comCDE* promoter from
181 *S. pneumoniae* D39, a strain that produces and recognizes CSP-1, was transcriptionally fused to a
182 *luc* reporter and integrated in its chromosome. Competence in D39 was efficiently induced by both
183 CSP-1 and CSP_{G22}, confirming that *S. mitis* G22 and *S. pneumoniae* D39 can cross-communicate
184 through distinct CSP peptides (Fig. 3C). Similar to G22, *S. pneumoniae* D39 was also affected by
185 mutations at position 14: Q14L (polar to nonpolar) reduced induction. In contrast to *S. mitis* G22, the
186 substitution Q14N (polar with another polar aminoacid), failed to restore it. Notably, the substitution
187 L14Q into CSP-2 (the second most frequent CSP in pneumococci) enabled competence induction.
188 These findings highligh the importance of Q14 in CSP recognition of pneumococci of the CSP-1
189 pherotype.

190 In the 253 *S. mitis* genomes analyzed, 2.8% encode CSP_{G22}, and 13.0% encode a CSP
191 containing Q14 (*SI Appendix*, Table S1), suggesting that more *S. mitis* strains could induce
192 competence in pneumococci of pherotype CSP-1.
193 These results reveal that cross-communications via CSP is possible between *S. mitis* and *S.*
194 *pneumoniae*, and that residue 14 plays a critical, but context-dependent, role in pheromone
195 recognition.
196
197 **CabAB mediates inhibition of *S. pneumoniae* in a contact-dependent manner**
198 Given that *S. mitis* G22 and *S. pneumoniae* D39 can cross-communicate through CSP, we
199 hypothesized both species would engage in competence-induced predation. Supporting this, *S. mitis*
200 G22 harbors the orphan immunity gene *cibC* (but not *cibAB*), suggesting it may be resistant to
201 pneumococcal CibAB attack (*SI Appendix*, Table S1).
202 To investigate the specific role of the competence associated bacteriocins CabAB in *S.*
203 *pneumoniae* inhibition, we first deleted two bacteriocin clusters (*blp4* and *blp1*) with known anti-
204 pneumococcal activity (23), from the genome of *S. mitis* G22, as their activity could obscure CabAB-
205 mediated effects. All experiments in this section were, thus, performed using *S. mitis* G22 Δ*blp4*Δ*blp1*
206 and its derivatives as described below.
207 We grew dual-species biofilms of *S. mitis* G22 Δ*blp4*Δ*blp1* and *S. pneumoniae* D39 under
208 competence-permissive conditions. After 24 h, both species persisted in the biofilm (Fig. 4A and *SI*
209 *Appendix*, Fig. 5). Deletion of *cab* from *S. mitis* led to increased pneumococcal loads, while
210 constitutive expression of *cab* via plasmid p(cab^+) (overexpressor mutant contains the native *cab* copy
211 and carries an additional constitutively expressed copy in plasmid p(cab^+)) reduced them, indicating
212 that the presence and expression levels of *cab* modulate competitive outcomes.
213 Bacteriocins are typically secreted to the extracellular environment (28). To test whether
214 CabAB exerts its activity as a secreted factor, we harvested cell-free supernatants (CFS) from *S. mitis*
215 strains and added them to pneumococcal cultures. CFS of *S. mitis* natively or overexpressing *cab* did
216 not inhibit *S. pneumoniae* growth (Fig. 4B), suggesting CabAB is not released into the medium. This

217 aligns with recent reports of bacteriocins, such as Listeriolysin S and contact-dependent inhibition by
218 glycine zipper proteins CdzCD (29, 30), that remain attached to the producer cell surface. In these
219 cases, inhibitory activity occurs via direct contact between producer and target cells.

220 To test whether CabAB could remain cell-associated, we heat-killed *S. mitis* strains (as
221 bacteriocins are typically resistant to high temperature treatments) and exposed them to *S.*
222 *pneumoniae*. Heat-killed *cab*$^+$ and p(*cab*$^+$) *S. mitis* extracts significantly inhibited pneumococcal
223 growth, while extracts from Δ*cab S. mitis* did not (Fig. 4B), supporting the idea that CabAB is retained
224 in producer cells.

225 We then tested whether direct contact between *S. mitis* and *S. pneumoniae* was required for
226 inhibition. Dual-species biofilms were grown either with or without a 0.4 µm transwell membrane
227 separating both species. When the strains were in direct contact with each other, *cab* expression was
228 associated with pneumococcal inhibition, whereas no inhibition was observed when both species
229 were separated (Fig. 4C). These effects were not due to differences in *S. mitis* growth, as bacterial
230 loads were consistent across conditions and genotypes (Fig. 4D).

231 We then sought to detect CabA and CabB on the surface of competent *S. mitis* cells. A mutant
232 lacking the native *cab* locus was used, into which we ectopically integrated cassettes containing
233 haemagglutinin-tagged (HA) CabA (*cabA-HA cabBC*) or CabB (*cabA cabB-HA cabC*), under native
234 regulation. Immunofluorescence microscopy of live *S. mitis* expressing *cabA-HA* using anti-HA
235 antibodies revealed discrete clusters of CabA on the cell surface (Fig. 4E). No signal was detected in
236 strains lacking the HA epitope, confirming specificity. Interestingly, no signal was observed in the
237 *cabB-HA* strain, suggesting that CabB may be less surface-exposed, that the N-terminal HA tag was
238 not accessible to antibody binding, or that tagging interfered with localization.

239 Together, these results demonstrate that *S. mitis* inhibits *S. pneumoniae* via CabAB in a
240 contact-dependent manner.

241

242 **CabAB is a two-peptide bacteriocin with LytA-dependent bactericidal activity**

243 CibAB has previously been shown to be a two-peptide bacteriocin, meaning its inhibitory activity
244 occurs only when both peptide components are present (8). To test if CabAB also functions as a two-

245 peptide bacteriocin, synthetic CabA and CabB were tested individually and in combination against *S.*
246 *pneumoniae* D39. No effect on pneumococcal growth was observed upon addition of DMSO (the
247 solvent used to resuspend the peptides), CabA alone, or CabB alone (Fig. 5A). In contrast, a single
248 treatment with equimolar amounts of CabA and CabB delayed *S. pneumoniae* growth for ~12 h,
249 indicating that both peptides are required for activity. This is consistent with the presence of multiple
250 GxxxG or GxxxG-like motifs in both bacteriocins (Fig. 5B), known to facilitate and stabilize two-
251 component bacteriocins (31-33).

252 We next investigated whether CabAB exerts bactericidal activity. Exponentially growing *S.*
253 *pneumoniae* D39 cultures were treated with CabAB or DMSO. CabAB-treated cultures showed
254 evident decrease in optical density, indicating lysis, while DMSO-treated controls did not (Fig. 5C).
255 Lysis induced by the related bacteriocin CibAB has been shown to depend on the action of the
256 pneumococcal autolysins LytA and LytC (8). Here, deletion of *lytC* from D39 had no effect on CabAB-
257 mediated lysis, whereas a Δ*lytA* mutant exhibited delayed growth but no lysis, indicating that LytA is
258 required for this phenotype.

259 Together, these findings show that *S. mitis* CabAB is a two-peptide bacteriocin with
260 bactericidal activity against *S. pneumoniae*, and that its lytic activity depends on the target cell LytA
261 autolysin.

262

263 **CabAB affects membrane homeostasis in *S. pneumoniae***

264 We sought to shed light on how CabAB affects pneumococcal physiology. To this end, *S. pneumoniae*
265 D39 cells were treated with CabAB or DMSO and imaged by scanning electron microscopy (SEM).
266 While DMSO-treated cultures displayed normal morphology, CabAB-treated cells appeared to be
267 encased in an extracellular matrix (Fig. 6A), suggesting leakage of intracellular material.

268 To test if membrane permeability was compromised, cells were stained with propidium iodine
269 (PI), a DNA-binding dye that only enters cells with compromised membranes. In DMSO-treated
270 cultures, only 3% were PI-positive, while CabAB-treated cultures contained 85% PI-positive cells (Fig.
271 6B). Doubling the concentration of CabAB further increased this proportion to 97%, indicating this
272 phenotype is concentration dependent. Deletion of *lytA* had no effect on these phenotypes,

273 demonstrating that membrane permeabilization occurs independently of autolysin-mediated lysis (*SI*
274 *Appendix*, Fig. S6).
275 Time series measurements showed that PI signal intensity peaked at 30 min post CabAB
276 exposure, still being detected after 120 min (Fig. 6C). We also assessed pneumococcal membrane
277 depolarization using the fluorescent dye $DiBAC_4(3)$, which enters cells only when their membranes
278 are depolarized. Compared to DMSO, CabAB treatment led to a rapid and sustained increase in
279 $DiBAC_4(3)$ signal (Fig. 6D), indicating membrane depolarization.
280 Since some characterized two-peptide bacteriocins act by forming pores (34-37), we tested
281 whether CabAB treatment causes efflux of intracellular components from target cells. In wild-type *S.*
282 *pneumoniae* treated with CabAB, 80% of total ATP was detected in the supernatant (Fig. 6E), in
283 agreement with our previous observation of cell lysis (Fig. 5C). Interestingly, in treated Δ*lytA S.*
284 *pneumoniae* cells, which are not lysed by CabAB (Fig. 5C), 30% of ATP was still released, suggesting
285 that CabAB induces leakage independently of cell lysis.
286 We next visualized CabAB-induced damages using transmission electron microscopy (TEM).
287 DMSO-treated cells appeared intact, whereas 17% of CabAB-treated cells contained large
288 intracellular aggregates (Fig. 6F). Based on our prior observations, we hypothesized these
289 aggregates would be membranous. Consistently, staining with the membrane dye FM4-64 revealed
290 intracellular foci in CabAB-treated cells, but not in control cells (Fig. 6G), confirming the formation of
291 membrane aggregates by CabAB.
292 Finally, lower-magnification fluorescent microscopy of CabAB-treated cultures stained with
293 DAPI and FM4-64 revealed frequent clumps of cells encased in nucleic acid and membrane material,
294 mirroring the SEM observations of surviving cells remaining embedded in an extracellular matrix (*SI*
295 *Appendix*, Fig. 7)
296 Altogether, these findings show that *S. mitis* CabAB disrupts membrane homeostasis in *S.*
297 *pneumoniae* by permeabilizing and depolarizing membranes, leading to release of its intracellular
298 content.
299
300 **CabAB facilitates the acquisition of pneumococcal DNA by *S. mitis* in biofilms**

301 As previously shown, CabAB promotes release of DNA from *S. pneumoniae* cultures. Since *cab*
302 expression is synchronized with the competence period, we hypothesized that CabAB could enhance
303 DNA acquisition and HGT within biofilms. To test this, we grew dual-species biofilms under conditions
304 designed to study HGT (Fig. 7A), where: (i) DNA transfer is unidirectional, since the DNA donor strain
305 (*S. pneumoniae* D39) carries a deletion of the major competence pilus subunit gene, *comGC,*
306 rendering it nontransformable; (ii) the *S. pneumoniae* DNA donor harbors chloramphenicol (Chl^R) and
307 tetracycline (Tet^R) resistance cassettes integrated at opposite ends of the chromosome; (iii) the DNA
308 recipients (*S. mitis* G22, wt and variants) are kanamycin resistant, allowing for discrimination between
309 non-transformed (Kan^R) and transformed *S. mitis* (Kan^R Chl^R, Kan^R Tet^R, and Kan^R Chl^R Tet^R); (iv)
310 biofilms are pre-grown under acidic pH for 24 h to promote biofilm establishment without inducing
311 competence; and (v) CSP_{G22} is added after 24 h to transiently induce competence. A noncompetent
312 *S. mitis* Δ*comE* mutant was used as a negative control, as it is unable to acquire Chl^R and/or Tet^R by
313 transformation.

314 To rule out the possibility that CabAB affects transformability rather than DNA availability, we
315 first replaced the donor strain with purified gDNA. Under these conditions, both *cab*$^+$ and Δ*cab S. mitis*
316 acquired resistance at similar frequencies (Fig. 7B), indicating that native *cab* expression does not
317 impact transformability. In contrast, overexpression of *cab* reduced transformation efficiency for one
318 antibiotic resistance, possibly due to the fitness burden associated with carrying p(*cab*$^+$).

319 In dual-species biofilms, *cab*$^+$ *S. mitis* efficiently acquired Chl^R and Tet^R from the DNA donor,
320 at a significantly higher frequency than the Δ*cab* mutant (Fig. 7C), indicating that CabAB contributes
321 to DNA acquisition. In contrast, overexpression of CabAB did not enhance transformation efficiency,
322 suggesting that a precise *cab* regulation might be necessary for optimal transformation.

323 Finally, we sought to investigate the specificity of CabAB-induced lysis. Synthetic CabAB was
324 tested against 26 bacterial species, including 18 streptococcal species, four additional non-
325 streptococcal Gram-positive and four Gram-negative species. All selected species are human
326 commensals or pathogens that can inhabit the oral and/or respiratory tract and could theoretically
327 encounter *S. mitis* and be exposed to Cab bacteriocins in natural environments. Addition of CabAB

328 to exponential cultures of these bacteria stalled the growth of some species (Fig. 7D and *SI Appendix*,
329 Fig. S8 and S9). The most sensitive to CabAB were Pyogenic Group streptococci (*S. pyogenes* and
330 *S. agalactiae*). Gram-negative bacteria (*Haemophilus influenzae*, *Klebsiella pneumoniae*, *Moraxella*
331 *catarrhalis*, and *Neisseria lactamica*) were largely unaffected. Despite growth inhibition in some
332 species, lysis was only observed in two - *S. pneumoniae* and *S. parasanguinis* - highlighting the
333 specificity of CabAB-mediated lysis.

334 These results suggest that CabAB provides a competitive advantage by inhibiting the growth
335 of some bacteria, but that it also enhances DNA release in biofilms by selectively lysing a few closely
336 related species during competence, notably *S. pneumoniae*, thereby promoting gene exchange.

337

338 **Discussion**

339 During competence, streptococci scavenge extracellular DNA. In *S. pneumoniae*, where competence-
340 induced predation is best characterized, the coordinated action of CibAB, LytA, LytC, and the murein
341 hydrolase CbpD leads to lysis of noncompetent siblings (8). This process promotes DNA release and
342 facilitates HGT (9, 38, 39).

343 Although extensive genomic data suggests that *S. mitis*, a close relative of *S. pneumoniae*,
344 frequently acquires *S. pneumoniae* DNA (14-20), the molecular mechanisms underlying this
345 exchange remained poorly understood. Understanding these mechanisms is relevant because
346 capsule acquisition by *S. mitis* can complicate DNA-based pneumococcal serotyping. In addition, *S.*
347 *mitis* has been associated with cases of infective endocarditis (19), highlighting the value of studying
348 how it acquires potentially pathogenic traits.

349 Here, we investigated the role of *S. mitis* competence-associated bacteriocins, CabAB, in
350 mediating interspecies interactions. We show that CabAB is a two-peptide bacteriocin produced
351 during the late phase of competence, when cells are primed for DNA uptake and recombination,
352 capable of lysing *S. pneumoniae* in a LytA-dependent manner. Although LytA is constitutively
353 expressed throughout growth, its concentration increases during competence, owing to a genomic
354 architecture comprising three constitutive promoters and one competence-induced promoter (7, 40-

355 42). In this context, it is tempting to speculate that by inducing *S. pneumoniae* competence via CSP
356 crosstalk, and therefore increasing LytA concentration, some *S. mitis* could further sensitize *S.*
357 *pneumoniae* to Cab bacteriocins. Nonetheless, CabAB-induced lysis appears to be independent of
358 pherotype of target cells, as both *S. pneumoniae* D39 (CSP-1; used in most experiments) and TIGR4
359 (CSP-2; included in the panel of 26 bacterial species) were lysed. These pherotypes account for the
360 vast majority (>95%) of pneumococcal strains (43-45).

361 Of the initial 332 *S. mitis* genomes analyzed, we were not able to retrieve the region upstream
362 of *comAB* from a substantial fraction of strains (23.8%), as their assemblies showed contig breaks
363 precisely at this locus. We propose this difficulty arises from the repetitive nature of the region, as
364 indicated by the presence of numerous SigX boxes. The number of boxes scaled linearly with the size
365 of *cab* loci, suggesting that SigX boxes have accumulated throughout these sequences. Repeats are
366 known to both promote and result from genomic rearrangements (46, 47). They are often remnants
367 of previous recombination events, with no known biological function (48). In this case, however,
368 accumulation of SigX boxes may provide a selective advantage by enhancing bacteriocin expression,
369 which could explain why they are enriched in this region. Consistent with this, the extensive genetic
370 rearrangements observed across multiple streptococcal species at this locus also suggests this is a
371 highly recombinogenic region (21, 22, 49).

372 Microscopic analysis revealed that CabAB-treated pneumococci often contain large
373 membrane-derived intracellular aggregates. Whether these structures are part of CabAB's
374 mechanism of action or represent a cellular stress response remains unclear. Intracellular vesicle
375 formation has been shown to be essential for the lytic activity of bacteriocin A37 (50). However, the
376 disordered morphology of CabAB-induced structures suggests an alternative process. We
377 hypothesize that aggregate formation may reflect a protective response, where membrane
378 invaginations at CabAB-enriched sites reduce metabolite leakage and trap affected membrane
379 material intracellularly.

380 We further demonstrate that CabAB-mediated inhibition of *S. pneumoniae* requires direct
381 contact between producer and target cells. Contact-dependent bacteriocin delivery has been
382 described in *Caulobacter crescentus* and *Listeria monocytogenes* (29, 30). In *L. monocytogenes*,

383 bacteriocins were only detected on the surface of producer cells following cell wall digestion. In
384 contrast, we detected CabAB on live *S. mitis* with intact cell walls, suggesting a distinct delivery
385 mechanism. Contact-dependent killing during competence is not unique to streptococci, despite
386 differences in killing factors. *Vibrio cholerae* produces a competence-induced type VI secretion
387 system that kills nonimmune cells, releasing DNA that becomes accessible for HGT (51). Contact
388 dependence may be particularly advantageous in biofilm contexts, a niche where extracellular DNA
389 could be subject to rapid degradation nucleases (52). Proximity within multispecies biofilms could
390 enhance transformation efficiency by increasing the local DNA concentration, given that DNA
391 abundance and size influence recombination success (53). Notably, biofilm conditions and cell-to-cell
392 contact have been shown to promote both the frequency and size of recombination events in
393 pneumococci, respectively (54, 55).

394 Strikingly, among 26 tested species, only *S. pneumoniae* and *S. parasanguinis* were lysed by
395 CabAB, suggesting a narrow-spectrum bactericidal activity. Whether this specificity is unique to
396 CabAB or shared among other Cab bacteriocins remains to be determined. Nonetheless, the ability
397 to selectively target phylogenetically related but distinct species suggests a potential trade-off
398 between maximizing recombination efficiency and accessing a broader gene pool. While high
399 sequence identity between donor and recipient promotes recombination (56), restricting lysis to
400 closely related species could expand the range of accessible alleles beyond conspecifics.

401 Importantly, CabAB also strongly inhibited the growth of other streptococcal pathogens,
402 including *S. pyogenes* and *S. agalactiae*, both of which are listed as priority pathogens by the World
403 Health Organization (25). This potent inhibitory activity suggests that the Cab arsenal carried by *S.*
404 *mitis* could be a promising source of antimicrobial agents against important clinical pathogens as
405 recently suggested by us (25).

406 In summary, our findings uncover a contact-dependent mechanism of bacteriocin delivery in
407 *S. mitis* that selectively targets closely related streptococci including *S. pneumoniae*. This process
408 promotes HGT and likely contributed to competitive fitness and evolutionary plasticity of streptococcal
409 populations.

410

411 ## Materials and Methods

412 ### Bacterial strains and culture conditions

413 Bacterial strains, oligonucleotides, plasmids and peptides used in the study are listed in *SI Appendix*,
414 Table S2. Streptococci were routinely grown in C+Y_{YB} (57) (pH 7.4, unless otherwise specified) and
415 plated on tryptic soy agar with 5% defibrinated sheep blood (blood agar, BA). When appropriate,
416 media was supplemented with antibiotics at the following concentrations: 150 µg.mL^{-1} kanamycin,
417 200 µg.mL^{-1} spectinomycin, 4 µg.mL^{-1} chloramphenicol, or 4 µg.mL^{-1} tetracycline.

418 *Staphylococcus aureus, Staphylococcus epidermidis* and *Moraxella catarrhalis* were grown in
419 tryptic soy broth (TSB); *Corynebacterium accolens* was grown in TSB with 0.5% Tween 80; *Klebsiella*
420 *pneumoniae* and *Escherichia coli* were grown in lysogeny broth; and *Neisseria lactamica*,
421 *Haemophilus influenzae* and *Dolosigranulum pigrum* were grown in C+Y_{YB} with 20 µg.mL^{-1} hemin and
422 20 µg.mL^{-1} NAD. For propagation of plasmids in *E. coli*, media was supplemented with 100 µg.mL^{-1}
423 kanamycin or 100 µg.mL^{-1} spectinomycin, as required.

424

425 ### Identification of *cab* bacteriocins and *cibABC* in *S. mitis*

426 Publicly available *S. mitis* genomes (n = 322) were downloaded from PubMLST. An additional 10
427 genomes from reference or commonly used *S. mitis* strains were included, resulting in a total of 332
428 genomes (*SI Appendix*, Table S1). To detect *cab* clusters, nucleotide sequences of *plsX-acpP* and
429 *comAB* (from *S. mitis* B6; GenBank Accession GCA_000027165.1), which flank the *cab* locus, were
430 aligned against all genomes using pairwise sequence alignment (Biopython v1.81; match = 2;
431 mismatch = -1; gap open = -5; gap extension = -0.5; minimum overall sequence identity ≥ 90%).
432 Genomes in which *plsX-acpP* and *comAB* were absent or located on separate contigs were excluded
433 from further analysis. This region was identified in 253 genomes.

434 To identify mature Cab bacteriocin sequences, extracted sequences were scanned for open
435 reading frames (ORFs) of 100-300 nucleotides, beginning with an ATG start codon and ending with
436 a TAA, TAG or TGA stop codon. Only ORFs whose translated sequences contained a
437 (M/L/V)XXXXGG double-glycine cleavage motif were retained. Mature Cab bacteriocins were

438 obtained by removing the N-terminal signal sequence upstream of the cleavage site. To explore
439 diversity of Cab bacteriocins, sequences were converted into amino acid frequency vectors. Pairwise
440 dissimilarities between sequences were calculated using the Bray-Curtis metric (ScyPy), followed by
441 agglomerative hierarchical clustering (scikit-learn). To determine the optimal number of clusters,
442 silhouette scores (scikit-learn) were computed for cluster numbers ranging from 2 to 50. The number
443 of clusters yielding the highest score was selected as optimal.

444 To assess the prevalence of *cibABC* in *S. mitis*, the nucleotide sequence of *cibABC* (from *S.*
445 *pneumoniae* D39, GenBank Accession NC_008533.2) was aligned against all *S. mitis* genomes using
446 NCBI BLASTn. Genomes with no detectable hit were considered *cibABC*-negative. For genomes with
447 partial matches (<100% query coverage), the locus was manually inspected to verify the presence or
448 absence of *cibA*, *cibB*, and *cibC* individually – a common occurrence in strains harboring *cibC* but not
449 *cibAB*.

450 To find SigX boxes, the consensus sequence (58) was searched within *cab* loci using Find
451 Individual Motif Occurrences (FIMO) v5.5.8 (59). Hits with *p*-value <0.001 were considered true SigX
452 boxes. The detection of Cab bacteriocins and putative SigX boxes was benchmarked against six *S.*
453 *mitis* strains with complete genomes and manually curated *cab* loci (23, 60).

454

455 **Phylogeny of *S. mitis***

456 Core genome single-nucleotide polymorphisms (SNPs) were called using Snippy v4.6.0
457 (https://github.com/tseemann/snippy) by aligning *S. mitis* genomes to the *S. mitis* B6 reference
458 genome. The resulting alignment was used to construct a maximum-likelihood phylogenetic tree with
459 FastTree v2.2 (61). The phylogeny was visualized and annotated using the Interactive Tree of Life
460 (iTOL) platform (62).

461

462 **Synthetic peptides**

463 Peptides were produced by solid-phase peptide synthesis with >95% purity (NZYTech) (*SI Appendix*,
464 Table S2) (23, 43-45). CSP and $BlpC_1$ pheromones were resuspended in sterile ddH_2O; $BlpC_4$ was

465 resuspended in 10% acetic acid; and CabA and CabB were resuspended in DMSO. Peptides were
466 serially diluted in sterile ddH_2O and stored at -20ºC.
467
468 **Transformation**
469 For transformation of *S. mitis* and *S. pneumoniae*, cells were grown to an OD_{600} of 0.5, diluted 1:100
470 in pre-warmed $C+Y_{YB}$ and grown until an OD_{600} of 0.04-0.1. Cells were treated with 1 µM of cognate
471 CSP and transformed with 0.4 µg linear DNA, 1 µg plasmid DNA, or 10 µg chromosomal DNA.
472 Transformants were recovered for 4 h and plated in selective medium. Linear, plasmid and genomic
473 DNA were purified using the Zymoclean Gel DNA Recovery Kit (Zymo Research), ZymoPURE
474 Plasmid Miniprep Kit (Zymo Research) and EZ1 DSP Virus Kit (Qiagen), respectively.
475 For heat-shock transformation of *E. coli* DH10B or DH5α, $CaCl_2$-competent cells were mixed
476 with 10% (v/v) of ligation reactions and incubated on ice for 15 min. Cells were then heat-shocked at
477 42ºC for 40 s, immediately chilled on ice, and recovered with 900 µL of SOC (2% tryptone, 0.5% yeast
478 extract, 10 mM NaCl, 2.5 mM KCl, 10 mM $MgCl_2$, 10 mM $MgSO_4$ and 20 mM glucose; pH 7) for 1 h
479 before plating in selective medium.
480
481 **Construction of a fluorescence-luminescence transcriptional reporter**
482 A DNA cassette containing a *hlpA-mNeonGreen* fusion and plasmid pBIR, which integrates in the
483 genome of *S. mitis* G22 and *S. pneumoniae* D39, were synthesized (Twist Bioscience). The reporter
484 cassette and plasmid were amplified and blunt end ligated to generate plasmid pJB10. The firefly
485 luciferase *luc* (from pPEP-LGZ) and plasmid pJB10 were amplified and blunt-end ligated to create
486 plasmid pJB11 encoding a dual fluorescence-luminescence reporter. Transcriptional fusions were
487 created by digesting both pJB11 and promoter fragments with BsaI, followed by ligation. Variants of
488 pJB11 were linearized with BamHI and transformed into *S. mitis* G22 or *S. pneumoniae* D39.
489 Transformants were selected in BA with chloramphenicol.
490
491 **Expression of *cabABC* and other competence genes**

492 *S. mitis* and *S. pneumoniae* strains harboring transcriptional fusions of competence promoters were
493 grown in C+Y_{YB} at pH 6.6 (to prevent natural competence induction) until an OD_{600} of 0.5. To evaluate
494 natural competence dynamics, acidic precultures were diluted 1:100 in C+Y_{YB} (pH 6.6, 7.4 or 8.2)
495 containing 340 µg/mL D-luciferin (Abcam). To assess the effect of different pheromones on
496 competence induction, acidic precultures were diluted to OD_{600} = 0.1 in C+Y_{YB} (pH 6.6) with 340 µg/mL
497 D-luciferin. Then, CSP or BlpC variants (up to 1 µM), were added. Cultures were transferred to white
498 96-well plates with clear bottoms (Nunc). The OD_{595} and luminescence was recorded every 10 min
499 for 24 h in a BioTek Neo2 Multimode Reader with a gain of 185. Luminescence values were
500 normalized to the OD_{595}. D-luciferin was resuspended in sterile ddH_2O to 15 $mg.mL^{-1}$ and kept at -80
501 ºC in single-use aliquots.
502
503 **Construction of ComE, SigX1 and SigX2 deletion mutants**
504 The upstream and downstream flanking regions of *comE, sigX1, sigX2* were amplified from *S. mitis*
505 G22 gDNA. Kanamycin and spectinomycin resistance genes were amplified from pKan and pPEP-
506 LGZ (63), respectively. DNAs were ligated using Gibson Assembly (New England Biolabs) and
507 amplified with nested primers. Transformants were selected in BA with kanamycin (for *comE* and
508 *sigX1*) or spectinomycin (for *sigX2*).
509
510 **Biofilms and transwells**
511 *S. mitis* and *S. pneumoniae* were grown to exponential phase and mixed at a 1:1 ratio (10^5 CFU of
512 each strain) in C+Y_{YB} with 1600 $U.mL^{-1}$ catalase. Two milliliters of the mixtures were added to tissue-
513 culture treated 12-well plates (Corning) and incubated 24 h at 34ºC with 5% CO_2. Non-adherent cells
514 were removed by aspiration, and biofilms were thoroughly resuspended in PBS.
515 For transwell biofilms, 1.5 mL of C+Y_{YB} containing catalase and 10^5 CFU of *S. pneumoniae*
516 was added to wells of tissue-culture treated 12-well plates. Transwell inserts containing a 0.4 µm pore
517 polycarbonate membrane (Corning) were placed in the wells, and 0.5 mL of C+Y_{YB} with catalase and
518 10^5 CFU of *S. mitis* were added to the upper insert. Biofilms were recovered from both compartments.

519 In dual-species biofilms, *S. pneumoniae* and *S. mitis* cells were enumerated by plating on BA
520 with chloramphenicol or kanamycin, respectively. In the transwell setup, where *S. pneumoniae* and
521 *S. mitis* were physically separated, biofilm suspensions from both compartments were also plated on
522 selective media to confirm that neither strain had crossed the membrane.
523
524 **Construction of an *S. mitis cab* overexpressor mutant**
525 The plasmid backbone was amplified from pDL278_P23-DsRed-Express2 (Addgene plasmid
526 #121505), and *cabABC* was amplified from *S. mitis* G22 gDNA. The two fragments were blunt-end
527 ligated, generating plasmid pJB09-*cabABC*, in which *cabABC* is placed under the control of the strong
528 constitutive P23 promoter. *S. mitis* transformants were selected in BA with spectinomycin.
529
530 **Inhibitory activity of cell-free supernatants and heat-killed cells**
531 *S. mitis* was grown to early stationary phase and centrifuged at 10,000 g for 30 min at 4ºC. Cell-free
532 supernatants (CFS) were obtained by filtration (0.22 µm). CFS were lyophilized by vacuum
533 evaporation using a SpeedVac concentrator (LabConco) and resuspended in ddH_2O to a
534 concentration of 10x before testing. $C+Y_{YB}$ medium was concentrated in parallel and used as a
535 negative control for inhibitory activity. Cell pellets were washed once in PBS and heat-killed for 15
536 min at 95 ºC. Complete lysis of pellet extracts was confirmed by plating in BA.
537 To test for inhibitory activity of CFS and heat-killed cells, *S. pneumoniae* D39 was grown to
538 an OD_{600} of 0.5, diluted 1:100 in fresh medium, and 180 µL of the dilution was added to clear 96-well
539 plates. Twenty microliters of treatments or water was added to each well and growth was monitored
540 by measuring the OD_{595} every 30 min for 24 h using a Tecan Infinite 200 Pro.
541
542 **Sensitivity of bacteria to CabAB**
543 Exponential-phase cultures of bacterial species (18 *Streptococcus* spp., four additional non-
544 streptococcal Gram-positive species, and four Gram-negative species) were diluted to OD_{600} 0.1 and
545 195 µL was added to wells of clear 96-well plates. CabAB (0.975 µM) or DMSO (0.00975%) was
546 added to wells and growth was recorded by measuring the OD_{595} every 10 min for 24 h using the

547 Tecan Infinite 200. Growth arrest was quantified by comparing the area under the curve (AUC)
548 between CabAB- and DMSO-treated cultures. All further assays using CabAB and DMSO treatments
549 were performed in the same conditions, unless specified otherwise.
550
551 **Construction of autolysis-deficient *S. pneumoniae* mutants**
552 The upstream and downstream regions of *lytA* and *lytC* were amplified from *S. pneumoniae* D39
553 gDNA. The PhunSweet cassette containing *pheS-sacB*-aph*A-3* which confers susceptibility to
554 chlorinated phenylalanine and sucrose, and resistance to kanamycin, was amplified from *S.*
555 *pneumoniae* D39 Δ*cps*::*PhunSweet* gDNA (64). DNAs were assembled using Gibson Assembly and
556 amplified with nested primers. *S. pneumoniae* D39 transformants were selected on BA with
557 kanamycin.
558 To remove the antibiotic resistance cassette, the flanking regions of *lytA* and *lytC* were
559 amplified, assembled with Gibson Assembly, and amplified with nested primers. Transformants were
560 recovered by counterselection on BA with 15 mM chlorinated phenylalanine and 10% sucrose.
561
562 **Scanning electron microscopy (SEM)**
563 *S. pneumoniae* D39 cultures (30 mL) were treated with DMSO or CabAB and incubated for 15 min at
564 37ºC. Cells were harvested by centrifugation (all centrifugations were carried out at 800 g for 10 min
565 at room temperature) and washed three times with PBS. Fixation was performed in 500 μL of 2.5%
566 glutaraldehyde and 1% paraformaldehyde in 0.1 M sodium cacodylate buffer for 30 min at room
567 temperature. Cells were washed three times with 0.1 M sodium cacodylate buffer and dehydrated in
568 increasingly higher ethanol concentrations (50%, 70%, 90%, 100%), by incubating 10 min in 500 μL
569 of each ethanol concentration. Ethanol was replaced with 500 μL tert-butyl alcohol and samples were
570 incubated at 30ºC for 1 h. Then, tert-butyl was removed and replaced with 500 μL of fresh tert-butyl
571 alcohol. Samples were kept at -20ºC overnight. Samples were then lyophilized under vacuum, gold-
572 sputtered using a Cressington 108 sputter coater, and imaged with a Hitachi SU-8010 scanning
573 electron microscope at 1.5kV.

574

575 **Transmission electron microscopy (TEM)**

576 *S. pneumoniae* D39 cultures (30 mL) were treated with DMSO or CabAB, incubated for 15 min at
577 37ºC, and recovered by centrifugation at 800 g. Cells were fixed with 2% formaldehyde, 2.5%
578 glutaraldehyde, 0.075% ruthenium red and 1.55 % lysine acetate in distilled water for 20 min at 4ºC.
579 Cells were washed twice in 0.075% ruthenium red, resuspended in 2% formaldehyde, 2.5%
580 glutaraldehyde and 0.075% ruthenium red, and incubated overnight at 4ºC. Cells were washed three
581 times with 0.075% ruthenium red and further processed at Instituto Gulbenkian de Ciência. Cells were
582 embedded in 2% low-melting point agarose and fixed with 1% osmium tetroxide and 0.06% ruthenium
583 red for 1 h at room temperature. Cells were washed once with 0.1 M sodium cacodylate buffer and
584 twice with distilled water. Dehydration was performed on ice using increasing concentrations of
585 ethanol (10%, 30%, 50%; 10 min each). Samples were stained overnight at 4ºC with 2% uranyl
586 acetate in 70% ethanol, followed by further dehydration with 90% ethanol and three times with 100%
587 ethanol. Infiltration was carried out with increasing concentrations of epoxy resin in ethanol (3:1, 1:1,
588 1:3), and 100% resin overnight, followed by two exchanges of 100% resin. Ultrathin sections were cut
589 and imaged on a Tecnai G2 Spirit BioTWIN Transmission Electron Microscope (FEI) equipped with
590 an Olympus-SIS Veleta CCD camera.

591 Large intracellular aggregates were observed in some CabAB-treated cells. To quantify these
592 structures, micrographs of CabAB- and DMSO-treated cells were blindly evaluated by two
593 researchers. Each researcher was first shown representative cells with and without aggregates, and
594 then independently counted the number of cells containing these structures. The final percentage of
595 cells with aggregates was calculated as the average between both researcher counts.

596

597 **Permeabilization and depolarization of *S. pneumoniae* membranes**

598 *S. pneumoniae* D39 cultures were treated with DMSO or CabAB. One-milliliter aliquots were taken at
599 0, 2, 5, 15, 30, 60, and 120 min post treatment and immediately chilled on ice. Cells were washed
600 twice with PBS and kept on ice. Cells were stained with 6 μM propidium iodine (Invitrogen) and 3 μM
601 $DiBAC_4(3)$ (Enzo Life Sciences) for 5 min at room temperature, protected from light. Cells were

602 centrifuged, resuspended in PBS, and added to black 96-well plates with clear bottoms (Nunc).
603 Fluorescence intensity was measured using a BioTek Neo2 Multimode Reader under the following
604 settings: shake for 5 s; propidium iodine – top reading, 535 ± 12 nm excitation, 617 ± 12 nm emission
605 and 120 gain; $DiBAC_4(3)$ – top reading, 492 ± 9 nm excitation, 518 ± 9 emission, 120 gain).
606 Fluorescent values were normalized to the OD_{595}.
607
608 **Efflux of ATP**
609 Cultures of *S. pneumoniae* were treated with DMSO or CabAB. Aliquots were taken at 0, 15 and 120
610 min post-treatment and kept on ice. Cells were centrifuged, and supernatants were filtered (0.22 µm)
611 and maintained on ice. Cells were permeabilized in DMSO for 10 min at room temperature. Both cells
612 and supernatants were diluted 1:10 in ddH_2O and kept on ice.
613 Extracellular and intracellular ATP was measured with the ATP Luminescent Cell Viability
614 Assay (Millipore) according to instructions. Luminescence was measured in a BioTek Neo2 Multimode
615 Reader using a gain of 150 and integration time of 10 s. An ATP standard curve confirmed linear
616 detection within the range of 0.2 µM to 2 mM ATP. Total ATP was calculated by summing
617 luminescence values from both the cell and supernatant fractions under each condition.
618
619 **Construction of *S. mitis* harboring HA-tagged bacteriocins**
620 DNAs containing HA (YPYDVPDYA)-tagged *cabA* and *cabB* were synthesized (Twist Bioscience).
621 The regions upstream (including the native promoter) and downstream (including a chloramphenicol
622 resistance cassette) of the *cab* operon were amplified from pJB11-*cabABC*. DNAs were assembled
623 by Gibson Assembly and amplified with nested primers. The resulting constructs were transformed
624 into the *S. mitis* Δ*cabABC* background, generating two mutant strains: *cabA-HA cabBC* and *cabA*
625 *cab-HA cabC.* Transformants were selected in BA with chloramphenicol.
626
627 **Confocal microscopy and immunofluorescence**

628 To quantify the percentage of cells that become membrane-permeable, *S. pneumoniae* was treated
629 with DMSO or CabAB. Cells were recovered by centrifugation (9600 g, 4ºC, 3 min) and washed three
630 times with PBS. Cells were stained with 30 µM propidium iodine and 5 µM SYTO 9 for 15 min at room
631 temperature, protected from light.

632 To determine whether large intracellular structures observed in CabAB-treated *S. pneumoniae*
633 cells corresponded to membranes, treated cells were washed three times with PBS and stained with
634 20 $\mu g.mL^{-1}$ FM4-64 and 15 $\mu g.mL^{-1}$ DAPI for 5 min at room temperature, protected from light.

635 For immunofluorescence of live competent bacteria, *S. mitis* harboring HA-tagged bacteriocins
636 were grown in acidic $C+Y_{YB}$ and diluted to OD_{600} = 0.1 in pre-warmed $C+Y_{YB}$. CSP_{G22} was added at 1
637 µM, and cells were incubated for 70 min at 37ºC and then chilled on ice. To retain the competent
638 status of cells, all subsequent steps were performed on ice using ice-cold solutions. Cells were
639 centrifuged (9600 g, 4ºC, 3 min) and washed twice in PBS. Blocking was performed in PBS with 5%
640 bovine serum albumin (BSA) for 1 h. Cells were pelleted and resuspended in 100 µL of primary rabbit
641 monoclonal anti-HA antibody (clone C29F4; Cell Signaling Technology) diluted 1:100 in PBS with 1%
642 BSA, and incubated for 1 h. Cells were washed twice in PBS with 0.1% Tween 20, resuspended in
643 100 µL of Alexa Fluor 488-conjugated goat anti-rabbit secondary antibody (Invitrogen) diluted 1:500
644 in PBS with 1% BSA, and incubated 1 h protected from light. Cells were washed twice with PBS
645 containing 0.1% Tween 20 and once with PBS. Cells were then stained with 20 $\mu g.mL^{-1}$ FM4-64 and
646 15 $\mu g.mL^{-1}$ DAPI for 5 at room temperature, covered from light.

647 Immediately before imaging, cells were mounted on thin 1.7% agarose pads. Fluorescence
648 imaging was performed using a Zeiss LSM 880 point scanning confocal microscope equipped with
649 an Airyscan detector. Samples were imaged with a Plan-Apochromat 63x/1.4 Oil DIC M27 objective
650 (Zeiss), using laser lines 405 nm (DAPI), 488 nm (SYTO 9 and Alexa Fluor 488), and 561 nm (FM4-
651 64 and propidium iodine). Imaging was performed at laser intensities of 2-3% and a gain of 700 for
652 DAPI, 700 for SYTO 9, 1000 for Alexa Fluor 488, 900 for FM4-64, and 700 for propidium iodine. The
653 Zeiss Zen v3.0 was used to control the microscope and for Airyscan processing. Image analysis was
654 conducted using ImageJ/FIJI v2.14 (65).
655

656 **Construction of a transformation-deficient *S. pneumoniae* mutant**

657 The upstream and downstream regions of *comGC* were amplified from *S. pneumoniae* D39 gDNA,
658 and *tetM* was amplified from *S. mitis* F22 gDNA. DNAs were ligated by Gibson Assembly and
659 amplified using nested primers. *S. pneumoniae* transformants were selected in BA with tetracycline.

660

661 **Horizontal gene transfer in biofilms**

662 Dual-species biofilms of *S. pneumoniae* D39-GFP Δ*comGC* (chloramphenicol and tetracycline
663 resistant; Chl^R Tet^R) and *S. mitis* (kanamycin resistant; Kan^R) were grown as described above, except
664 that $C+Y_{YB}$ was adjusted to pH 6.6 to prevent natural competence induction. After 24h, non-adherent
665 cells were removed by aspiration, and 2 mL of fresh $C+Y_{YB}$ (pH 7.4) containing catalase and 1 μM of
666 CSP_{G22} were added to biofilms. After 6 h of incubation at 34ºC with 5% CO_2, biofilm cells were
667 thoroughly resuspended in PBS and recovered by centrifugation.

668 Cells were plated on the following selective media: (i) BA with kanamycin to quantify total *S.*
669 *mitis* (Kan^R); (ii) BA with kanamycin and chloramphenicol to detect *S. mitis* transformants that have
670 acquired chloramphenicol resistance (Kan^R Chl^R), either with or without tetracycline resistance; (iii)
671 BA with kanamycin and tetracycline to detect *S. mitis* transformants that acquired tetracycline
672 resistance (Kan^R Tet^R), either with or without chloramphenicol resistance; (iv) BA with kanamycin,
673 chloramphenicol and tetracycline to identify *S. mitis* transformants that acquired both resistances
674 (Kan^R Chl^R Tet^R); (v) and BA with chloramphenicol and tetracycline (without kanamycin) to detect *S.*
675 *pneumoniae* loads.

676 Transformants were counted after 48 h of incubation. *S. mitis* transformation frequencies were
677 calculated as the ratio between the number of transformants (Kan^R colonies also resistant to
678 chloramphenicol and/or tetracycline) and the total number of Kan^R colonies. *S. mitis* G22 Δ*comE* was
679 used as a non-transformable control, in which acquisition of chloramphenicol and tetracycline
680 resistance should not occur via transformation.

681

682 **Statistical analyses**

683 The two-tailed unpaired *Mann-Whitney U* test with Benjamini and Hochberg correction for FDR was
684 used to compare bacterial loads. Student's *t*-test with Benjamini and Hochberg correction for FDR
685 was used to compare gene expression. The ratio paired *t*-test was used for the statistical analysis of
686 bacterial proportions in multi-species biofilms. All statistical analysis were computed using GraphPad
687 Prism 9.0 and considered significant at *P*-value ≤0.05.
688
689 **Data availability**
690 All data is available from the corresponding author upon reasonable request.
691
692 **Acknowledgements**
693 We are grateful to Jan-Willem Veening (University of Lausanne) and Morten Kjos (Norwegian
694 University of Life Sciences) for providing plasmids pPEP-LGZ and Jason Rosch (St. Jude Children's
695 Research Hospital) for providing *S. pneumoniae* strain harboring a PhunSweet cassette. We also
696 acknowledge Luisa N. Hiller (Carnegie Mellon University) and Adriano O. Henriques (ITQB NOVA)
697 for fruitful discussions.
698
699 **Funding**
700 This work was supported by FCT – Fundação para a Ciência e Tecnologia, I.P., through project
701 STOPneumo (PTDC/BIA-MIC/30703/2017), MOSTMICRO-ITQB R&D Unit (UIDB/04612/2020,
702 UIDP/04612/2020), LS4FUTURE Associated Laboratory (LA/P/0087/2020), and PPBI - Portuguese
703 Platform of BioImaging (PPBI-POCI-01-0145-FEDER-022122) co-funded by national funds from OE
704 - "Orçamento de Estado" and by european funds from FEDER - "Fundo Europeu de Desenvolvimento
705 Regional". J. Borralho and J. Lança were supported by PhD fellowships (2021.07866.BD -
706 doi.org/10.54499/2021.07866.BD and UI/BD/153385/2022 - doi.org/10.54499/UI/BD/153385/2022).
707
708 **References**
709 1. F. Griffith, The significance of pneumococcal types. *J Hyg (Lond)* **27**, 113-159 (1928).

710 2. L. S. Håvarstein, G. Coomaraswamy, D. A. Morrison, An unmodified heptadecapeptide
711 pheromone induces competence for genetic transformation in *Streptococcus pneumoniae*.
712 *Proc Natl Acad Sci U S A* **92**, 11140-11144 (1995).
713 3. L. S. Håvarstein, P. Gaustad, I. F. Nes, D. A. Morrison, Identification of the streptococcal
714 competence-pheromone receptor. *Mol Microbiol* **21**, 863-869 (1996).
715 4. F. M. Hui, D. A. Morrison, Genetic transformation in *Streptococcus pneumoniae*: nucleotide
716 sequence analysis shows *comA*, a gene required for competence induction, to be a member
717 of the bacterial ATP-dependent transport protein family. *J Bacteriol* **173**, 372-381 (1991).
718 5. E. V. Pestova, L. S. Håvarstein, D. A. Morrison, Regulation of competence for genetic
719 transformation in *Streptococcus pneumoniae* by an auto-induced peptide pheromone and a
720 two-component regulatory system. *Mol Microbiol* **21**, 853-862 (1996).
721 6. M. S. Lee, D. A. Morrison, Identification of a new regulator in *Streptococcus pneumoniae*
722 linking quorum sensing to competence for genetic transformation. *J Bacteriol* **181**, 5004-5016
723 (1999).
724 7. S. N. Peterson *et al.*, Identification of competence pheromone responsive genes in
725 *Streptococcus pneumoniae* by use of DNA microarrays. *Mol Microbiol* **51**, 1051-1070 (2004).
726 8. S. Guiral, T. J. Mitchell, B. Martin, J. P. Claverys, Competence-programmed predation of
727 noncompetent cells in the human pathogen *Streptococcus pneumoniae*: genetic
728 requirements. *Proc Natl Acad Sci U S A* **102**, 8710-8715 (2005).
729 9. O. Johnsborg, V. Eldholm, M. L. Bjørnstad, L. S. Håvarstein, A predatory mechanism
730 dramatically increases the efficiency of lateral gene transfer in *Streptococcus pneumoniae* and
731 related commensal species. *Mol Microbiol* **69**, 245-253 (2008).
732 10. P. Shen, J. A. Lees, G. C. W. Bee, S. P. Brown, J. N. Weiser, Pneumococcal quorum sensing
733 drives an asymmetric owner-intruder competitive strategy during carriage via the competence
734 regulon. *Nat Microbiol* **4**, 198-208 (2019).
735 11. J. Hohwy, J. Reinholdt, M. Kilian, Population dynamics of *Streptococcus mitis* in its natural
736 habitat. *Infect Immun* **69**, 6055-6063 (2001).

737 12. G. Salvadori, R. Junges, D. A. Morrison, F. C. Petersen, Competence in *Streptococcus*
738 *pneumoniae* and close commensal relatives: mechanisms and implications. *Front Cell Infect*
739 *Microbiol* **9**, 94 (2019).
740 13. G. Salvadori *et al.*, High-resolution profiles of the *Streptococcus mitis* CSP signaling pathway
741 reveal core and strain-specific regulated genes. *BMC Genomics* **19**, 453 (2018).
742 14. E. Potgieter, L. J. Chalkley, Relatedness among penicillin-binding protein 2b genes of
743 *Streptococcus mitis*, *Streptococcus oralis*, and *Streptococcus pneumoniae*. *Microb Drug*
744 *Resist* **1**, 35-42 (1995).
745 15. R. Hakenbeck, Transformation in *Streptococcus pneumoniae*: mosaic genes and the
746 regulation of competence. *Res Microbiol* **151**, 453-456 (2000).
747 16. F. C. Lessa *et al.*, *Streptococcus mitis* expressing pneumococcal serotype 1 capsule. *Sci Rep*
748 **8**, 17959 (2018).
749 17. F. Pimenta *et al.*, *Streptococcus infantis*, *Streptococcus mitis*, and *Streptococcus oralis* strains
750 with highly similar *cps5* loci and antigenic relatedness to serotype 5 pneumococci. *Front*
751 *Microbiol* **9**, 3199 (2018).
752 18. F. Ganaie, A. R. Branche, M. Peasley, J. W. Rosch, M. H. Nahm, Effect of oral streptococci
753 expressing pneumococcus-like cross-reactive capsule types on World Health Organization
754 recommended pneumococcal carriage detection procedure. *Clin Infect Dis* **75**, 647-656
755 (2022).
756 19. A. Kalizang'oma *et al.*, Population genomics of *Streptococcus mitis* in UK and Ireland
757 bloodstream infection and infective endocarditis cases. *Nat Commun* **15**, 7812 (2024).
758 20. U. B. Skov Sørensen, K. Yao, Y. Yang, H. Tettelin, M. Kilian, Capsular polysaccharide
759 expression in commensal *Streptococcus* species: genetic and antigenic similarities to
760 *Streptococcus pneumoniae*. *mBio* **7** (2016).
761 21. D. Denapaite *et al.*, The genome of *Streptococcus mitis* B6 - what is a commensal? *PLoS One*
762 **5**, e9426 (2010).

763 22. L. N. Ikryannikova *et al.*, Inhibitory effect of streptococci on the growth of *M. catarrhalis* strains
764 and the diversity of putative bacteriocin-like gene loci in the genomes of *S. pneumoniae* and
765 its relatives. *AMB Express* **7**, 218 (2017).
766 23. J. Borralho *et al.*, Inhibition of pneumococcal growth and biofilm formation by human isolates
767 of *Streptococcus mitis* and *Streptococcus oralis*. *Appl Environ Microbiol* **91**, e0133624 (2025).
768 24. S. Lehtinen, N. J. Croucher, F. Blanquart, C. Fraser, Epidemiological dynamics of bacteriocin
769 competition and antibiotic resistance. *Proc Biol Sci* **289**, 20221197 (2022).
770 25. H. Sati *et al.*, The WHO Bacterial Priority Pathogens List 2024: a prioritisation study to guide
771 research, development, and public health strategies against antimicrobial resistance. *Lancet*
772 *Infect Dis* **25**, 1033-1043 (2025).
773 26. M. Kilian *et al.*, Evolution of *Streptococcus pneumoniae* and its close commensal relatives.
774 *PLoS One* **3**, e2683 (2008).
775 27. G. Pozzi *et al.*, Competence for genetic transformation in encapsulated strains of
776 *Streptococcus pneumoniae*: two allelic variants of the peptide pheromone. *J Bacteriol* **178**,
777 6087-6090 (1996).
778 28. I. F. Nes, D. B. Diep, H. Holo, Bacteriocin diversity in *Streptococcus* and *Enterococcus*. *J*
779 *Bacteriol* **189**, 1189-1198 (2007).
780 29. J. Meza-Torres *et al.*, Listeriolysin S: A bacteriocin from *Listeria monocytogenes* that induces
781 membrane permeabilization in a contact-dependent manner. *Proc Natl Acad Sci U S A* **118**,
782 e2108155118 (2021).
783 30. L. García-Bayona, M. S. Guo, M. T. Laub, Contact-dependent killing by
784 *Caulobacter crescentus* via cell surface-associated, glycine zipper proteins. *Elife* **6** (2017).
785 31. C. Oppegård, J. Schmidt, P. E. Kristiansen, J. Nissen-Meyer, Mutational analysis of putative
786 helix-helix interacting GxxxG-motifs and tryptophan residues in the two-peptide bacteriocin
787 lactococcin G. *Biochemistry* **47**, 5242-5249 (2008).
788 32. B. Ekblad *et al.*, Structure-function analysis of the two-peptide bacteriocin plantaricin EF.
789 *Biochemistry* **55**, 5106-5116 (2016).

790 33. B. Ekblad, P. E. Kristiansen, NMR structures and mutational analysis of the two peptides
791 constituting the bacteriocin plantaricin S. *Sci Rep* **9**, 2333 (2019).
792 34. G. Moll *et al.*, Lactococcin G is a potassium ion-conducting, two-component bacteriocin. *J*
793 *Bacteriol* **178**, 600-605 (1996).
794 35. O. McAuliffe *et al.*, Lacticin 3147, a broad-spectrum bacteriocin which selectively dissipates
795 the membrane potential. *Appl Environ Microbiol* **64**, 439-445 (1998).
796 36. G. N. Moll *et al.*, Complementary and overlapping selectivity of the two-peptide bacteriocins
797 plantaricin EF and JK. *J Bacteriol* **181**, 4848-4852 (1999).
798 37. X. Zhang *et al.*, Two-peptide bacteriocin PlnEF causes cell membrane damage to
799 Lactobacillus plantarum. *Biochim Biophys Acta* **1858**, 274-280 (2016).
800 38. H. Wei, L. S. Håvarstein, Fratricide is essential for efficient gene transfer between
801 pneumococci in biofilms. *Appl Environ Microbiol* **78**, 5897-5905 (2012).
802 39. H. Steinmoen, E. Knutsen, L. S. Håvarstein, Induction of natural competence in *Streptococcus*
803 *pneumoniae* triggers lysis and DNA release from a subfraction of the cell population. *Proc Natl*
804 *Acad Sci U S A* **99**, 7681-7686 (2002).
805 40. S. Peterson, R. T. Cline, H. Tettelin, V. Sharov, D. A. Morrison, Gene expression analysis of
806 the *Streptococcus pneumoniae* competence regulons by use of DNA microarrays. *J Bacteriol*
807 **182**, 6192-6202 (2000).
808 41. R. Rimini *et al.*, Global analysis of transcription kinetics during competence development in
809 *Streptococcus pneumoniae* using high density DNA arrays. *Mol Microbiol* **36**, 1279-1292
810 (2000).
811 42. E. García, Structure, function, and regulation of LytA: the N-acetylmuramoyl-L-alanine
812 amidase driving the "suicidal tendencies" of *Streptococcus pneumoniae-a review*.
813 *Microorganisms* **13**, 827 (2025).
814 43. A. M. Whatmore, V. A. Barcus, C. G. Dowson, Genetic diversity of the streptococcal
815 competence (*com*) gene locus. *J Bacteriol* **181**, 3144-3154 (1999).
816 44. M. Carrolo, F. R. Pinto, J. Melo-Cristino, M. Ramirez, Pherotypes are driving genetic
817 differentiation within *Streptococcus pneumoniae*. *BMC Microbiol* **9**, 191 (2009).

818 45. D. F. Vestrheim, P. Gaustad, I. S. Aaberge, D. A. Caugant, Pherotypes of pneumococcal
819 strains co-existing in healthy children. *Infect Genet Evol* **11**, 1703-1708 (2011).
820 46. R. A. Aras, J. Kang, A. I. Tschumi, Y. Harasaki, M. J. Blaser, Extensive repetitive DNA
821 facilitates prokaryotic genome plasticity. *Proc Natl Acad Sci U S A* **100**, 13579-13584 (2003).
822 47. D. Wang, S. Li, F. Guo, K. Ning, L. Wang, Core-genome scaffold comparison reveals the
823 prevalence that inversion events are associated with pairs of inverted repeats. *BMC Genomics*
824 **18**, 268 (2017).
825 48. T. J. Treangen, A. L. Abraham, M. Touchon, E. P. Rocha, Genesis, effects and fates of repeats
826 in prokaryotic genomes. *FEMS Microbiol Rev* **33**, 539-571 (2009).
827 49. C. Bogaardt, A. J. van Tonder, A. B. Brueggemann, Genomic analyses of pneumococci reveal
828 a wide diversity of bacteriocins - including pneumocyclicin, a novel circular bacteriocin. *BMC*
829 *Genomics* **16**, 554 (2015).
830 50. J. S. Puls *et al.*, *Staphylococcus epidermidis* bacteriocin A37 kills natural competitors with a
831 unique mechanism of action. *ISME J* **18**, wrae044 (2024).
832 51. S. Borgeaud, L. C. Metzger, T. Scrignari, M. Blokesch, The type VI secretion system of *Vibrio*
833 *cholerae* fosters horizontal gene transfer. *Science* **347**, 63-67 (2015).
834 52. L. Zhu, Z. Kuang, B. A. Wilson, G. W. Lau, Competence-independent activity of pneumococcal
835 EndA mediates degradation of extracellular DNA and nets and is important for virulence. *PLoS*
836 *One* **8**, e70363 (2013).
837 53. G. Salvadori, R. Junges, D. A. Morrison, F. C. Petersen, Overcoming the barrier of low
838 efficiency during genetic transformation of *Streptococcus mitis*. *Front Microbiol* **7**, 1009 (2016).
839 54. L. A. Cowley *et al.*, Evolution via recombination: cell-to-cell contact facilitates larger
840 recombination events in *Streptococcus pneumoniae*. *PLoS Genet* **14**, e1007410 (2018).
841 55. L. R. Marks, R. M. Reddinger, A. P. Hakansson, High levels of genetic recombination during
842 nasopharyngeal carriage and biofilm formation in *Streptococcus pneumoniae*. *mBio* **3**,
843 e00200-12 (2012).

844 56. J. Majewski, P. Zawadzki, P. Pickerill, F. M. Cohan, C. G. Dowson, Barriers to genetic
845 exchange between bacterial species: *Streptococcus pneumoniae* transformation. *J Bacteriol*
846 **182**, 1016-1023 (2000).
847 57. K. E. Stevens, D. Chang, E. E. Zwack, M. E. Sebert, Competence in *Streptococcus*
848 *pneumoniae* is regulated by the rate of ribosomal decoding errors. *mBio* **2**, e00071-11 (2011).
849 58. E. A. Campbell, S. Y. Choi, H. R. Masure, A competence regulon in *Streptococcus*
850 *pneumoniae* revealed by genomic analysis. *Mol Microbiol* **27**, 929-939 (1998).
851 59. C. E. Grant, T. L. Bailey, W. S. Noble, FIMO: scanning for occurrences of a given motif.
852 *Bioinformatics* **27**, 1017-1018 (2011).
853 60. S. Handem, B. Ferreira, C. Valente, R. Sá-Leão, Genomic and functional insights into
854 commensal streptococci with anti-pneumococcal activity. *BMC Genomics* **26**, 577 (2025).
855 61. M. N. Price, P. S. Dehal, A. P. Arkin, FastTree 2--approximately maximum-likelihood trees for
856 large alignments. *PLoS One* **5**, e9490 (2010).
857 62. I. Letunic, P. Bork, Interactive Tree of Life (iTOL) v6: recent updates to the phylogenetic tree
858 display and annotation tool. *Nucleic Acids Res* **52**, W78-W82 (2024).
859 63. M. Kjos *et al.*, Expression of *Streptococcus pneumoniae* bacteriocins is induced by antibiotics
860 via regulatory interplay with the competence system. *PLoS Pathog* **12**, e1005422 (2016).
861 64. H. Echlin, J. W. Rosch, Advancing genetic tools in *Streptococcus pneumoniae*. *Genes (Basel)*
862 **11**, 965 (2020).
863 65. J. Schindelin *et al.*, Fiji: an open-source platform for biological-image analysis. *Nat Methods*
864 **9**, 676-682 (2012).
865

866 **Figure Legends**

867 **Fig. 1.** *Streptococcus mitis* genomes encode a plethora of competence-associated bacteriocins (*cab*).
868 (A) Core-SNP phylogeny of 253 *S. mitis* genomes and distribution of competence-induced
869 bacteriocins A and B (*cibAB*), dedicated immunity (*cibC*), and competence-associated bacteriocin

870 (*cab*) genes. (B) Prevalence of CibAB and 95 Cab variants in the *S. mitis* population. (C) Rarefaction
871 analysis of mature Cab amino acid sequences found in the *S. mitis* population.
872
873 **Fig. 2.** Cab bacteriocins are expressed at the late phase of competence. (A) Genetic organization of
874 *cab* cluster of strain *S. mitis* G22, containing two putative bacteriocin (*cabAB*) and an immunity protein
875 (*cabC*) upstream of the ABC-transporter *comAB* genes. The *cabABC* operon promoter (P*cabABC*)
876 contains five tandem copies of SigX-binding sites (SigX box; SigX is the alternative sigma factor that
877 controls gene expression during the late phase of competence). (B) Expression of *cabABC* in *S. mitis*
878 G22 containing a P*cabABC*-luciferase (*luc*) reporter, ectopically inserted in its genome. Expression of
879 *cabABC* was inferred by expression of *luc*. *S. mitis* was pre-grown in acidic medium to avoid natural
880 competence development and synthetic cognate competence-stimulating peptide (CSP_{G22}) was
881 added to wild-type *S. mitis* and mutants lacking competence regulators. (C) Dose-response of
882 *cabABC* expression across CSP_{G22} concentrations for the *S. mitis luc* reporter containing either the
883 full-length P*cabABC* promoter (which contains five SigX boxes), or a truncated version containing
884 only the most proximal SigX box. (D) Number of SigX boxes within *cab* clusters of varied sizes. Data
885 in panels B and C represent three to four independent experiments. Unpaired *t*-tests were performed
886 to compare *cab* expression. **** $P < 0.0001$.
887
888 **Fig. 3.** *S. mitis* and *S. pneumoniae* crosstalk through production of distinct CSP pheromones. (A)
889 Effect of CSP pheromones of close streptococci on *cabABC* expression in *S. mitis* G22 and alignment
890 of tested CSP variants (purple – Q14 amino acid residue, present only in inducing peptides). *S. mitis*
891 G22 P*cabABC-luc* was pre-grown in acidic medium, to which exogenous CSP was added. (B) Effect
892 of CSP with substitutions in residue 14 in the activation of *cabABC* expression in *S. mitis* G22. (C)
893 Effect of CSP with substitutions in residue 14 in the activation of competence in *S. pneumoniae* of
894 pherotype CSP-1 (P*comCDE-luc*). Dotted lines represent average luminescence value for nontreated
895 controls. Experiments were repeated three times, independently. Unpaired *t*-tests were performed to
896 compare *cab* expression. **** $P < 0.0001$. ns not significant.

897

898 **Fig. 4.** *S. mitis* bacteriocins CabAB mediate contact-dependent growth inhibition of *S. pneumoniae*.
899 Experiments were done using *S. mitis* G22 Δ*blp4*Δ*blp1* and *S. pneumoniae* D39. The bacteriocin
900 clusters *blp4* and *blp1* were first deleted from the genome of *S. mitis* G22 as they have anti-
901 pneumococcal activity (23), which could obscure CabAB-mediated effects. (A) Proportion of *S. mitis*
902 and *S. pneumoniae* in dual-species biofilm grown for 24 h in competence-permissive conditions. *S.*
903 *mitis* mutant p(*cab*$^+$) contains the native *cabABC* copy, and an additional copy under constitutive
904 regulation (promoter *p23*) in a multicopy plasmid. (B) *S. mitis* was grown in competence-permissive
905 conditions. Cell-free supernatants (CFS) were recovered and cell pellets were boiled. CFS and heat-
906 killed cells were added to *S. pneumoniae* cultures and growth was monitored. (C) Bacterial loads of
907 *S. pneumoniae* grown in the presence of *S. mitis* in direct contact (left) or separated with a 0.4 μm
908 pore transwell membrane (right). (D) Corresponding bacterial loads of *S. mitis* G22 in experiment (C).
909 (E) Representative images of CabA-HA and CabB-HA immunodetection on the surface of live
910 competent *S. mitis* cells containing the native *cabABC* (negative control), *cabA-HA cabBC* or *cabA*
911 *cabB-HA cabC* genotypes. *S. mitis* cultures were induced with CSP_{G22}, incubated with a primary anti-
912 HA rabbit antibody, and then with an Alexa Fluor 488-conjugated goat anti-rabbit secondary antibody.
913 At least ten independent fields were detected per experiment/condition. Experiments were repeated
914 at least three times, independently. The ratio paired *t*-test was used to compare bacterial proportions
915 in dual-species biofilms. The two-tailed unpaired Mann-Whitney U test was used to compare bacterial
916 loads. ** $P < 0.01$. *** $P < 0.001$. ns not significant.

917

918 **Fig. 5.** CabAB is a two-peptide bacteriocin with LytA-dependent bactericidal activity against *S.*
919 *pneumoniae.* (A) *S. pneumoniae* was treated with synthetic CabA, CabB, an equimolar mixture of
920 CabA and CabB, or with DMSO (solvent where peptides were resuspended). Growth was recorded
921 for 24 h. (B) Presence of GxxxG and GxxxG-like amino acid motifs in CabA and CabB sequences.
922 (C) Exponential cultures of wild-type and autolysin-deficient *S. pneumoniae* were treated with DMSO
923 (grey) or synthetic CabAB (purple). Growth was recorded for 24 h. For easier visualization of lysis

924 (decrease in optical density), the first 12 h of growth is represented. Experiments were repeated three
925 times independently.
926
927 **Fig. 6.** CabAB leads to permeabilization and depolarization of *S. pneumoniae* membranes, leading
928 to metabolite leakage. (A) *S. pneumoniae* treated with DMSO or CabAB and imaged by scanning
929 electron microscopy (SEM). (B) Quantification of membrane-permeable *S. pneumoniae* (stained with
930 propidium iodine (PI)) upon treatment with DMSO or increasing concentrations of CabAB. (C-D)
931 Quantification of populational membrane permeability (C) and depolarization (D) upon DMSO or
932 CabAB treatment at several timepoints. (E) Proportion of extracellular *vs.* total ATP in wild-type and
933 Δ*lytA S. pneumoniae* cultures upon DMSO or CabAB treatment. (F) Representative transmission
934 electron microscopy (TEM) image and quantification of intracellular aggregates in DMSO- (n = 118
935 cells) or CabAB- treated *S. pneumoniae* (n = 138 cells). (G) Labeling of large intracellular aggregates
936 by membrane dye FM4-64 in CabAB-treated *S. pneumoniae*. SEM and TEM were done once. Other
937 data was taken from at least three independent experiments.
938
939 **Fig. 7.** Expression of *cabAB* facilitates horizontal gene transfer in dual-species biofilms. (A)
940 Experimental setup to study gene transfer in dual-species biofilms. The *S. pneumoniae* DNA donor is
941 nontransformable due to a *comGC* deletion, and contains chloramphenicol and tetracycline resistance
942 cassettes at opposite ends of the chromosome (Chl^R and Tet^R); the *S. mitis* DNA receiver is labeled
943 with a kanamycin resistance cassette (Kan^R); biofilms were pre-grown at a starting 1:1 ratio for 24 h
944 in acidic medium to prevent natural competence induction; cells were aspirated and fresh medium
945 containing CSP_{G22} was added to biofilms to transiently induce competence; after 6 h of incubation,
946 cells were plated; *S. mitis* transformants were recovered and counted by selection in plates with
947 kanamycin and combinations of chloramphenicol and/or tetracycline. (B-C) Acquisition of Chl^R and/or
948 Tet^R by *S. mitis* in biofilms containing purified donor gDNA (B) or the strain itself (C). (D) Growth
949 inhibition and lysis of 26 bacterial species when treated with CabAB *vs.* DMSO during their
950 exponential phase. Growth was recorded for 24 h. Lysis is shown when a decrease from the initial
951 culture optical density was observed in all replicates. Experiments were repeated three times,

952 independently. Transformation efficiencies were compared using unpaired *t*-tests. LOD limit of

953 detection. * $P < 0.05$. ** $P < 0.01$.

954

Figure 1

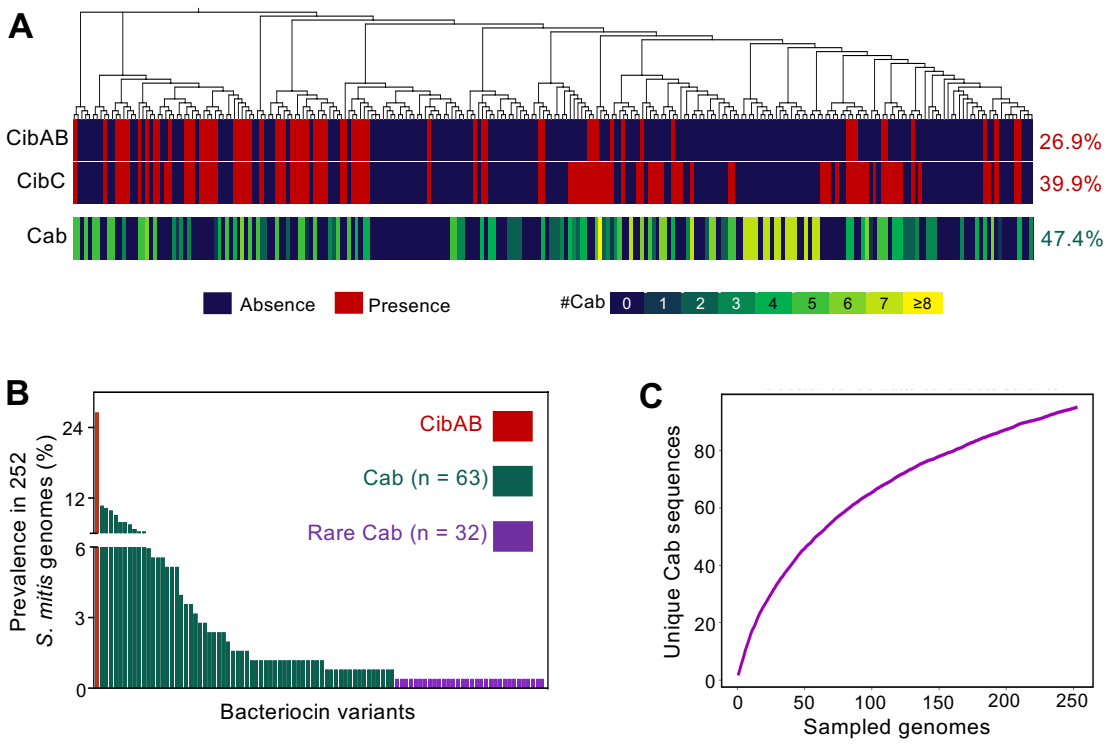
A
CibAB
CibC
Cab
26.9%
39.9%
47.4%
Absence
Presence
#Cab
0
1
2
3
4
5
6
7
≥8
B
Prevalence in 252 S. mitis genomes (%)
24
12
6
3
0
CibAB
Cab (n = 63)
Rare Cab (n = 32)
Bacteriocin variants
C
Unique Cab sequences
80
60
40
20
0
0
50
100
150
200
250
Sampled genomes

Figure 2

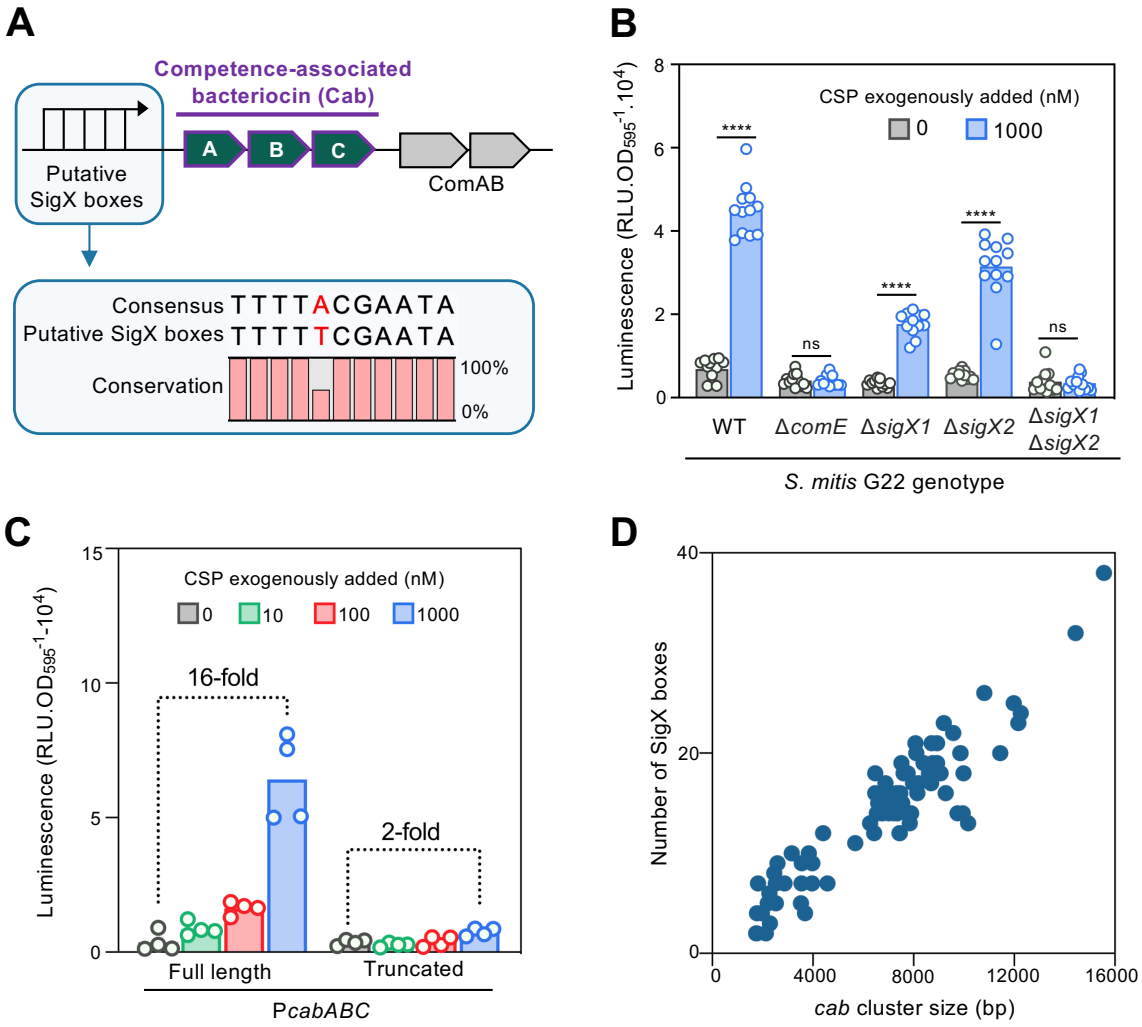
A
Competence-associated bacteriocin (Cab)
Putative SigX boxes
A
B
C
ComAB
Consensus TTTTACGAATA
Putative SigX boxes TTTTTCGAATA
Conservation
100%
0%
B
Luminescence (RLU.OD595-1.10^4)
CSP exogenously added (nM)
0
1000
****
ns
****
****
ns
WT
ΔcomE
ΔsigX1
ΔsigX2
ΔsigX1 ΔsigX2
S. mitis G22 genotype
C
Luminescence (RLU.OD595-1.10^4)
CSP exogenously added (nM)
0
10
100
1000
16-fold
2-fold
Full length
Truncated
PcabABC
D
Number of SigX boxes
cab cluster size (bp)

Figure 3

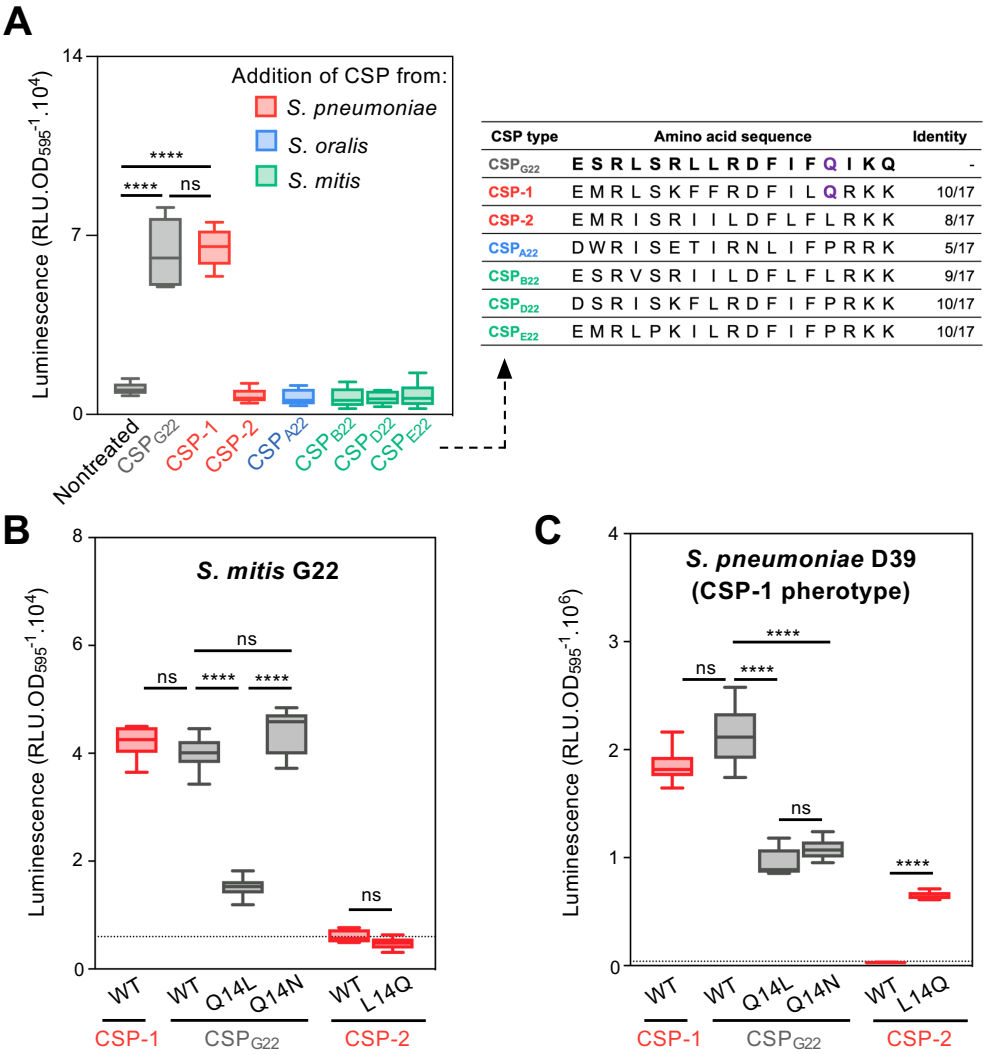

CSP type	Amino acid sequence	Identity
CSP_{G22}	**E S R L S R L L R D F I F Q I K Q**	-
CSP-1	E M R L S K F F R D F I L Q R K K	10/17
CSP-2	E M R I S R I I L D F L F L R K K	8/17
CSP_{A22}	D W R I S E T I R N L I F P R R K	5/17
CSP_{B22}	E S R V S R I I L D F L F L R K K	9/17
CSP_{D22}	D S R I S K F L R D F I F P R K K	10/17
CSP_{E22}	E M R L P K I L R D F I F P R K K	10/17

Figure 4

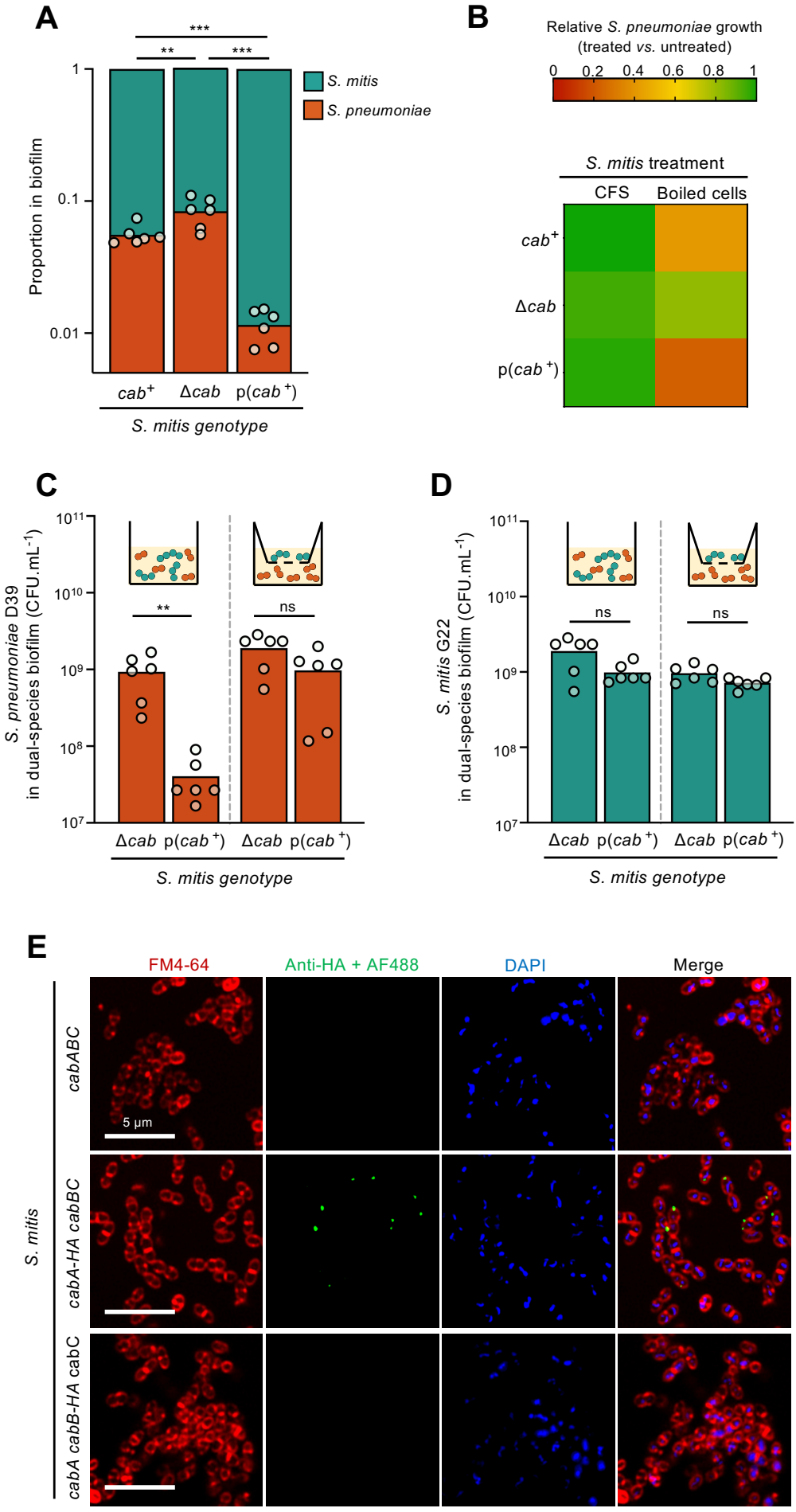
A
***
**
***
1
0.1
0.01
Proportion in biofilm
S. mitis
S. pneumoniae
cab+
Δcab
p(cab+)
S. mitis genotype
B
Relative S. pneumoniae growth
(treated vs. untreated)
0
0.2
0.4
0.6
0.8
1
S. mitis treatment
CFS
Boiled cells
cab+
Δcab
p(cab+)
C
S. pneumoniae D39
in dual-species biofilm (CFU.mL-1)
10^11
10^10
10^9
10^8
10^7
**
ns
Δcab
p(cab+)
Δcab
p(cab+)
S. mitis genotype
D
S. mitis G22
in dual-species biofilm (CFU.mL-1)
10^11
10^10
10^9
10^8
10^7
ns
ns
Δcab
p(cab+)
Δcab
p(cab+)
S. mitis genotype
E
FM4-64
Anti-HA + AF488
DAPI
Merge
S. mitis
cabABC
cabA-HA cabBC
cabA cabB-HA cabC
5 µm

Figure 5

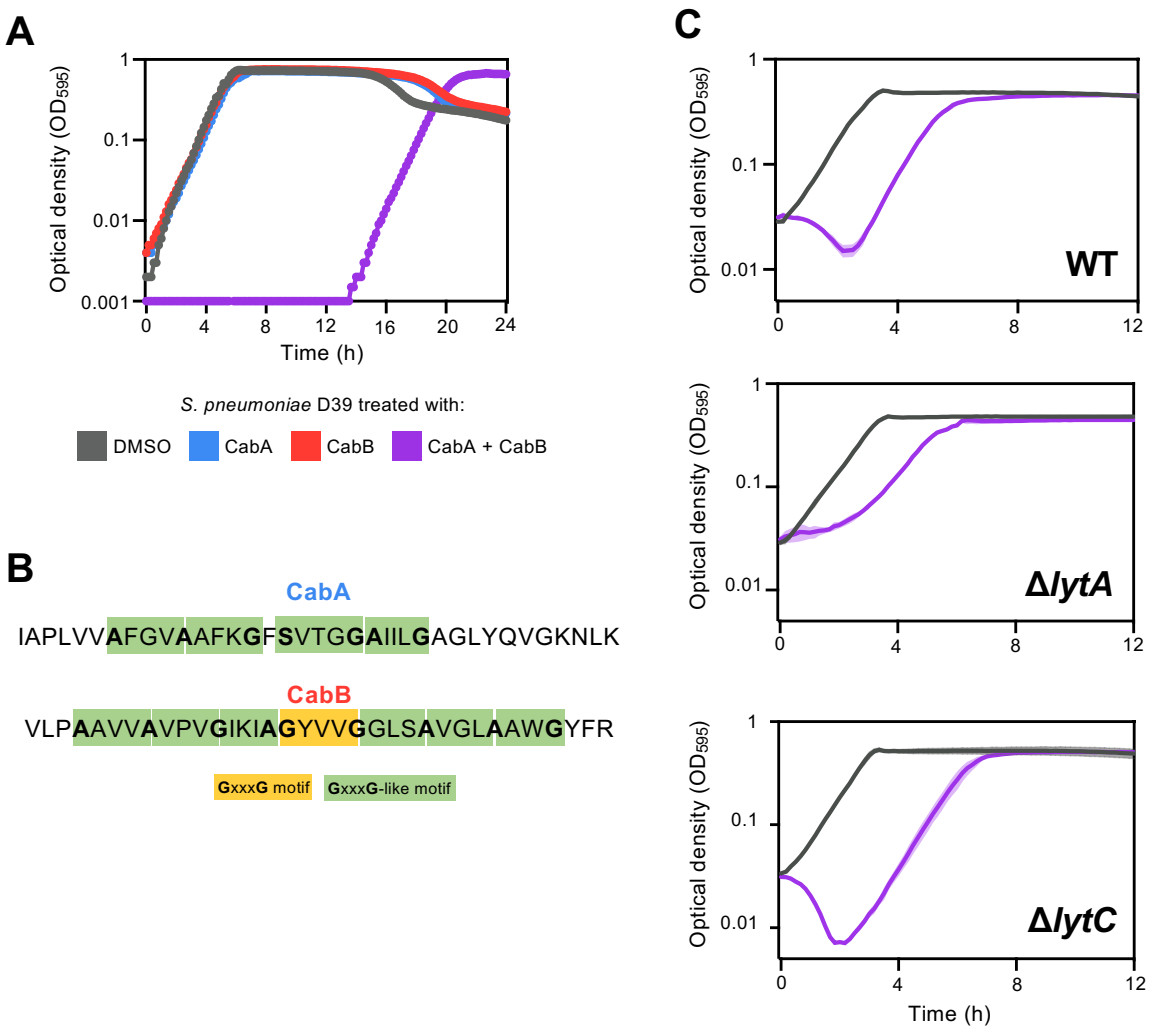
A
Optical density (OD595)
1
0.1
0.01
0.001
0
4
8
12
16
20
24
Time (h)
S. pneumoniae D39 treated with:
DMSO
CabA
CabB
CabA + CabB
B
CabA
IAPLVVAFGVAAFKGFSVTGGAIILGAGLYQVGKNLK
CabB
VLPAAVVAVPVGIKIAGYVVGGLSAVGLAAWGYFR
GxxxG motif
GxxxG-like motif
C
Optical density (OD595)
1
0.1
0.01
0
4
8
12
WT
ΔlytA
ΔlytC
Time (h)

Figure 6

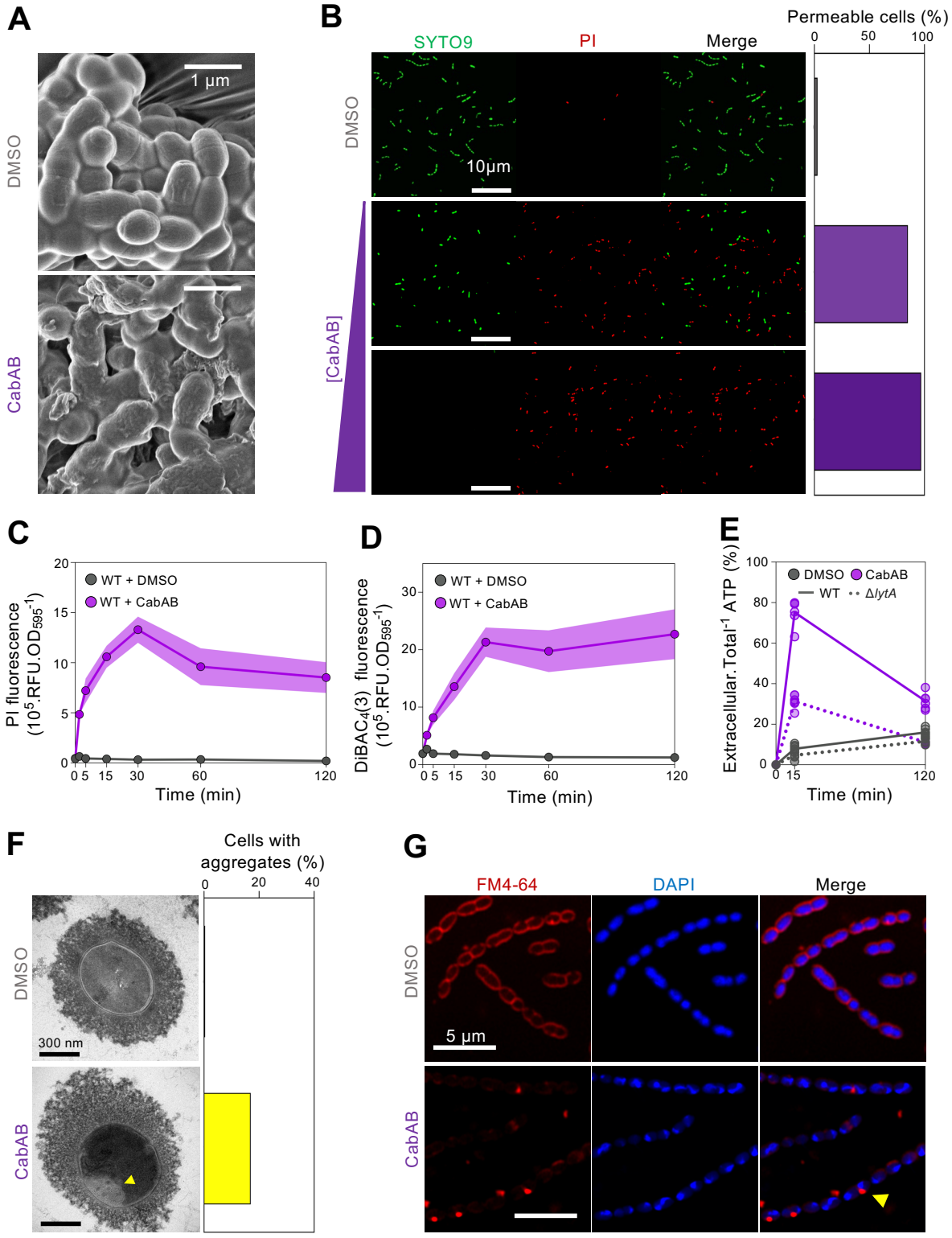
A
DMSO
CabAB
1 µm
B
SYTO9
PI
Merge
Permeable cells (%)
0
50
100
DMSO
[CabAB]
10µm
C
PI fluorescence
(10^5.RFU.OD595^-1)
WT + DMSO
WT + CabAB
Time (min)
D
DiBAC4(3) fluorescence
(10^5.RFU.OD595^-1)
WT + DMSO
WT + CabAB
Time (min)
E
Extracellular.Total^-1 ATP (%)
DMSO
CabAB
WT
ΔlytA
Time (min)
F
Cells with aggregates (%)
DMSO
CabAB
300 nm
G
FM4-64
DAPI
Merge
DMSO
CabAB
5 µm

Figure 7

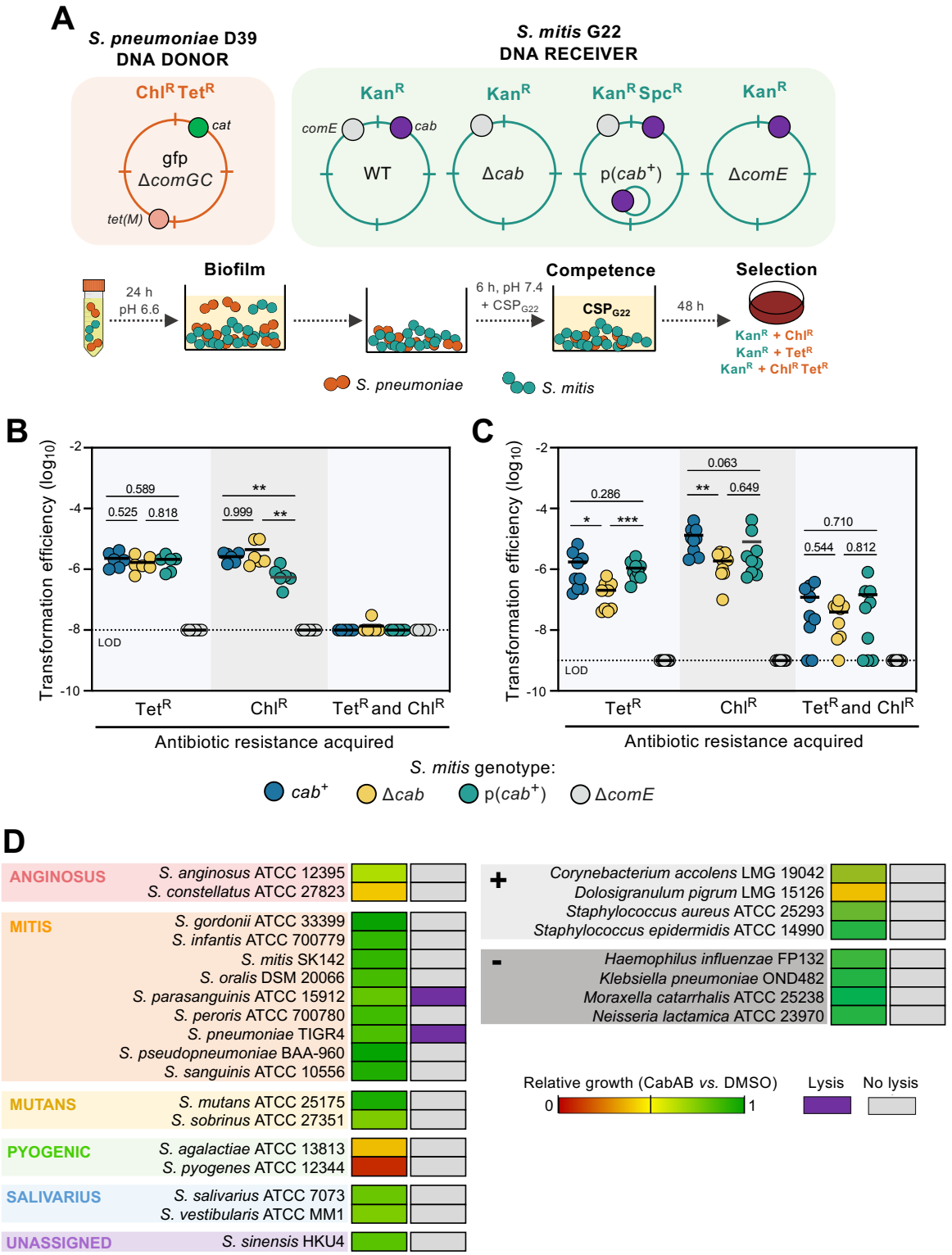
A
S. pneumoniae D39
DNA DONOR
ChlR TetR
cat
gfp
ΔcomGC
tet(M)
S. mitis G22
DNA RECEIVER
KanR
comE
cab
WT
KanR
Δcab
KanR SpcR
p(cab+)
KanR
ΔcomE
Biofilm
24 h
pH 6.6
Competence
6 h, pH 7.4
+ CSPG22
CSPG22
48 h
Selection
KanR + ChlR
KanR + TetR
KanR + ChlR TetR
S. pneumoniae
S. mitis
B
Transformation efficiency (log10)
-2
-4
-6
-8
-10
0.589
0.525
0.818
**
0.999
**
LOD
TetR
ChlR
TetR and ChlR
Antibiotic resistance acquired
C
0.286
*
***
0.063
**
0.649
0.710
0.544
0.812
LOD
TetR
ChlR
TetR and ChlR
Antibiotic resistance acquired
S. mitis genotype:
cab+
Δcab
p(cab+)
ΔcomE
D
ANGINOSUS
S. anginosus ATCC 12395
S. constellatus ATCC 27823
MITIS
S. gordonii ATCC 33399
S. infantis ATCC 700779
S. mitis SK142
S. oralis DSM 20066
S. parasanguinis ATCC 15912
S. peroris ATCC 700780
S. pneumoniae TIGR4
S. pseudopneumoniae BAA-960
S. sanguinis ATCC 10556
MUTANS
S. mutans ATCC 25175
S. sobrinus ATCC 27351
PYOGENIC
S. agalactiae ATCC 13813
S. pyogenes ATCC 12344
SALIVARIUS
S. salivarius ATCC 7073
S. vestibularis ATCC MM1
UNASSIGNED
S. sinensis HKU4
+
Corynebacterium accolens LMG 19042
Dolosigranulum pigrum LMG 15126
Staphylococcus aureus ATCC 25293
Staphylococcus epidermidis ATCC 14990
-
Haemophilus influenzae FP132
Klebsiella pneumoniae OND482
Moraxella catarrhalis ATCC 25238
Neisseria lactamica ATCC 23970
Relative growth (CabAB vs. DMSO)
0
1
Lysis
No lysis

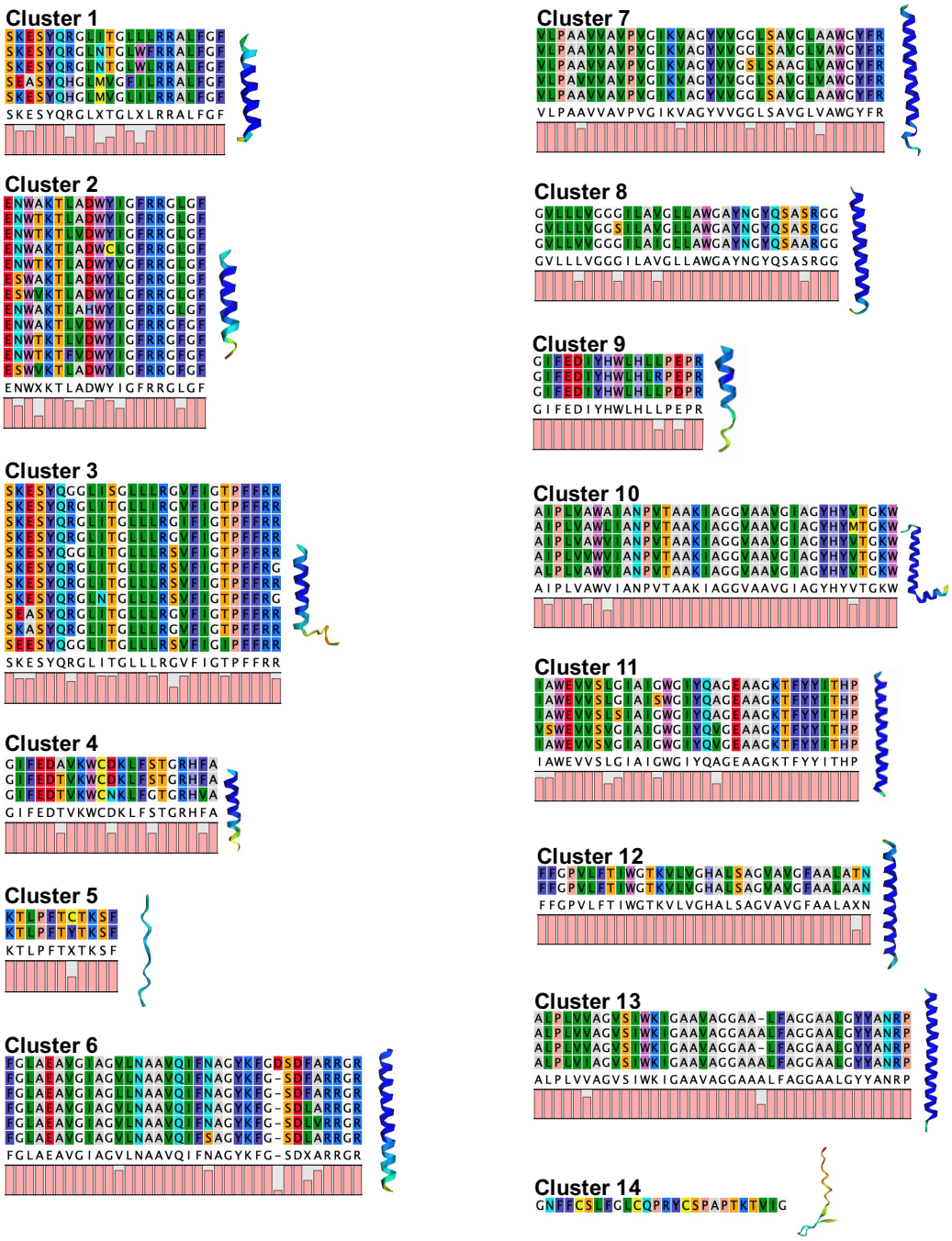

Fig. S1. Alignment-based clustering of Cab variants. The 95 Cab variants found *S. mitis* populations were clustered based on pairwise sequence alignments (see Materials and Methods). Alignments for Cab sequences within each cluster is shown, with associated Alphafold2 (ColabFold v1.5.5) structural model of the most prevalent variant. Amino acids are colored according to biochemical traits (RasMol coloring). Structures are colored according to plDDT (predicted local distance difference test) confidence.

(continues on next page)

Fig. S1. (cont.)

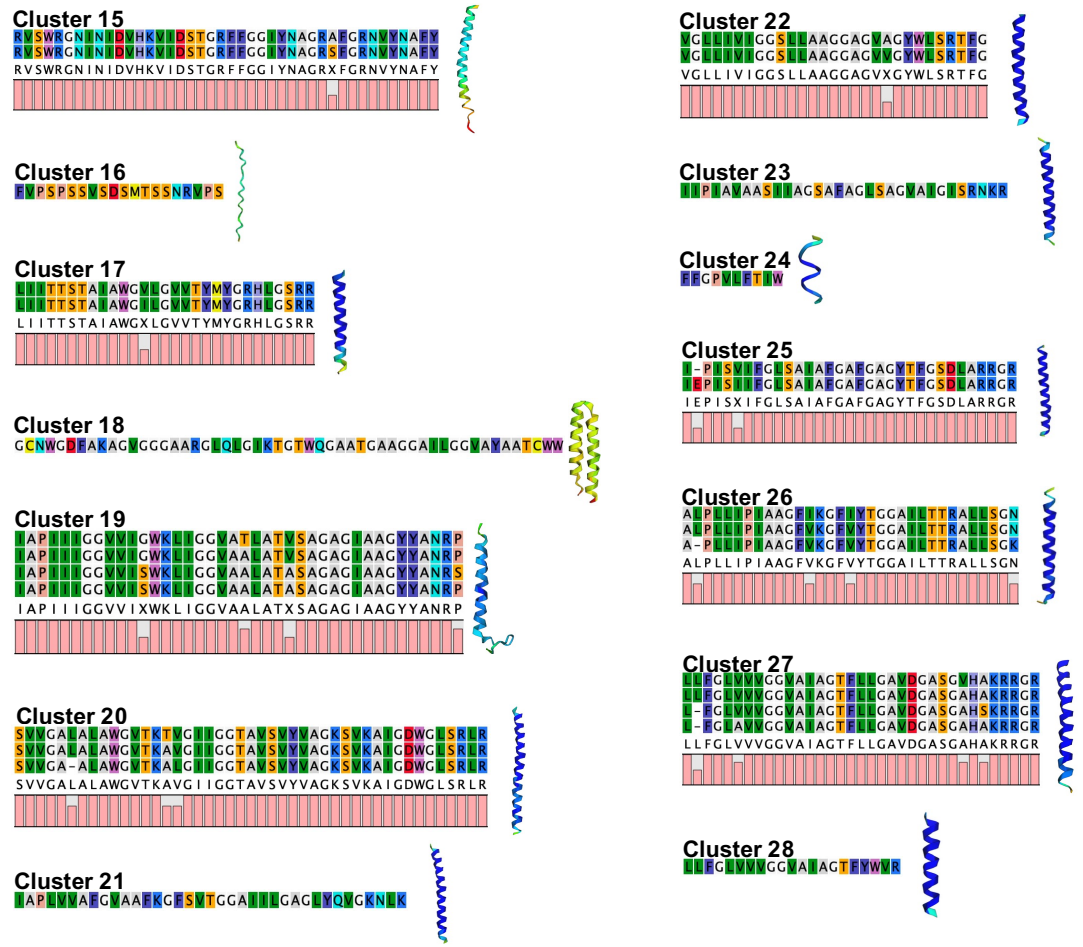

- **Acidic** - Asp (D), Glu (E)
- **Sulfur-containing** – Cys (C), Met (M)
- **Basic** – Lys (K), Arg (R)
- **Polar uncharged** – Ser (S), Thr (T)
- **Aromatic** – Phe (F), Tyr (Y)
- **Polar uncharged (amide)** – Asn (N), Gln (Q)
- **Small/flexible** – Gly (G)
- **Aliphatic hydrophobic** – Leu (L), Val (V), Ile (I)
- **Small hydrophobic** – Ala (A)
- **Aromatic bulky** – Trp (W)
- **Weakly basic** – His (H)
- **Cyclic/ring** – Pro (P)

pIDDT: Very low (<50) Low (60) OK (70) Confident (80) Very high (>90)

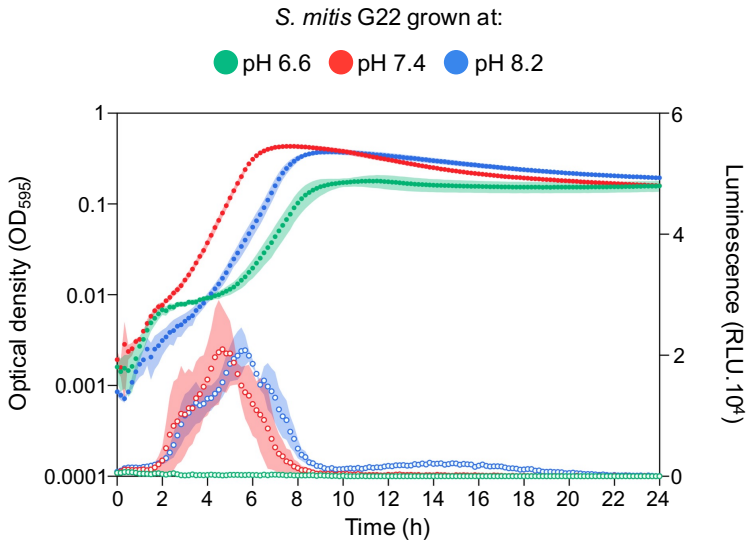

Fig. S2. *S. mitis* competence is inhibited in medium with acidic pH. *S. mitis* G22 harboring an early-competence reporter (P*comCDE-luc*) was pre-grown in medium at pH 6.6, before being diluted 1:100 in fresh medium at pH 6.6, 7.4, or 8.2. Optical density (closed circles) and luminescence (open circles) values were measured every 10 min for 24 h. Experiment was repeated three times independently.

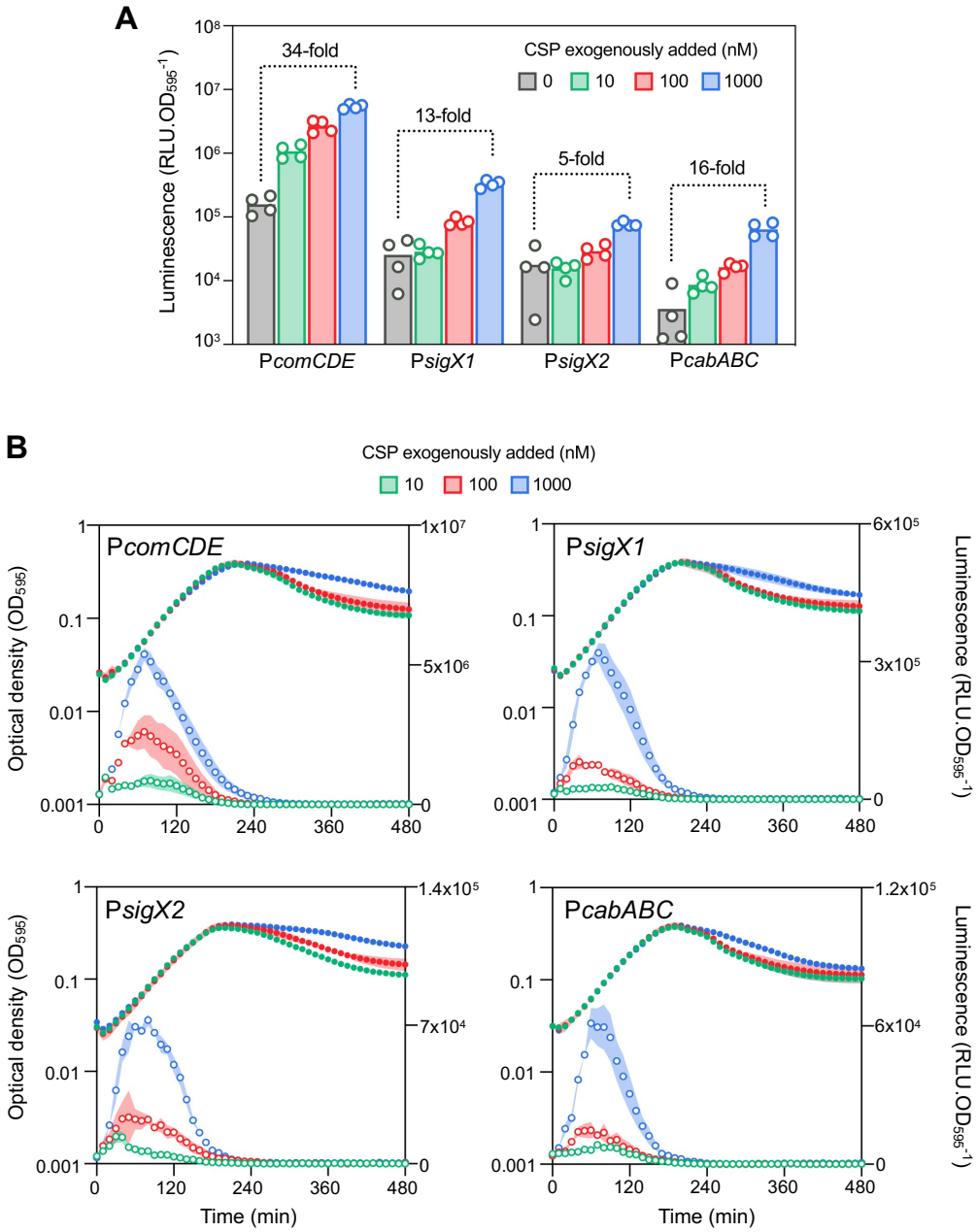

Fig. S3. Expression of *cabABC* follows the same dynamics of other competence genes. (A) Expression of *comCDE*, *sigX1*, *sigX2* and *cabABC* evaluated by luminescence produced by luminescent reporter *S. mitis*. Cells were pre-grown in acidic pH and diluted in fresh medium containing synthetic CSP_{G22}. Values represent the highest expression value ($RLU.OD_{595}^{-1}$) obtained during the 3 h post CSP_{G22} treatment. (B) Dynamics of *comCDE*, *sigX1*, *sigX2* and *cabABC* expression in *S. mitis*. Optical density – closed circles. Luminescence – open circles. Experiments were repeated 3 times independently for 24 h. For clarity only the first 8 h are shown, since there is no visible expression of the four reporters after this period.

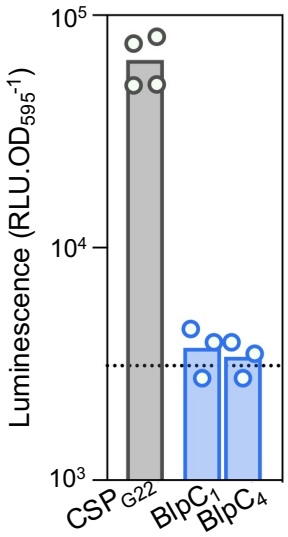

Fig. S4. Expression of *cabABC* is not induced by bacteriocin-like peptide pheromones (BlpC)**.** *S. mitis* G22 harboring a P*cabABC-luc* reporter was pre-grown in acidic pH and diluted in fresh medium containing 1 µM of synthetic CSP_{G22} (grey), 1 µM of $BlpC_1$ or $BlpC_4$ pheromones (blue) or left untreated (dashed line). $BlpC_1$ or $BlpC_4$ are encoded in two *blp*-type bacteriocin clusters elsewhere in the genome of G22.

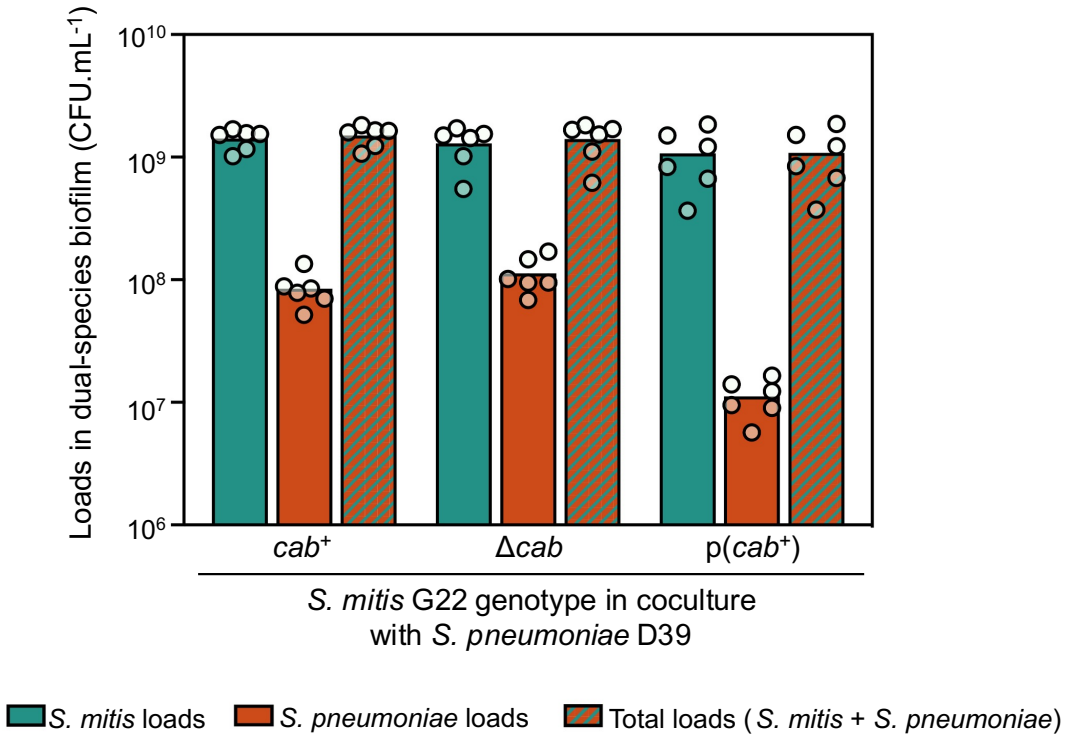

Fig. S5. Expression of *cab* by *S. mitis* reduces *S. pneumoniae* loads in dual-species biofilms. Figure individual and total bacterial loads of biofilm proportions presented in Figure 4A of the main text. *S. pneumoniae* and *S. mitis* of different *cab* genotypes were grown in 24 h biofilms in competence-permissive conditions. *S. mitis* and *S. pneumoniae* cell loads were enumerated by plating in BA with kanamycin or chloramphenicol, respectively. The experiment was repeated three times, independently.

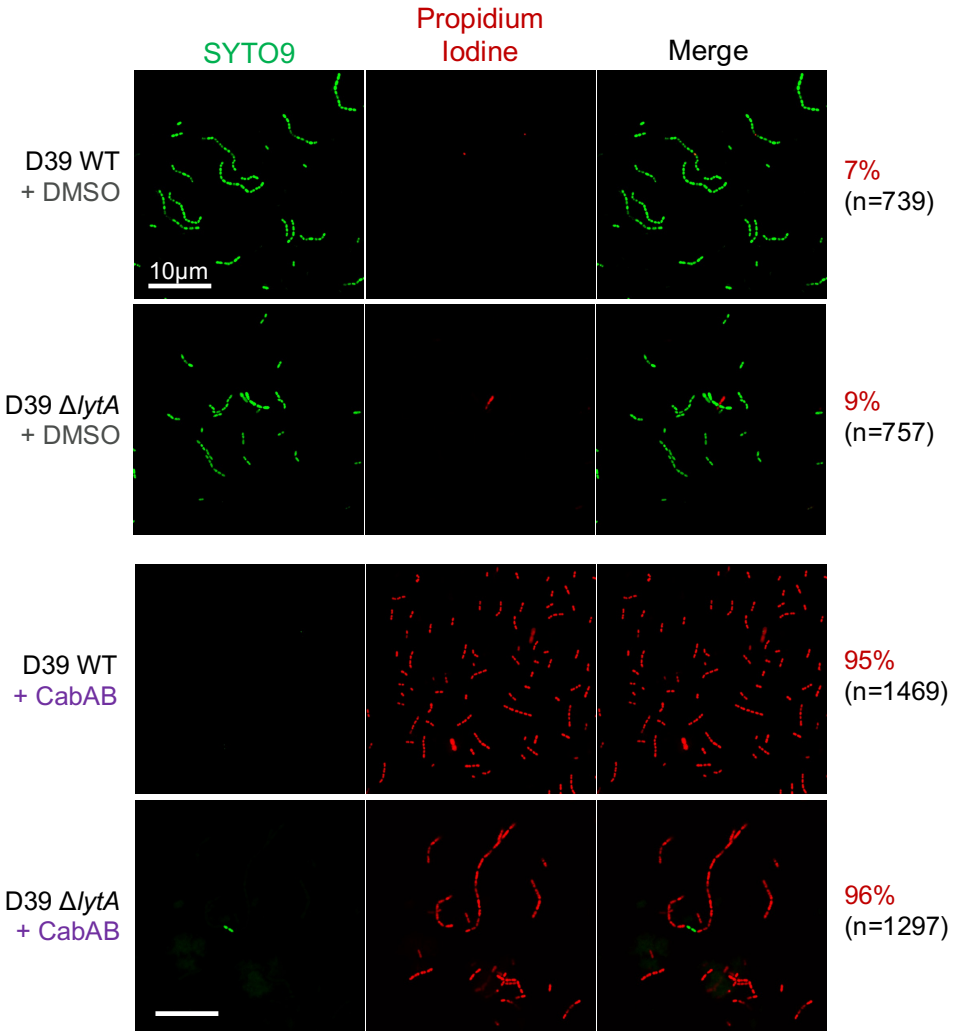

Fig. S6. Permeabilization of *S. pneumoniae* membranes does not depend on autolysin LytA. Confocal imaging of wild-type and Δ*lytA S. pneumoniae* treated with DMSO or synthetic CabAB peptides. Membrane permeabilization is shown in red, by entry of propidium iodine. The total number and percentage of permeable cells is shown next to panels. Microscopy images are representative of three independent experiments.

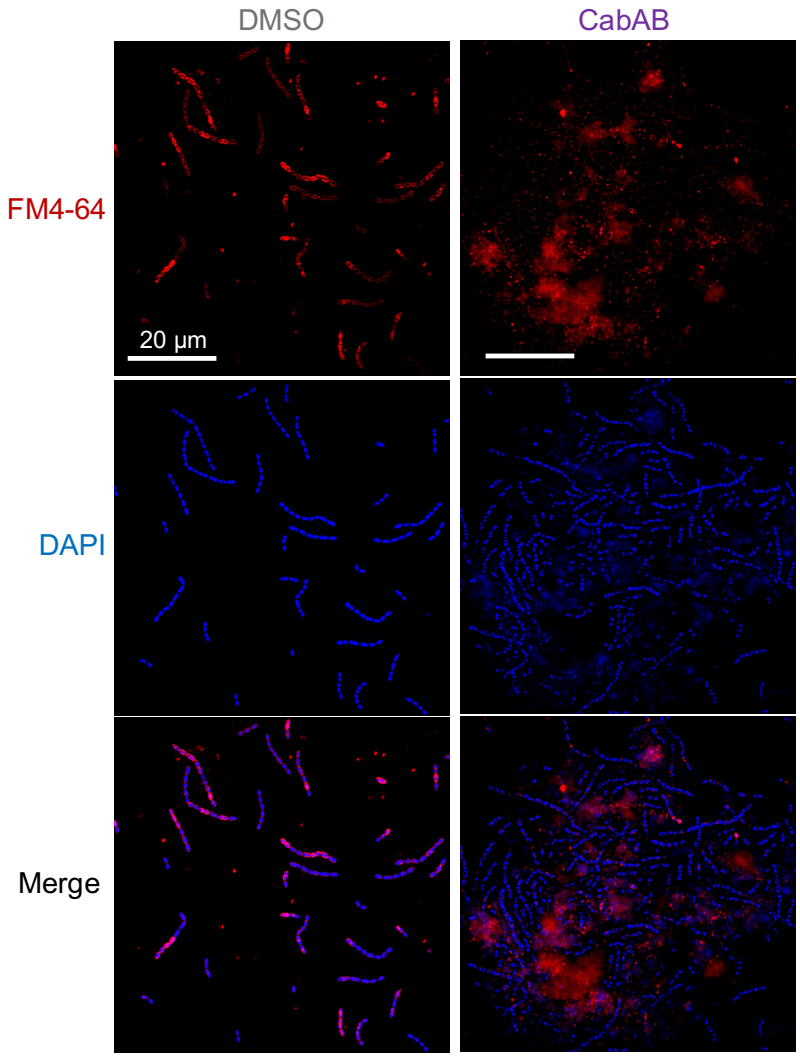

Fig. S7. CabAB treatment induces formation of large clumps of *S. pneumoniae* cells encased in a matrix of DNA and membrane material. *S. pneumoniae* D39 was treated with DMSO or CabAB and stained with FM4-64 (membrane dye) and DAPI (nucleic acid dye), before being imaged in a confocal microscope. Experiment was repeated three times, independently.

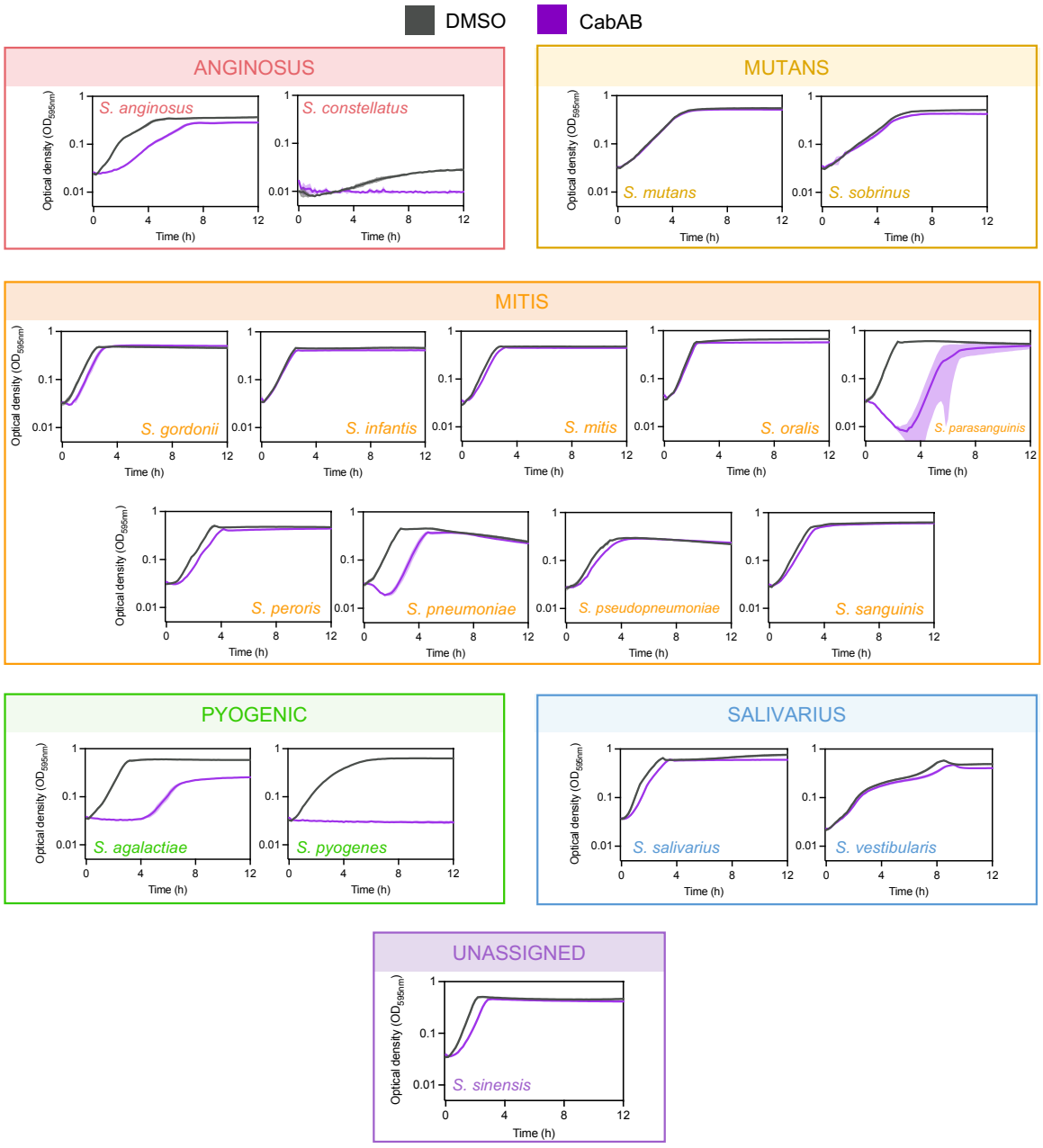

Fig. S8. Individual growth curves of 18 streptococcal species and their sensitivity to CabAB. Exponential cultures of streptococcal species were diluted to OD_{600} 0.1 in appropriate medium and treated with either DMSO or CabAB. Optical density was measured every 10 min for 24 h. For clarity, the first 12 h are shown. Species are colored according to streptococcal group. The experiment was repeated three times, independently. Summary data of the growth curves can be found in the main manuscript.

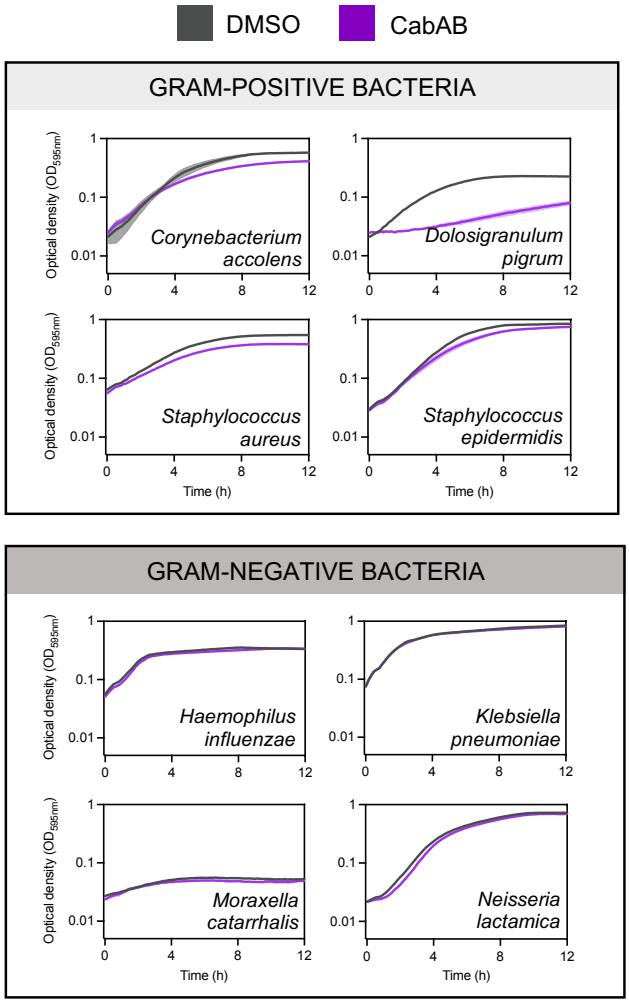

Fig. S9. Individual growth curves of 4 non-streptococcal Gram-positive and 4 Gram-negative bacteria and their sensitivity to CabAB. Exponential cultures of species were diluted to OD_{600} in appropriate medium and treated with either DMSO or CabAB. Optical density was measured every 10 min for 24 h. For clarity, the first 12 h are shown. Species are colored according to Gram staining. The experiment was repeated three times, independently. Summary data of the growth curves can be found in the main manuscript.

Table S1. *Streptococcus mitis* genomes used in the study.

Strain	Region flanked by *plsX-acpP and* comAB recovered from genome (Y/N)	Presence of *cab* (Y/N)	*cab* locus length (bp)	Number of unique Cabs	Number of SigX boxes in *cab* locus	Presence of *cibAB* (Y/N)	Presence of *cibC* (Y/N)	Mature CSP sequence	4th last amino acid in CSP	Genbank accession	Location of region flanked by *plsX-acpP* and *comAB*
103U_S92	Y	Y	9862	4	20	Y	Y	EMRKPDGALFNLFRRR	F	GCA_946186075.1	23700 to 33569 (contig 5)
125U_S4	Y	N	-	-	-	N	N	EMRRSNNNFFNFLRRI	L	GCA_946184935.1	121366 to 123329 (contig 6)
128U_S6	N	-	-	-	-	-	-	-	-	GCA_946186995.1	-
12P_S5	Y	Y	6869	5	15	N	N	EIRQTHNIFFNFFKRR	F	GCA_946186085.1	27830 to 34698 (contig 6)
13P_S6	Y	Y	9282	5	16	Y	Y	EIRQTHNIFFNFFKRR	F	GCA_946187105.1	25159 to 34440 (contig 14)
14P_S7	Y	Y	2287	2	3	N	N	ESRVSDLILDFLFQRKK	Q	GCA_946186685.1	19479 to 21765 (contig 2)
161U_S19	Y	N	-	-	-	Y	Y	EMRKPDGALFNLFRRR	F	GCA_946188375.1	109310 to 116321 (contig 4)
1P_S1	Y	N	-	-	-	N	N	EIRIADKIFFNLFKRR	F	GCA_946183265.1	10854 to 17772 (contig 11)
22P_S11	N	-	-	-	-	-	-	-	-	GCA_946183395.1	-
27P_S14	Y	Y	7997	5	17	N	Y	EIRKTSNSLLNFFKRR	F	GCA_946184735.1	22263 to 30259 (contig 10)
32P_S19	Y	Y	6869	5	15	N	N	EIRQTHNIFFNFFKRR	F	GCA_946223905.1	28620 to 35488 (contig 11)
38P_S23	Y	Y	6883	3	17	N	N	ESRLSKLLRDFIFKIKQ	K	GCA_946183455.1	26015 to 32897 (contig 9)
3P_S2	N	-	-	-	-	-	-	-	-	GCA_946183495.1	-
44P_S26	Y	N	-	-	-	N	N	EIRIADKIFFNLFKRR	F	GCA_946186695.1	36560 to 43673 (contig 10)
50P_S29	Y	Y	7547	4	15	Y	Y	ESRLSRLLRDFIFQIKQ	Q	GCA_946188075.1	25384 to 32930 (contig 8)
52P_S30	N	-	-	-	-	-	-	-	-	GCA_946186135.1	-
61P_S37	N	-	-	-	-	-	-	-	-	GCA_946183505.1	-
62P_S38	Y	Y	7457	5	15	N	N	ESRLPKIRFDFIFPRKK	P	GCA_946183485.1	24444 to 24837 (contig 5)
68U_S84	Y	N	-	-	-	N	N	EIRQTHNIFFNFFKRR	F	GCA_946183445.1	13397 to 18312 (contig 11)
7P_S3	N	-	-	-	-	-	-	-	-	GCA_946185985.1	-
B1_S23	Y	Y	3685	6	4	N	Y	EMRKMNEKSFNFFNIFRRR	F	GCA_946189985.1	18059 to 21743 (contig 6)
B10_S32	N	-	-	-	-	-	-	-	-	GCA_946183015.1	-
B100_S21	N	-	-	-	-	-	-	-	-	GCA_946186585.1	-
B1015B24C5	Y	Y	8698	4	17	N	Y	EMRKSNSTFFHFLRRI	L	GCA_905220945.1	27478 to 36175 (contig 5)
B1015G24C3	Y	Y	3544	6	7	N	Y	ESRVSDLILDFLFQRKK	Q	GCA_905221115.1	3577 to 7120 (contig 16)
B1015H24C1	Y	Y	9990	4	18	Y	Y	ESRVSDLILDFLFQRKK	Q	GCA_905221235.1	24516 to 34505 (contig 8)
B1015H24C3	Y	N	-	-	-	N	N	ESRLPKILLDFLFLRKK	L	GCA_905221375.1	45744 to 49408 (contig 11)
B1015H24C4	Y	N	-	-	-	N	N	EMRRIGSVLLNFFKRR	F	GCA_905221455.1	110170 to 117841 (contig 8)
B102_S23	N	-	-	-	-	-	-	-	-	GCA_946183435.1	-
B105_S26	Y	Y	3557	4	9	N	Y	EMRKMNEKSFNFFNIFRR	I	GCA_946185425.1	22400 to 25956 (contig 13)
B106_S27	Y	Y	6472	5	16	N	N	ESRLSRLLRDFILQRKK	Q	GCA_946184175.1	27052 to 33524 (contig 3)
B107_S28	Y	N	-	-	-	N	N	EMRKMNEKSFNFFNIFRRR	F	GCA_946184385.1	73855 to 74301 (contig 3)
B110_S31	Y	N	-	-	-	N	N	ESRLPKIRFDFIFPRKK	P	GCA_946185245.1	58142 to 67806 (contig 5)
B111_S32	Y	N	-	-	-	Y	Y	EIRIADKIFFNLFKRR	F	GCA_946185595.1	35645 to 42337 (contig 8)
B112_S33	Y	Y	8000	5	17	N	Y	EMRLPKILRDFIFPRKK	P	GCA_946185795.1	16961 to 24960 (contig 6)
B113_S34	Y	Y	7352	5	14	N	N	EMRKPDGALFNLFRRR	F	GCA_946186035.1	28045 to 35396 (contig 4)
B114_S35	Y	Y	7477	1	16	Y	Y	ESRLPKILLDFIFPRKK	P	GCA_946184755.1	130119 to 137595 (contig 5)
B116_S37	Y	N	-	-	-	Y	Y	EMRRIDKMFINFLKRR	L	GCA_946186655.1	65112 to 74936 (contig 6)
B117_S38	Y	N	-	-	-	N	Y	EMRKMNEKSFNFFNIFRRR	F	GCA_946184245.1	112994 to 121923 (contig 7)
B119_S40	Y	N	-	-	-	N	N	ESRVSDLILDFLFQRKK	Q	GCA_946184705.1	31961 to 19319 (contig 13)
B12_S34	Y	Y	6838	5	15	N	N	EMRKPDGALFNLFRRR	F	GCA_946187535.1	27777 to 34614 (contig 5)
B121_S42	Y	N	-	-	-	N	Y	ESRVSDLILDFLFQRKK	Q	GCA_946184465.1	3398 to 5219 (contig 19)
B122_S43	Y	Y	9952	5	14	Y	Y	EIRQTHNIFFNFFKRR	F	GCA_946183295.1	27547 to 37498 (contig 7)
B124_S44	Y	N	-	-	-	N	N	EMRKMNEKSFNFFNIFRRR	F	GCA_946184765.1	33241 to 41252 (contig 13)
B125_S45	Y	Y	6733	3	14	Y	Y	EIRIADKIFFNLFKRR	F	GCA_946186825.1	10414 to 17146 (contig 9)
B126_S46	Y	Y	7012	5	14	Y	Y	EMRRIDKMFINFLKRR	L	GCA_946183535.1	26548 to 33559 (contig 6)
B128_S47	N	-	-	-	-	-	-	-	-	GCA_946187305.1	-
B129_S48	N	-	-	-	-	-	-	-	-	GCA_946183555.1	-
B13_S35	Y	N	-	-	-	Y	Y	EIRQTHNIFFNFFKRR	F	GCA_946184335.1	124084 to 131222 (contig 4)
B132_S51	Y	Y	5685	5	11	N	N	ESRVSDLILDFLFQRKK	Q	GCA_946188115.1	26091 to 31775 (contig 7)
B133-2_S52	N	-	-	-	-	-	-	-	-	GCA_946187925.1	-
B134_S53	N	-	-	-	-	-	-	-	-	GCA_946183695.1	-
B137_S55	Y	N	-	-	-	N	N	EMRKPDGALFNLFRRR	F	GCA_946183685.1	37817 to 47227 (contig 10)
B139_S57	Y	N	-	-	-	Y	Y	ESRMPKILRDFIFPRKK	P	GCA_946183965.1	129975 to 133398 (contig 6)
B14_S36	Y	N	-	-	-	Y	Y	DMRISESIRNLIFPRKKK	R	GCA_946188365.1	132557 to 140438 (contig 5)

(continues on next page)

Table S1. (cont.)

B140_S58	Y	Y	7981	7	17	N	Y	EMRKMNEKSFNFFNIFRRR	F	GCA_946188035.1	21526 to 21918 (contig 7)
B146_S64	N	-	-	-	-	-	-	-	-	GCA_946184845.1	-
B147_S65	Y	N	-	-	-	Y	Y	EMRKMNEKSFNFFNIFRRR	F	GCA_946188285.1	33777 to 37954 (contig 129
B148_S66	N	-	-	-	-	-	-	-	-	GCA_946185855.1	-
B15_S37	Y	N	-	-	-	N	N	EMRKMNDKSFNLFNFFRRR	F	GCA_946188735.1	108533 to 116391 (contig 7)
B151_S69	N	-	-	-	-	-	-	-	-	GCA_946185905.1	-
B153_S71	Y	Y	10165	3	13	Y	Y	ESRLPKIRFDFIFPRKK	P	GCA_946188725.1	12287 to 22451 (contig 7)
B155_S73	N	-	-	-	-	-	-	-	-	GCA_946185295.1	-
B156_S74	N	-	-	-	-	-	-	-	-	GCA_946189305.1	-
B157_S75	Y	N	-	-	-	N	N	ESRLSRLLRDFIFQIKQ	Q	GCA_946188715.1	47861 to 48593 (contig 11)
B158_S76	N	-	-	-	-	-	-	-	-	GCA_946188825.1	-
B159_S77	Y	N	-	-	-	Y	Y	ESRLPKIRFDFIFPRKK	P	GCA_946188815.1	126333 to 135213 (contig 1)
B161_S79	Y	N	-	-	-	N	N	ESRLPKIRFDFIFPRKK	P	GCA_946188505.1	121745 to 133038 (contig 7)
B162_S80	N	-	-	-	-	-	-	-	-	GCA_946188645.1	-
B163_S81	N	-	-	-	-	-	-	-	-	GCA_946188665.1	-
B165_S83	Y	Y	7454	5	12	N	N	ESRLPKIRFDFIFPRKK	P	GCA_946188525.1	9840 to 17293 (contig 6)
B166_S84	N	-	-	-	-	-	-	-	-	GCA_946188555.1	-
B167_S85	Y	N	-	-	-	N	Y	ESRLPKILLDFLFLRKK	L	GCA_946188435.1	51984 to 55661 (contig 7)
B168_S86	Y	N	-	-	-	N	N	ESRLPKILLDFLFLRKK	L	GCA_946188425.1	129601 to 136812 (contig 5)
B169_S87	Y	N	-	-	-	N	Y	EMRLPKILRDFIFPRKK	P	GCA_946189595.1	100635 to 105207 (contig 7)
B170_S88	Y	Y	2522	2	7	N	N	EMRKMNEKSFNFFNIFRRR	F	GCA_946189625.1	16848 to 19369 (contig 119
B172_S90	N	-	-	-	-	-	-	-	-	GCA_946189565.1	-
B173_S91	N	-	-	-	-	-	-	-	-	GCA_946188785.1	-
B174_S92	Y	N	-	-	-	N	Y	EMRKPDGALFNLFRRR	F	GCA_946189255.1	44630 to 50769 (contig 13)
B176_S94	N	-	-	-	-	-	-	-	-	GCA_946188865.1	-
B19_S40	Y	Y	6430	2	12	N	Y	ESRVSDLILDFLFQRKK	Q	GCA_946190005.1	24129 to 30558 (contig 12)
B20_S41	N	-	-	-	-	-	-	-	-	GCA_946190035.1	-
B21_S42	N	-	-	-	-	-	-	-	-	GCA_946189125.1	-
B22_S43	Y	N	-	-	-	Y	Y	EMRKPDGALFNLFRRR	F	GCA_946189035.1	45816 to 51979 (contig 12)
B26_S45	Y	Y	7324	1	14	N	N	EMRRIDKIFINFLKRR	L	GCA_946189055.1	36560 to 43883 (contig 12)
B3_S25	Y	Y	6276	6	13	Y	Y	EMRKMNEKSFNFFNIFRRR	F	GCA_946189635.1	27034 to 33309 (contig 11)
B30_S48	Y	N	-	-	-	Y	Y	ESRVSDILLDFLFRRKK	R	GCA_946189895.1	13875 to 25318 (contig 11)
B31_S49	Y	Y	7447	5	12	Y	Y	EMRKMNDKSFNLFNFFRRR	F	GCA_946188485.1	24297 to 31743 (contig 13)
B33_S51	Y	Y	11446	5	20	Y	Y	ESRLPKIRFDFIFPRKK	P	GCA_946188605.1	9714 to 21159 (contig 14)
B34_S52	Y	N	-	-	-	N	N	EMRKMNEKSFNFFNIFNIFRR	F	GCA_946189235.1	27396 to 35035 (contig 17)
B37_S55	Y	N	-	-	-	N	Y	EIRKTSNSLLNFFKRR	F	GCA_946188755.1	8105 to 15978 (contig 6)
B38_S56	N	-	-	-	-	-	-	-	-	GCA_946188795.1	-
B4_S26	Y	N	-	-	-	N	N	EMRKMNEKSFNFFNIFRRR	F	GCA_946189945.1	13981 to 20965 (contig 29)
B42_S60	Y	N	-	-	-	Y	Y	ESRLPKIRFDFIFPRKK	P	GCA_946188675.1	147283 to 158055 (contig 5)
B43_S61	Y	Y	7325	4	16	Y	Y	EIRQTHNIFFNFFKRR	F	GCA_946188595.1	23294 to 30618 (contig 15)
B44_S62	Y	Y	6767	5	14	Y	Y	ESRLPKIRFDFIFPRKK	P	GCA_946188765.1	24640 to 31406 (contig 5)
B45_S63	Y	N	-	-	-	Y	Y	EIRQTHNIFFNFFKRR	F	GCA_946189355.1	8513 to 9245 (contig 6)
B46_S64	N	-	-	-	-	-	-	-	-	GCA_946188655.1	-
B47_S65	Y	N	-	-	-	N	Y	EMRKSNNNFFHFLRRI	L	GCA_946188745.1	43466 to 50055 (contig 7)
B49_S67	N	-	-	-	-	-	-	-	-	GCA_946188965.1	-
B5_S27	N	-	-	-	-	-	-	-	-	GCA_946189025.1	-
B50_S68	Y	N	-	-	-	Y	Y	ESRLPKIRFDFIFPRKK	P	GCA_946188955.1	126680 to 135327 (contig 7)
B52_S70	Y	N	-	-	-	N	N	ETRKTINSLLNLFKRR	F	GCA_946189865.1	13665 to 14681 (contig 16)
B54_S72	N	-	-	-	-	-	-	-	-	GCA_946188925.1	-
B55_S73	Y	N	-	-	-	N	N	ESRLSRLLRDFIFQIKQ	Q	GCA_946188895.1	49166 to 58656 (contig 9)
B56_S74	N	-	-	-	-	-	-	-	-	GCA_946188995.1	-
B57_S75	Y	N	-	-	-	N	Y	EMRRIDKMFINFLKRR	L	GCA_946188985.1	117917 to 125697 (contig 4)
B59_S77	N	-	-	-	-	-	-	-	-	GCA_946188875.1	-
B60_S78	Y	N	-	-	-	N	N	EMRKPDGALFNLFRRR	F	GCA_946189965.1	124476 to 131218 (contig 4)
B61_S79	Y	N	-	-	-	Y	Y	EIRKSNSALVNFFKRR	F	GCA_946188855.1	55573 to 66461 (contig 10)
B63_S81	Y	Y	7221	5	14	N	Y	ESRVSDLILDFLFQRKK	Q	GCA_946189015.1	10888 to 18108 (contig 15)
B65_S83	Y	N	-	-	-	N	N	ESRVSDILLDFLFRRKK	R	GCA_946189955.1	118327 to 122899 (contig 3)
B67_S85	Y	Y	3156	4	10	Y	Y	EMRKSNNTFFNFLRRI	L	GCA_946188885.1	7767 to 10922 (contig 13)
B69_S87	N	-	-	-	-	-	-	-	-	GCA_946188945.1	-
B73_S91	Y	Y	8931	3	19	N	N	ESRVSDILLDFLFRRKK	R	GCA_946188935.1	13555 to 22485 (contig 9)

(continues on next page)

Table S1. (cont.)

B74_S92	Y	N	-	-	-	N	N	EIRQTHNIFFNFFKRR	F	GCA_946188975.1	10138 to 10870 (contig 11)
B76_S94	Y	Y	7437	4	12	N	N	ESRLSRLLRDFIFQIKQ	Q	GCA_946189935.1	30822 to 38258 (contig 8)
B77_S95	Y	N	-	-	-	N	Y	EIRKTSNSLLNFFKRR	F	GCA_946189755.1	118938 to 126810 (contig 5)
B78_S96	Y	Y	8714	4	21	Y	Y	EMRRIDKMFINFLKRR	L	GCA_946189875.1	25049 to 33762 (contig 5)
B79_S1	Y	Y	3832	6	10	Y	Y	EMRKMNEKSFNFFNIFRRR	F	GCA_946188405.1	8778 to 12609 (contig 18)
B82_S4	Y	N	-	-	-	N	N	EMRKMNEKSFNFFNIFRRR	F	GCA_946188465.1	68030 to 72644 (contig 9)
B85_S7	Y	N	-	-	-	N	N	ESRLPKIRFDFIFPRKK	P	GCA_946189515.1	124429 to 125974 (contig 6)
B88_S10	Y	N	-	-	-	N	Y	EMRLPKILRDFIFPRKK	P	GCA_946189785.1	67460 to 77667 (contig 6)
B89L_S11	Y	Y	8758	4	19	Y	Y	EMRKPDGALFNLFRRR	F	GCA_946188455.1	23760 to 32517 (contig 5)
B9_S31	Y	N	-	-	-	N	N	EMRKMNEKSFNFFNIFRRR	F	GCA_946189075.1	32842 to 41229 (contig 13)
B91_S12	Y	N	-	-	-	Y	Y	EMRLSKFLRDFILQRKN	Q	GCA_946189535.1	19728 to 28296 (contig 10)
B93_S14	N	-	-	-	-	-	-	-	-	GCA_946189095.1	-
B95_S16	Y	N	-	-	-	N	N	MKNTVKLEQFVALKEKTCRR FEVGKLEKQLIVYLISSKEDK	K	GCA_946188475.1	57945 to 58714 (contig 10)
B96_S17	Y	Y	7329	1	16	N	N	EIRIADKIFFNLFKRR	F	GCA_946189115.1	35203 to 42531 (contig 12)
B97_S18	Y	N	-	-	-	N	N	EIRQTHNIFFNFFKRR	F	GCA_946189825.1	102775 to 103025 (contig 4)
B99_S20	N	-	-	-	-	-	-	-	-	GCA_946189005.1	-
GCF_000027165.1_ASM2716v1	Y	Y	9068	5	18	Y	Y	EMRKPDGALFNLFRRR	F	GCA_000027165.1_ASM2716v1	53854 to 62921 (contig 1)
GCF_000148505.1_ASM14850v1	N	-	-	-	-	-	-	-	-	GCA_000148505.1_ASM14850v1	-
GCF_000148525.1_ASM14852v1	Y	Y	4573	7	7	N	N	ESRVSDILLDFLFRRKK	R	GCA_000148525.1_ASM14852v1	23154 to 27726 (contig 22)
GCF_000148545.1_ASM14854v1	N	-	-	-	-	-	-	-	-	GCA_000148545.1_ASM14854v1	-
GCF_000148585.2_ASM14858v3	Y	Y	8195	5	17	Y	Y	EIRQTHNIFFNFFKRR	F	GCA_000148585.2_ASM14858v3	46590 to 54784 (contig 1)
GCF_000220045.1_ASM22004v2	Y	N	-	-	-	N	N	ESRLSRLLRDFIFQIKQ	Q	GCA_000220045.1_ASM22004v2	113804 to 121511 (contig 10)
GCF_000220085.1_ASM22008v2	Y	Y	7601	3	18	N	N	EMRRIDKIFNFLKRR	L	GCA_000220085.1_ASM22008v2	33312 to 40912 (contig 6)
GCF_000222785.1_ASM22278v2	Y	N	-	-	-	Y	Y	EMRLPKILRDFIFPRKK	P	GCA_000222785.1_ASM22278v2	80829 to 88913 (contig 17)
GCF_000257805.1_ASM25780v1	Y	N	-	-	-	N	N	EMRRIDKIFINFLKRR	L	GCA_000257805.1_ASM25780v1	30349 to 36794 (contig 56)
GCF_000257865.1_ASM25786v1	Y	N	-	-	-	N	N	EMRKMNEKSFNFFNIFRRR	F	GCA_000257865.1_ASM25786v1	108462 to 111048 (contig 56)
SK579v1.0	Y	N	-	-	-	N	N	EIRKSNSALVNFFKRR	F	GCA_000257905.1_SmitisSK579v1.0	51648 to 53976 (contig 13)
GCF_000385815.1_ASM38581v1	N	-	-	-	-	-	-	-	-	GCA_000385815.1_ASM38581v1	-
Smit.str17_34_v1.0	Y	Y	8147	3	16	N	N	ESRISDLLLDFLFQRKK	Q	GCA_000430305.1_Smit.str17_34_v1.	24690 to 32836 (contig 5)
Smit.str18_56_v1.0	Y	N	-	-	-	N	N	ETRKTINSLLNLFKRR	F	GCA_000430345.1_Smit.str18_56_v1.	6585 to 7319 (contig 12)
Smit.str29_42_v1.0	Y	N	-	-	-	Y	Y	EIRQTHNIFFNFFKRR	F	GCA_000430365.1_Smit.str29_42_v1.	28257 to 34755 (contig 8)
Sm.str21_39_v1.0	Y	N	-	-	-	N	N	EMRLPKILRDFIFPRKK	P	GCA_000506725.1_Sm.str21_39_v1.0	107853 to 111953 (contig 6)
Sm.str27_7_v1.0	Y	N	-	-	-	N	N	EIRQTHNIFFNFFKRR	F	GCA_000506765.1_Sm.str27_7_v1.0	48091 to 54587 (contig 8)
GCF_000722685.1_ASM72268v1	Y	Y	6593	3	15	N	N	EIRKSNSALVNFFKRR	F	GCA_000722685.1_ASM72268v1	33237 to 39817 (contig 3)
GCF_000722695.1_ASM72269v1	Y	Y	8106	4	20	N	Y	EMRLPKILRDFIFPRKK	P	GCA_000722695.1_ASM72269v1	28640 to 36745 (contig 2)
GCF_000722705.1_ASM72270v1	Y	Y	7521	3	19	N	Y	EMRRIDKMFINFLKRR	L	GCA_000722705.1_ASM72270v1	26310 to 33830 (contig 1)
GCF_000722755.1_ASM72275v1	Y	N	-	-	-	N	N	ETRKTINSLLNLFKRR	F	GCA_000722755.1_ASM72275v1	19662 to 20232 (contig 8)
GCF_000722765.2_ASM72276v2	Y	Y	7760	4	18	N	Y	EMRKSNNNFFHFLRRI	L	GCA_000722765.2_ASM72276v2	49608 to 57367 (contig 1)
GCF_000722775.1_ASM72277v1	Y	Y	8930	3	21	N	N	EIRKTSNSLLNFFKRR	F	GCA_000722775.1_ASM72277v1	27763 to 36692 (contig 6)
GCF_000722815.1_ASM72281v1	Y	Y	1789	3	4	N	N	EMRRSNNNFFNFLRRI	L	GCA_000722815.1_ASM72281v1	20061 to 21849 (contig 1)
GCF_000722835.1_ASM72283v1	N	-	-	-	-	-	-	-	-	GCA_000722835.1_ASM72283v1	-
GCF_000724165.1_ASM72416v1	Y	N	-	-	-	N	N	Not found	-	GCA_000724165.1_ASM72416v1	438770 to 446249 (contig 12)
GCF_000960005.1_ASM96000v1	Y	Y	8611	2	18	Y	Y	EMRKPDGALFNLFRRR	F	GCA_000960005.1_ASM96000v1	29135 to 37745 (contig 1)
GCF_000960025.1_ASM96002v1	Y	Y	12265	4	24	N	N	ESRLPKIRFDFIFPRKK	P	GCA_000960025.1_ASM96002v1	32833 to 45097 (contig 3)
GCF_000960065.1_ASM96006v1	Y	N	-	-	-	N	N	DMRISESIRNLIFPRKKK	R	GCA_000960065.1_ASM96006v1	33075 to 43002 (contig 5)
GCF_001070035.1_ASM107003v1	N	-	-	-	-	-	-	-	-	GCA_001070035.1_ASM107003v1	-
GCF_001070205.1_ASM107020v1	N	-	-	-	-	-	-	-	-	GCA_001070205.1_ASM107020v1	-
GCF_001070375.1_ASM107037v1	N	-	-	-	-	-	-	-	-	GCA_001070375.1_ASM107037v1	-
GCF_001070705.1_ASM107070v1	Y	N	-	-	-	N	N	ESRLSKLLRDFIFKIKQ	K	GCA_001070705.1_ASM107070v1	91104 to 97864 (contig 13)
GCF_001070985.1_ASM107098v1	Y	N	-	-	-	Y	Y	EMRKPDGALFNLFRRR	F	GCA_001070985.1_ASM107098v1	125336 to 135287 (contig 33)
GCF_001074635.1_ASM107463v1	N	-	-	-	-	-	-	-	-	GCA_001074635.1_ASM107463v1	-
GCF_001281025.1_ASM128102v1	Y	N	-	-	-	Y	Y	EMRKSNNNFFNFLRRI	L	GCA_001281025.1_ASM128102v1	326587 to 336055 (contig 1)
GCF_001546795.1_ASM154679v1	N	-	-	-	-	-	-	-	-	GCA_001546795.1_ASM154679v1	-
GCF_001560895.1_ASM156089v1	Y	Y	2200	2	5	N	N	EMRKSNNTFFNFLRRI	-	GCA_001560895.1_ASM156089v1	73674 to 75873 (contig 1)
GCF_001579045.1_ASM157904v1	Y	N	-	-	-	Y	Y	EMRLPKILRDFIFPRKK	P	GCA_001579045.1_ASM157904v1	416341 to 423519 (contig 63)
GCF_001588595.1_ASM158859v1	Y	N	-	-	-	N	N	ETRKTINSLLNLFKRR	F	GCA_001588595.1_ASM158859v1	14693 to 15462 (contig 4)
GCF_001588605.1_ASM158860v1	Y	N	-	-	-	N	N	ETRKTINSLLNLFKRR	F	GCA_001588605.1_ASM158860v1	34154 to 34922 (contig 15)
GCF_001588625.1_ASM158862v1	Y	Y	9205	5	23	N	N	EMRKPDGALFNLFRRR	F	GCA_001588625.1_ASM158862v1	9739 to 18943 (contig 27)
GCF_002005545.1_ASM200554v1	Y	Y	3980	6	9	N	N	EMRLPKILRDFIFPRKK	P	GCA_002005545.1_ASM200554v1	495219 to 499198 (contig 1)

(continues on next page)

Table S1. (cont.)

GCF_002014755.1_ASM201475v1	Y	N	-	-	-	N	N	EIRQTHNIFFNFFKRR	F	GCA_002014755.1_ASM201475v1	115535 to 123729 (contig 6)
GCF_002014795.1_ASM201479v1	Y	Y	8075	4	21	N	Y	EMRKPDGALFNLFRRR	F	GCA_002014795.1_ASM201479v1	26394 to 34468 (contig 6)
GCF_002014875.1_ASM201487v1	Y	N	-	-	-	Y	Y	EIRQTHNIFFNFFKRR	F	GCA_002014875.1_ASM201487v1	63548 to 69821 (contig 7)
GCF_002096735.1_ASM209673v1	Y	Y	9752	2	14	N	N	EMRKSNNNFFNFLRRI	L	GCA_002096735.1_ASM209673v1	14476 to 24227 (contig 13)
GCF_002096755.1_ASM209675v1	N	-	-	-	-	-	-	-	-	GCA_002096755.1_ASM209675v1	-
GCF_002096765.1_ASM209676v1	Y	Y	6682	6	16	Y	Y	EMRKPDGALFNLFRRR	F	GCA_002096765.1_ASM209676v1	26701 to 33382 (contig 48)
GCF_002096775.1_ASM209677v1	Y	N	-	-	-	Y	Y	ESRLPKIRFDFIFPRKK	P	GCA_002096775.1_ASM209677v1	23754 to 24138 (contig 24)
GCF_002096815.1_ASM209681v1	Y	N	-	-	-	Y	Y	EMRRIDKMFINFLKRR	L	GCA_002096815.1_ASM209681v1	14082 to 19251 (contig 18)
GCF_002096835.1_ASM209683v1	Y	N	-	-	-	Y	Y	ESRVSDILLDFLFRRKK	R	GCA_002096835.1_ASM209683v1	4746 to 5469 (contig 19)
GCF_002096845.1_ASM209684v1	N	-	-	-	-	-	-	-	-	GCA_002096845.1_ASM209684v1	-
GCF_002096895.1_ASM209689v1	Y	N	-	-	-	N	N	DSRISKYLRDFIFPRKK	P	GCA_002096895.1_ASM209689v1	125698 to 126269 (contig 19)
GCF_002096925.1_ASM209692v1	N	-	-	-	-	-	-	-	-	GCA_002096925.1_ASM209692v1	-
GCF_002096935.1_ASM209693v1	Y	Y	6733	3	14	N	N	EIRIADKIFFNLFKRR	F	GCA_002096935.1_ASM209693v1	24923 to 31655 (contig 25)
GCF_002860825.1_ASM286082v1	Y	Y	3524	6	5	N	N	EMRKSNNTFFNFLRRI	L	GCA_002860825.1_ASM286082v1	18587 to 22110 (contig 13)
GCF_002860865.1_ASM286086v1	Y	Y	2525	2	5	N	N	ESRVSDLILDFLFQRKK	Q	GCA_002860865.1_ASM286086v1	58524 to 61048 (contig 3)
GCF_002860905.1_ASM286090v1	Y	Y	3156	4	10	Y	Y	EMRRIDKIFINFLKRR	L	GCA_002860905.1_ASM286090v1	18653 to 21808 (contig 8)
GCF_002871315.1_ASM287131v1	Y	Y	3524	6	5	N	N	EMRKSNNTFFNFLRRI	L	GCA_002871315.1_ASM287131v1	18509 to 22032 (contig 13)
GCF_003942775.1_ASM394277v1	N	-	-	-	-	-	-	-	-	GCA_003942775.1_ASM394277v1	-
GCF_003942885.1_ASM394288v1	N	-	-	-	-	-	-	-	-	GCA_003942885.1_ASM394288v1	-
GCF_003942965.1_ASM394296v1	Y	N	-	-	-	N	N	Not found	-	GCA_003942965.1_ASM394296v1	11262 to 11512 (contig 3)
GCF_003942995.1_ASM394299v1	Y	N	-	-	-	Y	Y	ESRVSDILLDFLFRRKK	R	GCA_003942995.1_ASM394299v1	30869 to 40944 (contig 14)
GCF_003943915.1_ASM394391v1	N	-	-	-	-	-	-	-	-	GCA_003943915.1_ASM394391v1	-
GCF_003943965.1_ASM394396v1	Y	N	-	-	-	N	Y	EMRRSNNNFFNFLRRI	L	GCA_003943965.1_ASM394396v1	40655 to 42425 (contig 16)
GCF_005144795.1_ASM514479v1	Y	Y	1780	2	4	Y	Y	ESRLSKIFLDFIFPRKK	P	GCA_005144795.1_ASM514479v1	13402 to 15181 (contig 16)
GCF_005844455.1_ASM584445v1	N	-	-	-	-	-	-	-	-	GCA_005844455.1_ASM584445v1	-
GCF_008763935.1_FS623	Y	Y	6780	5	16	Y	Y	ESRLPKIRFDFIFPRKK	P	GCA_008763935.1_FS623	107171 to 113950 (contig 5)
GCF_009495695.1_ASM949569v1	N	-	-	-	-	-	-	-	-	GCA_009495695.1_ASM949569v1	-
GCF_009495705.1_ASM949570v1	Y	Y	7465	7	16	N	N	EIRKTSNSLLNFFKRR	F	GCA_009495705.1_ASM949570v1	23517 to 30981 (contig 17)
GCF_009495735.1_ASM949573v1	Y	N	-	-	-	N	N	ESRVSDLILDFLFQRKK	Q	GCA_009495735.1_ASM949573v1	88623 to 96087 (contig 8)
GCF_009495895.1_ASM949589v1	Y	Y	7465	7	16	N	N	EIRKTSNSLLNFFKRR	F	GCA_009495895.1_ASM949589v1	23636 to 31100 (contig 8)
GCF_009495955.1_ASM949595v1	Y	N	-	-	-	N	N	EIRKTSNSLLNFFKRR	F	GCA_009495955.1_ASM949595v1	58616 to 66080 (contig 10)
GCF_009496035.1_ASM949603v1	Y	N	-	-	-	N	N	EIRKTSNSLLNFFKRR	F	GCA_009496035.1_ASM949603v1	88623 to 96087 (contig 9)
GCF_009496045.1_ASM949604v1	Y	N	-	-	-	N	N	EIRKTSNSLLNFFKRR	F	GCA_009496045.1_ASM949604v1	88615 to 96079 (contig 9)
GCF_009496065.1_ASM949606v1	Y	Y	7465	7	16	N	N	EIRKTSNSLLNFFKRR	F	GCA_009496065.1_ASM949606v1	23577 to 31041 (contig 10)
GCF_009496075.1_ASM949607v1	Y	Y	7465	7	16	N	N	EIRKTSNSLLNFFKRR	F	GCA_009496075.1_ASM949607v1	23517 to 30981 (contig 11)
GCF_009496165.1_ASM949616v1	Y	Y	7465	7	16	N	N	EIRKTSNSLLNFFKRR	F	GCA_009496165.1_ASM949616v1	23517 to 30981 (contig 8)
GCF_009496185.1_ASM949618v1	N	-	-	-	-	-	-	-	-	GCA_009496185.1_ASM949618v1	-
GCF_009496205.1_ASM949620v1	N	-	-	-	-	-	-	-	-	GCA_009496205.1_ASM949620v1	-
GCF_009496295.1_ASM949629v1	Y	N	-	-	-	Y	Y	ESRLPKIRFDFIFPRKK	P	GCA_009496295.1_ASM949629v1	124953 to 131821 (contig 6)
GCF_009496335.1_ASM949633v1	Y	N	-	-	-	N	N	EIRKTSNSLLNFFKRR	F	GCA_009496335.1_ASM949633v1	88622 to 96086 (contig 8)
GCF_009496355.1_ASM949635v1	Y	N	-	-	-	N	N	EIRKTSNSLLNFFKRR	F	GCA_009496355.1_ASM949635v1	88623 to 96087 (contig 7)
GCF_009496385.1_ASM949638v1	Y	Y	2273	2	6	N	N	EMRKSNNTFFNFLRRI	L	GCA_009496385.1_ASM949638v1	111359 to 113631 (contig 5)
GCF_009496395.1_ASM949639v1	Y	Y	7465	7	16	N	N	EIRKTSNSLLNFFKRR	F	GCA_009496395.1_ASM949639v1	23577 to 31041 (contig 8)
GCF_009496435.1_ASM949643v1	Y	N	-	-	-	N	N	EIRKTSNSLLNFFKRR	F	GCA_009496435.1_ASM949643v1	88623 to 96087 (contig 8)
GCF_009496505.1_ASM949650v1	Y	Y	7465	7	16	N	N	EIRKTSNSLLNFFKRR	F	GCA_009496505.1_ASM949650v1	23517 to 30981 (contig 6)
GCF_009496725.1_ASM949672v1	Y	Y	7465	7	16	N	N	EIRKTSNSLLNFFKRR	F	GCA_009496725.1_ASM949672v1	23577 to 31041 (contig 7)
GCF_009496735.1_ASM949673v1	Y	Y	7465	7	16	N	N	EIRKTSNSLLNFFKRR	F	GCA_009496735.1_ASM949673v1	23577 to 31041 (contig 7)
GCF_009496755.1_ASM949675v1	Y	N	-	-	-	N	N	EIRKTSNSLLNFFKRR	F	GCA_009496755.1_ASM949675v1	18419 to 25883 (contig 15)
GCF_009496795.1_ASM949679v1	Y	Y	7465	7	16	N	N	EIRKTSNSLLNFFKRR	F	GCA_009496795.1_ASM949679v1	23577 to 31041 (contig 8)
GCF_009496805.1_ASM949680v1	Y	Y	7465	7	16	N	N	EIRKTSNSLLNFFKRR	F	GCA_009496805.1_ASM949680v1	23577 to 31041 (contig 8)
GCF_009496815.1_ASM949681v1	Y	Y	7465	7	16	N	N	EIRKTSNSLLNFFKRR	F	GCA_009496815.1_ASM949681v1	23577 to 31041 (contig 9)
GCF_009496825.1_ASM949682v1	N	-	-	-	-	-	-	-	-	GCA_009496825.1_ASM949682v1	-
GCF_009496835.1_ASM949683v1	Y	Y	7465	7	16	N	N	EIRKTSNSLLNFFKRR	F	GCA_009496835.1_ASM949683v1	23577 to 31041 (contig 9)
GCF_009496895.1_ASM949689v1	Y	Y	7465	7	16	N	N	EIRKTSNSLLNFFKRR	F	GCA_009496895.1_ASM949689v1	23517 to 30981 (contig 15)
GCF_009496905.1_ASM949690v1	Y	N	-	-	-	N	N	EIRKTINGLLNFFKRR	F	GCA_009496905.1_ASM949690v1	51468 to 56727 (contig 9)
GCF_009730515.1_ASM973051v1	Y	Y	8195	5	17	N	N	EIRQTHNIFFNFFKRR	-	GCA_009730515.1_ASM973051v1	31493 to 39687 (contig 1)
GCF_900459425.1_42042_B02	Y	N	-	-	-	N	N	EIRQTHNIFFNFFKRR	F	GCA_900459425.1_42042_B02	116797 to 124991 (contig 2)
MSCx	Y	Y	8886	4	18	Y	Y	DSRISKYLRDFIFPRKK	P	GCA_905187535.1	25487 to 34372 (contig 11)
NM2_1	Y	N	-	-	-	N	N	EIRKTSNSLLNFFKRR	F	GCA_905187515.1	32077 to 39698 (contig 13)

(continues on next page)

Table S1. (cont.)

NM4_2	Y	N	-	-	-	N	Y	EIRKTSNSLLNFFKRR	F	GCA_905187545.1	32687 to 40308 (contig 13)
NM5_2	N	-	-	-	-	-	-	-	-	GCA_905187495.1	-
P11_S4	Y	N	-	-	-	N	N	EMRKPDGALFNLFRRR	F	GCA_946189525.1	42441 to 48870 (contig 6)
P164_S40	N	-	-	-	-	-	-	-	-	GCA_946189105.1	-
P21_S10	Y	Y	7902	6	14	N	N	EMRKPDGALFNLFRRR	F	GCA_946189045.1	26201 to 34102 (contig 7)
P28_S15	Y	N	-	-	-	Y	Y	ESRLPKIRFDFIFPRKK	P	GCA_946188915.1	120578 to 128595 (contig 6)
P42_S25	N	-	-	-	-	-	-	-	-	GCA_946189085.1	-
P55_S33	Y	Y	7359	5	16	Y	Y	EMRKPDGALFNLFRRR	F	GCA_946189995.1	28034 to 35392 (contig 7)
P59_S35	Y	N	-	-	-	Y	Y	ESRLPKIRFDFIFPRKK	P	GCA_946189495.1	151368 to 161798 (contig 4)
P60_S36	N	-	-	-	-	-	-	-	-	GCA_946190025.1	-
S1071B24C1	Y	Y	2587	2	9	N	N	ESRISDLLLDFLFQRKK	Q	GCA_905221505.1	3951 to 6537 (contig 12)
S1071B24C2	Y	Y	2461	2	8	N	N	ESRISDLLLDFLFQRKK	Q	GCA_905221525.1	3630 to 6090 (contig 13)
S1071G24C1	Y	N	-	-	-	N	N	EMRKIDDALFNLFNFFRRR	F	GCA_905221535.1	47372 to 58002 (contig 11)
S1071G24C2	Y	N	-	-	-	N	N	EMRKIDDALFNLFNFFRRR	F	GCA_905221545.1	47372 to 58002 (contig 11)
S1071G24C3	Y	Y	2461	2	8	N	N	ESRISDLLLDFLFQRKK	Q	GCA_905221005.1	3630 to 6090 (contig 12)
S1071G24C4	N	-	-	-	-	-	-	-	-	GCA_905221035.1	-
S1071G24C5	N	-	-	-	-	-	-	-	-	GCA_905221045.1	-
S1072B24C4	Y	Y	2873	4	7	N	N	EMRMLKSPFSFLFPRKK	P	GCA_905221065.1	23060 to 25952 (contig 4)
S1072B24C5	Y	Y	2873	4	7	N	N	EMRMLKSPFSFLFPRKK	P	GCA_905221055.1	23060 to 25952 (contig 4)
S1072G24C4	Y	N	-	-	-	N	N	ESRISDLLLDFLFQRKK	Q	GCA_905221105.1	26882 to 35329 (contig 7)
S1075M24C2	Y	N	-	-	-	Y	Y	ESRVADLLLDFLFQRKK	Q	GCA_905221085.1	103323 to 113219 (contig 6)
S1075M24C3	Y	N	-	-	-	N	N	ESRISDLLLDFLFQRKK	Q	GCA_905221095.1	31726 to 42537 (contig 11)
S1075M24C5	Y	Y	10812	2	26	N	N	ESRISDLLLDFLFQRKK	Q	GCA_905221075.1	27291 to 37102 (contig 8)
S1086G24C1	N	-	-	-	-	-	-	-	-	GCA_905221125.1	-
S1088B24C2	Y	Y	6473	2	18	N	Y	ESRVSDLILDFLFQRKK	Q	GCA_905221135.1	26672 to 33144 (contig 6)
S1088M24C1	Y	N	-	-	-	N	N	EMRIADKIFFNLFKRR	F	GCA_905221145.1	54156 to 65018 (contig 7)
S1091B24C4	Y	N	-	-	-	N	N	EMRKPDGALFNLFRRR	F	GCA_905221155.1	125261 to 134199 (contig 4)
S1092G24C1	Y	Y	1740	2	2	N	N	DMRISGSIRNLIFPRKKK	R	GCA_905221165.1	12912 to 14651 (contig 9)
S1092G24C3	Y	Y	1768	2	2	N	N	EIRKKSNSLLNFFKRR	F	GCA_905221175.1	13104 to 14871 (contig 5)
S1092G24C4	N	-	-	-	-	-	-	-	-	GCA_905221185.1	-
S1093G24C1	Y	Y	8698	4	17	N	Y	EMRKSNSTFFHFLRRI	L	GCA_905221195.1	27478 to 36175 (contig 5)
S1093G24C2	Y	N	-	-	-	N	N	ESRLPKILRDFIFPRKK	P	GCA_905221205.1	66159 to 73603 (contig 4)
S1093G24C3	Y	N	-	-	-	N	N	EMRKTSYSLLNLFKRR	F	GCA_905221225.1	104898 to 109878 (contig 7)
S1096G24C5	N	-	-	-	-	-	-	-	-	GCA_905221215.1	-
S1096M24C3	Y	Y	9580	5	22	N	N	EIRKTSNSLFNFFKRR	F	GCA_905221245.1	11901 to 21480 (contig 6)
S1096M24C5	N	-	-	-	-	-	-	-	-	GCA_905221285.1	-
U10_S50	Y	N	-	-	-	Y	Y	EMRRIDKMFINFLKRR	L	GCA_946188615.1	136100 to 146454 (contig 6)
U104_S93	Y	Y	9859	4	20	Y	Y	EMRKPDGALFNLFRRR	F	GCA_946188685.1	23700 to 33558 (contig 6)
U105_S94	N	-	-	-	-	-	-	-	-	GCA_946188575.1	-
U109_S95	Y	N	-	-	-	N	N	EIRKTSNSLFNFFKRR	F	GCA_946188695.1	67998 to 77255 (contig 5)
U114_S96	Y	N	-	-	-	Y	Y	EMRRIDKMFINFLKRR	L	GCA_946188415.1	84542 to 94928 (contig 4)
U117_S1	Y	N	-	-	-	N	N	DSRISKYLRDFIFPRKK	P	GCA_946188585.1	15202 to 15765 (contig 7)
U12_S51	Y	N	-	-	-	Y	Y	ESRLPKIRFDFIFPRKK	P	GCA_946224775.1	52874 to 63087 (contig 6)
U122_S2	Y	N	-	-	-	N	Y	EIRKTSNSLLNFFKRR	F	GCA_946189145.1	149195 to 157067 (contig 2)
U123_S3	Y	N	-	-	-	N	N	ESRVSDILLNFLFRRKK	R	GCA_946190065.1	49685 to 50417 (contig 16)
U126_S5	Y	Y	8396	4	19	Y	Y	ESRVSDLILDFLFQRKK	Q	GCA_946190085.1	25538 to 25928 (contig 3)
U13_S52	Y	N	-	-	-	N	N	ESRLSKLLRDFIFKIKQ	K	GCA_946190075.1	21460 to 34396 (contig 12)
U131_S7	Y	N	-	-	-	N	N	ESRVSDLILDFLFQRKK	Q	GCA_946190095.1	127239 to 129511 (contig 5)
U134_S8	Y	Y	1964	3	4	N	N	EMRRSNNNFFNFLRRI	L	GCA_946190055.1	12955 to 14918 (contig 6)
U135_S9	Y	Y	1964	3	4	N	N	EMRRSNNNFFNFLRRI	L	GCA_946190045.1	12955 to 14918 (contig 6)
U14_S53	N	-	-	-	-	-	-	-	-	GCA_946190385.1	-
U143_S13	Y	N	-	-	-	N	N	EIRKKSNSLLNFFKRR	F	GCA_946190395.1	13391 to 14114 (contig 3)
U144_S14	Y	N	-	-	-	N	Y	EMRKMNEKSFNFFNIFRRR	F	GCA_946190245.1	31975 to 35539 (contig 15)
U148_S15	Y	Y	1964	3	4	N	N	EMRRSNNNFFNFLRRI	L	GCA_946190215.1	12955 to 14918 (contig 6)
U15_S54	Y	Y	3970	1	7	N	N	ESRVSDLILDFLFQRKK	Q	GCA_946190375.1	44742 to 48711 (contig 14)
U16_S55	Y	N	-	-	-	Y	Y	ESRLPKIRFDFIFPRKK	P	GCA_946190205.1	52874 to 63087 (contig 9)
U164_S21	Y	N	-	-	-	N	N	DSRISKYLRDFIFPRKK	P	GCA_946190365.1	56909 to 62429 (contig 9)
U165-2_S22	N	-	-	-	-	-	-	-	-	GCA_946186005.1	-
U23_S57	Y	N	-	-	-	N	N	EMRRIDKMFINFLKRR	L	GCA_946190355.1	34140 to 39308 (contig 18)

(continues on next page)

Table S1. (cont.)

U24_S58	Y	N	-	-	-	N	N	EMRRIDKMFINFLKRR	L	GCA_946190345.1	13215 to 18383 (contig 16)
U25_S59	N	-	-	-	-	-	-	-	-	GCA_946224995.1	-
U28_S60	N	-	-	-	-	-	-	-	-	GCA_946225005.1	-
U32_S62	Y	Y	6537	3	14	N	N	EMRRIDKIFINFLKRR	L	GCA_946224725.1	25517 to 32053 (contig 4)
U35_S65	Y	N	-	-	-	N	N	EMRRIDKIFINFLKRR	L	GCA_946224685.1	125817 to 132353 (contig 5)
U36_S66	N	-	-	-	-	-	-	-	-	GCA_946224705.1	-
U39_S69	N	-	-	-	-	-	-	-	-	GCA_946224645.1	-
U40_S70	Y	Y	1815	3	7	N	N	EIRKTINGLLNFFKRR	F	GCA_946190305.1	49454 to 51267 (contig 3)
U48_S72	N	-	-	-	-	-	-	-	-	GCA_946224865.1	-
U52_S74	N	-	-	-	-	-	-	-	-	GCA_946190225.1	-
U54_S75	Y	N	-	-	-	N	N	EMRRIDKMFINFLKRR	L	GCA_946190185.1	18384 to 28422 (contig 12)
U56_S76	Y	N	-	-	-	N	N	ETRKTINSLLNLFKRR	F	GCA_946190325.1	71434 to 73220 (contig 5)
U57_S77	Y	N	-	-	-	N	N	ETRKTINSLLNLFKRR	F	GCA_946190235.1	37034 to 38822 (contig 12)
U61_S78	N	-	-	-	-	-	-	-	-	GCA_946190115.1	-
U63_S79	Y	N	-	-	-	N	N	ETRKTINSLLNLFKRR	F	GCA_946190175.1	37034 to 38822 (contig 15)
U65_S81	Y	N	-	-	-	N	N	EMRRIDKMFINFLKRR	L	GCA_946190125.1	10058 to 15226 (contig 20)
U67_S83	Y	Y	7327	1	14	Y	Y	EMRRIDKMFINFLKRR	L	GCA_946190165.1	35610 to 42936 (contig 11)
U8_S49	Y	N	-	-	-	Y	Y	ESRLPKIRFDFIFPRKK	P	GCA_946190315.1	52874 to 63087 (contig 6)
U92_S86	Y	N	-	-	-	N	N	ETRKTINSLLNLFKRR	F	GCA_946190145.1	58367 to 59135 (contig 6)
U98_S90	Y	N	-	-	-	N	N	EIRIADKIFFNLFKRR	F	GCA_946190155.1	14745 to 15455 (contig 11)
U99_S91	Y	N	-	-	-	N	N	EIRIADKIFFNLFKRR	F	GCA_946190155.1	14745 to 15455 (contig 12)
WTCHG_774611_72895361	N	-	-	-	-	-	-	-	-	GCA_946190255.1	-
WTCHG_774611_72965368	Y	N	-	-	-	N	N	ESRVSDILLDFLFRRKK	R	GCA_946190195.1	114512 to 120897 (contig 4)
WTCHG_774611_73005372	Y	Y	12164	2	23	N	N	EMRKMNDKSFNLFNFFRRR	F	GCA_946190135.1	24172 to 36335 (contig 6)
WTCHG_774611_73015373	N	-	-	-	-	-	-	-	-	GCA_946190275.1	-
WTCHG_774611_73075379	Y	N	-	-	-	Y	Y	EMRKPDGALFNLFRRR	F	GCA_946190295.1	119791 to 129649 (contig 6)
WTCHG_774611_73095381	Y	N	-	-	-	N	N	EMRKMNDKSFNLFNFFRRR	F	GCA_946190335.1	118632 to 130795 (contig 6)
WTCHG_774611_73775353	Y	Y	11984	5	25	N	N	EIRLSKFLRDFILQRKK	Q	GCA_946190285.1	28199 to 40182 (contig 5)
WTCHG_774611_73825358	Y	Y	11984	5	25	N	N	EIRLSKFLRDFILQRKK	Q	GCA_946190255.1	28199 to 40182 (contig 5)
WTCHG_774611_73845360	Y	N	-	-	-	N	N	EMRKMNDKSFNLFNFFRRR	F	GCA_946185975.1	118632 to 130795 (contig 6)
B22	Y	Y	15566	11	38	N	Y	ESRVSRIILDFLFLRKK	L	GCA_965111745.1	61443 to 77008 (contig 1)
C22	Y	Y	7274	3	15	N	Y	ESRLSRLLRDFIFQIKQ	Q	GCA_965111725.1	50761 to 58034 (contig 1)
D22	Y	Y	2127	2	2	N	N	DSRISKFLRDFIFPRKK	P	GCA_965111735.1	34443 to 36569 (contig 1)
E22	Y	Y	14434	1	32	Y	Y	EMRLPKILRDFIFPRKK	P	GCA_965111705.1	263852 to 278285 (contig 1)
F22	Y	Y	7848	5	13	Y	Y	ESRVSRIILDFLFLRKK	L	GCA_965111715.1	42896 to 50743 (contig 1)
G22	Y	Y	4404	2	12	N	Y	ESRLSRLLRDFIFQIKQ	Q	GCA_965111695.1	57304 to 61707 (contig 1)
B6	Y	Y	9068	5	18	Y	Y	EMRKPDGALFNLFRRR	F	GCA_000027165.1	53854 to 62921 (contig 1)
FDA684	Y	Y	8195	5	17	N	N	EIRQTHNIFFNFFKRR	F	GCA_009730515.1	31493 to 39687 (contig 1)
SK637	Y	Y	7760	4	18	N	Y	EMRKSNNNFFHFLRRI	L	GCA_000722765.2	49608 to 57367 (contig 1)
SVGS061	Y	Y	2200	2	5	N	N	EMRKSNNTFFNFLRRI	L	GCA_001560895.1	73674 to 75873 (contig 1)

The genomic region between *plsX-acpP* and *comAB* was extracted from publicly available *S. mitis* genomes. Of the 332 genomes analyzed, this region was successfully retrieved from 253; the remaining genomes contained contig breaks and were excluded from further analyses. The 253 genomes were screened for the presence of competence-associated bacteriocin (*cab*), competence-induced bacteriocins A and B (*cibAB*), and the cognate immunity protein (*cibC*) genes. The number of SigX boxes in cab loci was determined. Mature CSP sequences of each strain was predicted by identifying small ORFs upstream of *comDE* that contained a double-glycine cleavage motif.

Table S2. Bacterial strains, plasmids, peptides and oligonucleotides used in study.

Bacterial strain, plasmid, oligonucleotide or peptide	Relevant genotype or sequence	Note	Source
Bacterial strains			
Corynebacterium accolens LMG 19042	Wild type	-	BCCM/LMG
Dolosigranulum pigrum LMG 15126	Wild type	-	BCCM/LMG
Escherichia coli DH5α	Wild type	-	Thermo Fisher
Escherichia coli DH10B	Wild type	-	Thermo Fisher
Haemophilus influenzae FP7132	Wild type		P. Lavado
Klebsiella pneumoniae OND482	Wild type	-	Simões *et al* ., 2022
Moraxella catarrhalis ATCC 25238	Wild type	-	ATCC
Neisseria lactamica ATCC 23970	Wild type	-	ATCC
Staphylococcus aureus ATCC 25293	Wild type	-	ATCC
Staphylococcus epidermidis ATCC 14990	Wild type	-	ATCC
Streptococcus agalactiae ATCC 13813	Wild type	-	ATCC
Streptococcus anginosus ATCC 12395	Wild type	-	ATCC
Streptococcus constellatus ATCC 27823	Wild type	-	ATCC
Streptococcus gordonii ATCC 33399	Wild type	-	ATCC
Streptococcus infantis ATCC 700779	Wild type	-	ATCC
Streptococcus mitis SK142	Wild type	-	ATCC
Streptococcus mitis F22	Wild type	-	Borralho, Handem and Lança *et al.,* 2025
Streptococcus mitis G22	Wild type	-	Borralho, Handem and Lança *et al.,* 2025
Streptococcus mitis G22 P*comCDE* -pJB11	*CIL* ::P*comCDE* -mNeonGreen-luciferase *cat*	chl^R	This study
Streptococcus mitis G22 *PsigX1-pJB11*	*CIL::PsigX1-mNeonGreen-luciferase cat*	chl^R	This study
Streptococcus mitis G22 *PsigX2-pJB11*	*CIL::PsigX2-mNeonGreen-luciferase cat*	chl^R	This study
Streptococcus mitis G22 *PcabABC-pJB11*	*CIL::PcabABC-mNeonGreen-luciferase cat*	chl^R	This study
Streptococcus mitis G22 *PcabABC* (truncated)-*pJB11*	*CIL::P* cabABC(truncated)-*mNeonGreen-luciferase cat*	chl^R	This study
Streptococcus mitis G22 Δ*comE PcabABC-pJB11*	Δ*comE::aphA-3 CIL::PcabABC-mNeonGreen-luciferase cat*	kan^R chl^R	This study
Streptococcus mitis G22 Δ*sigX1 PcabABC-pJB11*	Δ*sigX1::aphA-3 CIL::PcabABC-mNeonGreen-luciferase cat*	kan^R chl^R	This study
Streptococcus mitis G22 Δ*sigX2 PcabABC-pJB11*	Δ*sigX2::ant(9) CIL::PcabABC-mNeonGreen-luciferase cat*	spc^R chl^R	This study
Streptococcus mitis G22 Δ*sigX1* Δ*sigX2 PcabABC-*	Δ*sigX1* ::*aphA-3* Δ*sigX2* ::*ant(9)* *CIL* ::P*cabABC-mNeonGreen-luciferase cat*	kan^R spc^R chl^R	This study
Streptococcus mitis Δ*blp4* Δ*blp1*	Δ*blp4* ::*lox72* Δ*blp1::aphA-3*	kan^R	Borralho, Handem and Lança *et al.,* 2025
Streptococcus mitis Δ*blp4* Δ*blp1* (markerless)	Δ*blp4* ::*lox72* Δ*blp1::lox72*	-	This study
Streptococcus mitis Δblp4 Δblp1 Δ*cabABC*	Δ*blp4* ::*lox72* Δ*blp1::lox72* Δ*cabABC* ::*aphA-3*	kan^R	This study
Streptococcus mitis p(*cab* $^+$)	Δ*blp4* ::*lox72* Δ*blp1::lox72* Δ*cabABC* ::*aphA-3* pJB09-P23-*cabABC*	spc^R kan^R	This study
Streptococcus mitis G22 *cabA-HA*	Δ*blp4* ::*lox72* Δ*blp1* ::*lox72* Δ*cabABC* ::*aphA-3 CIL::cabA-HA cabBC cat*	kan^R chl^R	This study
Streptococcus mitis G22 *cabB-HA*	Δ*blp4* ::*lox72* Δ*blp1* ::*lox72* Δ*cabABC* ::*aphA-3 CIL::cabA cabB-HA cabC cat*	kan^R chl^R	This study
Streptococcus mitis Δ*blp4* Δ*blp1* Δ*comE*	Δ*blp4* ::*lox72* Δ*blp1* ::*lox72* Δ*comE* ::*aphA-3*	kan^R	This study
Streptococcus mutans ATCC 25175	Wild type	-	ATCC
Streptococcus oralis DSM 20066	Wild type	-	DSMZ

(continues on next page)

Table S2. (cont.)

Streptococcus parasanguinis ATCC 15912	Wild type	-	ATCC
Streptococcus peroris ATCC 700780	Wild type	-	ATCC
Streptococcus pneumoniae D39	Wild type	-	Avery *et al.,* 1944
Streptococcus pneumoniae D39 PhunSweet	*Δcps ::pheS-sacB-aphA-3*	kan^R	Echlin and Rosch, 2020
Streptococcus pneumoniae D39 P*comCDE* -pJB11	*CIL* ::P*comCDE* -mNeonGreen-luciferase *cat*	chl^R	This study
Streptococcus pneumoniae D39 Δ*lytA*	*ΔlytA ::pheS-sacB-aphA-3*	kan^R	This study
Streptococcus pneumoniae D39 Δ*lytA* (markerless)	Δ*lytA*	-	This study
Streptococcuspneumoniae D39 Δ*lytC*	*ΔlytC ::pheS-sacB-aphA-3*	kan^R	This study
Streptococcuspneumoniae D39 Δ*lytC* (markerless)	Δ*lytC*	-	This study
Streptococcus pneumoniae D39-GFP	P*hlpA -hlpA-gfp cat*	chl^R	Valente *et* al., 2022
Streptococcus pneumoniae D39-GFP ΔcomGC	P*hlpA -hlpA-gfp cat ΔcomGC ::tet(M)*	tet^R	This study
Streptococcus pneumoniae TIGR4	Wild type	-	ATCC
Streptococcus pseudopneumoniae BAA-960	Wild type	-	ATCC
Streptococcus pyogenes ATCC 12344	Wild type	-	ATCC
Streptococcus salivarius ATCC 7073	Wild type	-	ATCC
Streptococcus sanguinis ATCC 10556	Wild type	-	ATCC
Streptococcus sinensis HKU4	Wild type	-	DSMZ
Streptococcus sobrinus ATCC 27351	Wild type	-	ATCC
Streptococcus vestibularis ATCC MM1	Wild type	-	ATCC
Plasmids			
pDL278-P23-DsRed-Express2	*P23-dsRed-Express2 pMB1 pVA380-1 ant(9)*	*E. coli*-streptococcal	Plasmid #121505 (Addgene)
pJB09-cabABC	pDL278-P23-DsRed-Express2 but Δ*dsRed-Express2 ::cabABC*	*E. coli*-streptococcal	This study
pBIR	*p15A aphA-3 tdTomato cat*	Integrates in *CIL* locus	This study (Twist Bioscience)
pPEP-LGZ	*luc sfGFP lacZ cat p15A ant(9)*	Integrates in *CEP* locus	Kjos *et al* ., 2016
pJB10	pBIR but Δ*tdTomato ::hlpA-mNeonGreen*	Integrates in *CIL* locus	This study
pJB11	pJB10 but *luc*	Integrates in *CIL* locus	This study
pJB11-PcomCDE(G22)	pJB11 but P*comCDE* reporter (*S. mitis* G22)	Integrates in *CIL* locus	This study
pJB11-PcomCDE(D39)	pJB11 but P*comCDE* reporter (S. *pneumoniae* D39)	Integrates in *CIL* locus	This study
pJB11-PsigX1	pJB11 but P*sigX1* reporter	Integrates in *CIL* locus	This study
pJB11-PsigX2	pJB11 but P*sigX2* reporter	Integrates in *CIL* locus	This study
pJB11-PcabABC	pJB11 but P*cabABC* reporter	Integrates in *CIL* locus	This study
pJB11-PcabABC(truncated)	pJB11 but P*cabABC* (truncated) reporter	Integrates in *CIL* locus	This study
pKan	*pMB1 lox66-p3-aphA-3-lox71*	Integrates in *cab* locus	Borralho, Handem and Lança *et al.*, 2025
Peptides			
$BlpC_1$	GLWEELYETITTPLKLRTTFKP	-	NZYTech
$BlpC_4$	GWWEELLHETILSKFKITKALELPVQL	-	NZYTech
CSP-1	EMRLSKFFRDFILQRKK	-	NZYTech
CSP-2	EMRISRIILDFLFLRKK	-	NZYTech
CSP-2(L14Q)	EMRISRIILDFLFQRKK	-	NZYTech

(continues on next page)

Table S2. (cont.)

CSP_{A22}	DWRISETIRNLIFPRRK	-	NZYTech
CSP_{B22}	ESRVSRIILDFLFLRKK	-	NZYTech
CSP_{D22}	DSRISKFLRDFIFPRKK	-	NZYTech
CSP_{E22}	EMRLPKILRDFIFPRKK	-	NZYTech
CSP_{G22}	ESRLSRLLRDFIFQIKQ	-	NZYTech
CSP_{G22}(Q14L)	ESRLSRLLRDFIFLIKQ	-	NZYTech
CSP_{G22}(Q14N)	ESRLSRLLRDFIFNIKQ	-	NZYTech
Oligonucleotides			
P1F_cab7_OE	ATGACAAATTTTGACAAAATGGAAC	Construction of plasmid pJB09-cabABC	This study
P1R_cab7_OE	CCCTATAGAACGTCTACTACCTC		
P1F_pDL278_OE	CTCGGTACCAAATTCCAGAAAAG		
P1F_pDL278_OE	GTTTGTCCTCCTTAACTAGTAATTAATAC		
P1F_hlpA_mNG_twist	AAAGCACTCAAAAGTTTACCTTATGG	Construction of plasmid pJB10	This study
P1R_hlpA_mNG_twist	CGCAAAAAACCCCGCTTCGGCGGGGTTTTTTCGCTTATTTATAC		
P1F_pBIR_backbone	ATCGGAGAAATTGGACACACC		
P1R_pBIR_backbone	CCCTATCAAAAGAATCTTGCTTGGC		
PF_luc_pPEP	GCTGAAGGAGGAATAATGAGATCC	Construction of plasmid pJB11	This study
PR_luc_pPEP	TTACAATTTGGGCTTTCCGCC		
PF_pJB10_backbone	GAATGGACGAGTTGTATAAG		
PR_pJB10_backbone	TTATTTATACAATTCATCCATACCC		
PF_reporter_PcomCDE(G22)	AGCTGGTCTCTGACTATATAGTAGCAAAGCTGGG	Construction of plasmid pJB11-PcomCDE (G22)	This study
PR_reporter_PcomCDE(G22)	CGATGGTCTCAAGTCAATAAAATCTCCTAAAATGTTTTTTTC		
PF_reporter_PcomCDE(D39)	AGCTGGTCTCTGACTATATAATAGCAAAGCTGGG	Construction of plasmid pJB11-PcomCDE (D39)	This study
PR_reporter_PcomCDE(D39)	CGATGGTCTCAAGTCAATAAAATCTCCTAAAATGTTTTTTC		
PF_reporter_PsigX1	AGCTGGTCTCTGACTCCCAAAGAGAGGCAAGACC	Construction of plasmid pJB11-PsigX1	This study
PR_reporter_PsigX1	CGATGGTCTCAAGTCTCTTTTCCCCTTTCTGTGTAC		
PF_reporter_PsigX2	AGCTGGTCTCTGACTCCCTGAGAGAGGCCCGTC	Construction of plasmid pJB11-PsigX2	This study
PR_reporter_PsigX2	CGATGGTCTCAAGTCAGTCTTCCCCTTTCTGTGTAC		
PF_reporter_PcabABC	AGCTGGTCTCTGACTAAATAACATCTTCACAACTAATCG	Construction of plasmid pJB11-PcabABC	This study
PR_reporter_PcabABC	CGATGGTCTCAAGTCCTTTTTTCTCCTTTATTTCTATTTTTTAG		
PF_reporter_PcabABC_trunc	AGCTGGTCTCTGACTTTTAGTTGTGTATTTTCGAATTG	Construction of plasmid pJB11-PcabABC (truncated)	This study
PR_reporter_PcabABC_trunc	CGATGGTCTCAAGTCCTTTTTTCTCCTTTATTTCTATTTTTTAG		
P1F_comE_G22	GGATTAAACAGTATGAGAGG	Deletion of *comE* in *S. mitis* G22	This study
P1F_comE_G22	GTCAATACCGTTCGTATAGCATACATTATACGAAGTTATTCATTCAAATTCCCTCTTAAATC		
P2F_comE_G22_pKan	CAAATTATTAGATTTAAGAGGGAATTTGAATGAATAACTTCGTATAATGTATGC		
P2R_comE_G22_pKan	CATTATATCAATTTCTTGCTAATTGTCAATCACTATAACTTCGTATAGCATAC		
P3F_comE_G22	GTTTTAGTACCGTTCGTATAATGTATGCTATACGAAGTTATAGTGATTGACAATTAGCAAGAAATTG		
P3R_comE_G22	TATTACCATTATAGGAAGCC		
P4F_comE_G22	TATAACAGGAGATAATTTTG		
P4R_comE_G22	ACAGAGCTGGAATAAGAGAAATCC		

(continues on next page)

Table S2. (cont.)

P1F_sigX1_G22	ATTGTCATCGCTGCGACAAAC	Deletion of *sigX1* in *S. mitis* G22	This study
P1R_sigX1_G22	GTCAATACCGTTCGTATAGCATACATTATACGAAGTTATCATTCTTTTCCCCTTTCTGTGTACAG		
P2F_sigX1_G22_pKan	GACTGTACACAGAAAGGGGAAAAGAATGATAACTTCGTATAATGTATGC		
P2R_sigX1_G22_pKan	CTTTTTTGCATGAATTCCTAATGGGTACGATAACTTCGTATAGCATAC		
P3F_sigX1_G22	GTTTTAGTACCGTTCGTATAATGTATGCTATACGAAGTTATCGTACCCATTAGGAATTCATGC		
P3R_sigX1_G22	CGCTACACATGGAATTCCAC		
P4F_sigX1_G22	AGCAATCTTGAAAGTTCATGCTAAG		
P4R_sigX1_G22	ATCCGGACAACGCTCGGGACCTAC		
P1F_sigX2_G22	TGCTTGTCAAAGCCTGGCTTTCTTG	Deletion of *sigX2* in *S. mitis* G22	This study
P1F_sigX2_G22	CATGCAAAACAATGAATAGGCATAGTCTTCCCCTTTCTGTGTAC		
P2F_sigX2_G22_pPEP	GACTGTACACAGAAAGGGGAAGACTATGCATGCAAAACAATGAATAGG		
P2R_sigX2_G22_pPEP	CTTTTTTGCATGAATTCCTAATGAGTACGCTAATTGAGAGAAGTTTCTATAG		
P3F_sigX2_G22	CTAATTGAGAGAAGTTTCTATAGCGTACTCATTAGGAATTCATGCAAA		
P3R_sigX2_G22	CCGCTACACATGGAATTCCACTC		
P4F_sigX2_G22	CTATTCAATCAAGATTAGTGGAAAC		
P4R_sigX2_G22	TAGTTAGCCGTCCCTTTCTGGTAAG		
P1F_PS_lytA_D39	GGTTTATCAGCGGTTCTCTGC	Deletion of *lytA* in *S. pneumoniae D39*	This study
P1R_PS_lytA_D39	CGGATCGATCCTTAATAGTGGGTTCCATATTCTACTCCTTATCAA		
P2F_PS_lytA_D39	GTTTTAATTGATAAGGAGTAGAATATGGAACCCACTATTAAGGATCGATC		
P2R_PS_lytA_D39	CTGTTCTGATTTGAAAGACATTCCATTATTACTAAAACAATTCATCCAGTAAAATATAAT		
P3F_PS_lytA_D39	CTGGATGAATTGTTTTATAATAATGGAATGTCTTTCAAATCAG		
P3R_PS_lytA_D39	TTTTACTTTCTGACAAAGGACG		
P4F_PS_lytA_D39	TTCAATTGTATCTATCGGCAG		
P4R_PS_lytA_D39	TTCCTCAATCTATATAACATAGCTTTATG		
P5F_PS_lytA_D39	GTTTTAATTGATAAGGAGTAGAATATGGAATAATAATGGAATGTCTTTCAAATCAG		
P5R_PS_lytA_D39	CTGTTCTGATTTGAAAGACATTCCATTATTATTCCATATTCTACTCCTTATCAA		
P1F_PS_lytC_D39	ACTAAAGGAAGATGGAACCAG	Deletion of *lytC* in *S. pneumoniae D39*	This study
P1R_PS_lytC_D39	CGGATCGATCCTTAATAGTGGGAGACATCTGAATGCTGTTCC		
P2F_PS_lytC_D39	CTAGGTGGAACAGCATTCAGATGTCTCCCACTATTAAGGATCGATC		
P2R_PS_lytC_D39	CACATCCCTCTTTCAAATCATCGCTTACTAAAACAATTCATCCAGTAAAATATAAT		
P3F_PS_lytC_D39	CTGGATGAATTGTTTTATAAGCGATGATTTGAAAGAGGG		
P3R_PS_lytC_D39	TTCTTAGTCATGCTTCCATCC		
P4F_PS_lytC_D39	CTCAAATTGAGGCCAAGAGAG		
P4R_PS_lytC_D39	GTCCAAGTTCGGCTGCAAG		
P5F_PS_lytC_D39	CTAGGTGGAACAGCATTCAGATGTCTTAAGCGATGATTTGAAAGAGGG		
P5R_PS_lytC_D39	CACATCCCTCTTTCAAATCATCGCTTAAGACATCTGAATGCTGTTCC		

(continues on next page)

Table S2. (cont.)

P1F_comGC_del	AATCGTTGACTTTGCAAGCAG	Deletion of *comGC* in *S. pneumoniae* D39	This study
P1R_comGC_del	TAATTTTCCTCCTATTTAGATCTTGCATGTATAGTTATTATACCAGGGGGACAGTGCAATGTCAATTTAAAAATTTACCTCCATATTTTGATACATG		
P2F_comGC_del	TTGACATTGCACTGTCCCCCTGGTATAATAACTATACATGCAAGATCTAAATAGGAGGAAAATTAATGAAAATTATTAATATTGGAGTTTTAGC		
P2R_comGC_del	CATTGACTTTACGATTTGCTCCTCCATTCTAAGTTATTTTATTGAACATATATCG		
P3F_comGC_del	GTACGATATATGTTCAATAAAATAACTTAGAATGGAGGAGCAAATCGTAAAGTC		
P3R_comGC_del	GTGACTGCGTAGAGGAGAAC		
P4F_comGC_del	TTCAGGCTGAGACGGAAAAAATTAG		
P4R_comGC_del	CAGATTTGAGTCCATAAACC		
P1F_cabAB_HA	CAAGCGCCAGGGTTTTCC	Construction of *S. mitis* harboring HA-tagged bacteriocins	This study
P1R_cabAB_HA	GTTCTGTTCCATTTTGTCAAAATTTGTCATCTTTTTTCTCCTTTATTTCTATTTTTTAG		
P2F_cabAB_HA	GTAAACTAAAAAATAGAAATAAAGGAGAAAAAAGATGACAAATTTTGACAAAATGGAAC		
P2F_cabAB_HA	CCAGGGGGACAGTGCAATGTCAATTATCCATTCTTTTTTTCTTTACTTC		
P3F_cabAB_HA	CATTCTTTTATATAGAAGTAAAGAAAAAAAGAATGGATAATTGACATTGCACTGTCCCC		
P3F_cabAB_HA	GCCCTCTGAGCGGATAACAATTTC		
P4F_cabAB_HA	ATCGGAGAAATTGGACACACC		
P4R_cabAB_HA	TTCGCAAATAGCGAAACCAATG		

chl^R - chloramphenicol resistant; kan^R - kanamycin resistant; tet^R - tetracycline resistant; spc^R - spectinomycin resistant.

SI References

1. A. S. Simões *et al*., Using whole genome sequencing to investigate a mock-outbreak of carbapenem-resistant *Klebsiella pneumoniae* in real-time. *Acta Med Port* **35**, 36–41 (2022).

2. J. Borralho *et al*., Inhibition of pneumococcal growth and biofilm formation by human isolates of *Streptococcus mitis* and *Streptococcus oralis*. *Appl Environ Microbiol* **91**, e01336-24 (2025).

3. O. T. Avery, C. M. MacLeod, M. McCarty, Studies on the chemical nature of the substance inducing transformation of pneumococcal types: induction of transformation by a desoxyribonucleic acid fraction isolated from pneumococcus type III. *J Exp Med* **79**, 137–158 (1944).

4. H. Echlin, J. W. Rosch, Advancing genetic tools in *Streptococcus pneumoniae*. *Genes (Basel*) **11**, 965 (2020).

5. C. Valente, A. R. Cruz, A. O. Henriques, R. Sá-Leão, Intra-species interactions in *Streptococcus pneumoniae* biofilms. *Front Cell Infect Microbiol* **11**, 803286 (2022).

6. M. Kjos *et al*., Expression of *Streptococcus pneumoniae* bacteriocins is induced by antibiotics via regulatory interplay with the competence system. *PLoS Pathog* **12**, e1005422 (2016).